UiT The Arctic University of Norway

Faculty of Science and Technology

Department of Physics and Technology

Implementing renewable energy technologies in buildings: impacts of local-specific conditions, intermittency and volatile power markets

Nikolai Enok Anfeltmo

EOM-3901 Master's thesis in energy, climate and environment 30 SP June 2024

Abstract

Increased implementations of small-scale renewable energy technologies in buildings can potentially save costs and reduce greenhouse gas emissions. The aim of this thesis is to analyse the total costs and climatic impact of implementations in major cities in Norway. Basing the analysis in data of hourly resolutions captures effects of how intermittency and volatility in the power market impacts production and cost for implementors in the major cities. A model with back-up electricity was developed with focus on the total costs and climatic impact of covering a building's electrical and heating needs, as opposed to analysing the technologies in isolation. Using hourly electricity prices from 2022 and 2018, and a fixed price scenario the performance of the implementations was analysed.

Results show that electricity prices are the main factor when judging economical performance and points particularly to photovoltaic systems (PV) as especially sensitive to electricity prices. Alternative configurations of PV systems on a typical house outperform south facing ones. Considerable reliance on back-up electricity results in worse economical results for air source heat pumps (ASHPs) and bioenergy combined heat and power (CHP) modules. Even with substantial temperature differences between locations, electricity prices are still the deciding factor. All technologies show purposefulness as implementations in the power market. Results show that ASHPs significantly reduces climatic impact, while PV systems climatically perform poorly in comparison to the Norwegian electricity mix. For the climatic impact of bioenergy CHPs it is concluded that the scope of this thesis does not provide for a confident basis to conclude on CHPs climatic impact.

Acknowledgements

First and foremost, I would like to extend my gratitude to my supervisor Professor Yngve Birkelund for valuable guidance, feedback, and interesting discussions. I would like to thank Anton Asplund, Tom Rasmussen and Asplan Viak Tromsø as a contributor for shaping the idea for this thesis. I would also like to thank Karen Byskov Lindberg for helping me access PROFet, and Volter for delivering technical data.

I am thankful for my family and friends for their moral support and for sharing moments and laughter together to help me recharge and focus for the thesis work.

I must especially thank my partner Johanna Mankova Buseth for being by my side for every step through this journey while also writing her own master's thesis. I value every moment we have shared and look forward to the rest of them.

Table of Contents

List of Tables

List of Figures

1 Introduction

The purposefulness of small-scale renewable energy technologies varies with the conditions of how and where they are implemented. Knowing which energy technology that will provide for the most saved costs and which will mitigate climatic impacts the most is of interest for actors that wish to implement renewable technologies. How these implementations are impacted by the power market and how implementations impact the power market is of interest for both small-scale investors, policymakers, power producers and grid operators.

Background

Fluctuations of power production potential, known as intermittency, is a key concern of adapting to renewable energy. Intermittency and volatility of the power market are interconnected as higher degrees of intermittency alters economical dynamics (Bunn & Muñoz, 2016), (Green & Vasilakos, 2010), (Aghaie, 2016). Glenk and Reichelstein (2022) uses "cannibalization" as a term to describe scenarios where high degrees of hourly-sensitive energy production, for instance solar and wind, causes the electricity price to fall when production reaches its daily peak. That is, electricity prices are affected by renewable energy intermittency. A situation where it is interesting to analyse how well renewable energy technologies perform, both in relation to which building-specific purpose it should supply and economically, rises in the wake of increased electricity price volatility. To properly analyse these dynamics data of hourly resolution is required, as averaged data will not capture all interesting aspects. For instance, Reichelstein and Sahoo (2015) found that the levelized cost of electricity (LCOE) for wind and solar is increased by 10% and reduced by 10% - 15% respectively when adjusted for time-of-day pricing.

Ambec and Crampes (2021) models that if electricity consumers adapt to price changes to counteract the intermittency of renewable energy production it leads to carbon emission reductions. There is a large consensus within the literature that cleverly designed power markets can solve challenges intermittency create (Jaraitė et al., 2019), (Jacobsen & Zvingilaite, 2010), (Kirkerud et al., 2021), (Gjerland & Gjerde, 2020).

Hydropower, which most of Norwegian power production is based on, is not a highly intermittent energy source, while solar and wind are (Pandey et al., 2021), (Delarue & Morris, 2015). With interconnectivity between the Norwegian and European power grid and the EU

seeking to increase its share of renewables, as stated in Knopf et al. (2015), intermittency challenges are increasingly important also in a Norwegian context.

Air-source heat pumps (ASHP), photovoltaic (PV) panels and bioenergy combined heat and power (CHP) production are examples of energy solutions to implement in buildings. ASHP are popular and purposeful implementation, also in cold regions (Sadeghi et al., 2022), (Wu et al., 2022), (Kamel & Fung, 2014). Masternak et al. (2014) points out Norway as an especially well-suited location for the use of ASHP for the purpose of lowering CO2 emissions, because of the high share of renewables supplying the grid. While one concern is the cold conditions, Gibb et al. (2023) reports that ASHPs are efficient even in conditions approaching $-30°C$. Investing in ASHPs are potentially very energy saving and economical as opposed to only basing heating needs on resistive electrical heating.

There is an increased interest in house-integrated PV systems in Norway (Winther et al., 2018). Zainali et al. (2023) reports a levelized cost of electricity (LCOE) for PV systems ranging from 0.85 to 1.15 SEK/kWh for single family dwellings in Sweden which is comparable to Norwegian conditions. There is no strong consensus of what the role and need of small-scale PV prosumers, consumers which also produces electricity to the grid, in the Norwegian power system are (Inderberg et al., 2020). PV systems with alternative configurations to south facing arrays show varying results, the system-specific results in Khatib and Deria (2022) show that the payback time and cost of energy between south and east-west facing systems are quite similar. In an electricity grid context Hartner et al. (2015) concludes that any benefits to alternative configurations diminishes with high shares of PV installed. The results from Khatib and Deria (2022) and Hartner et al. (2015), are based on energy markets in Palestine and Germany/Austria, respectively. Both report electricity costs peaking at noon, which in a Norwegian context is not necessarily the same.

Compared to PV and ASHP the literature on small scale bioenergy CHP systems specifically is scarce, but generally some assume biomass for power and heating will be increasingly important both in Norway and the EU (Jåstad et al., 2021), (Mandley et al., 2020). Hagos et al. (2017) states that ASHPs are favoured over bioenergy heating systems due to high biomass fuel prices and low electricity prices. The premise for this conclusion might not still be true, as electricity prices have risen considerably. Additionally, biomass-based solutions do not have intermittency issues and could be beneficial for power grid stabilization (Nord et al., 2021).

Project goals

In this thesis it was of particular importance to use hourly values of temperature, electricity prices and solar conditions to analyse the performance of renewable energy technologies. The hourly local-specific performance was judged on a basis reflected by real-life building needs. The method is constructed in an automated way which allows for the option to construct estimations for many locations. With a basis of realistic performance, the aim of the study was to identify how the climatic impact and economy of energy technology implementations varied with the different local-specific conditions and different electricity price scenarios. Using values in an hourly temporal resolution, as opposed to yearly, seasonal, or daily averages, is a relatively new approach to energy estimations. Due to the intermittency of implementing energy technologies and volatility in the power market using actual hour-to-hour variations can capture insights which might otherwise be overlooked. For the market segment of prosumers, price variability could be exploited to save costs, and even produce revenue. Price variability and complexities of intermittency are often overlooked for small scale systems.

2022 and 2018 and a fixed price electricity scenarios are especially interesting as this capture ranges of volatility and price variation both between price zones and the years themselves. Modelling the performance of PV, ASHP and CHP in these scenarios for major cities leads to specific questions of how the technologies compare against each other based on climatic impact, economy and role in the power market. Additionally, are there any differences within Norway for which technologies that should be prioritized given local-specific conditions and electricity price scenario.

Organization

The thesis is structured with an initial theoretical and methodological framework, before results are presented and discussed in the same chapter. Lastly, a conclusion and suggestion to future research are presented.

2 Theory

2.1 Statistical and economic measures

2.1.1 Levelized cost of electricity (LCOE)

A central concept for assessing energy technologies is levelized cost of electricity (LCOE) which applies discount rates to the yearly cash flow and energy production of the technology. In Williams & Rubert (2019) LCOE is defined as

$$LCOE = \frac{NPV}{NPE}. \tag{1}$$

Where NPV and NPE are net present value and net present energy respectively defined as

$$NPV = \sum_{t=1}^{n} \frac{C_t + O_t + V_t}{(1+r)^t} \tag{2}$$

and

$$NPE = \sum_{t=1}^{n} \frac{E_t}{(1+r)^t}. \tag{3}$$

Where C_t, O_t, V_t, E_t, r, and t being respectively capital cost, fixed operating cost, variable operating costs, energy generated in year t, and r is the discount rate. LCOE describes the relation between yearly variabilities of the parameters and how this is affected by discount rates.

With a simplified model, without discount rates or varying performance (1) is simplified to

$$LCOE = \frac{C_1}{E_1 \cdot t_{life}} \tag{4}$$

Where $C_1$is the capital cost of year 1, i.e. the investment cost, and all yearly or varying costs neglected, E_1 is the electricity produced in the first year. In this form, there is no variation in the PV system performance over the years. As one of the main aims of the thesis is to analyse impacts of hourly price variations, discount rates is not utilized in calculations.

2.1.2 Yearly attributed cost

Attributing the investment cost of an energy technology implementation to each year of lifetime returns results for the totality of costs evenly distributed to all lifetime years. The yearly attributed cost, C_{year}, is defined as

$$C_{year} = \frac{I}{t_{life}}. \tag{5}$$

Where C_{year}, I and t_{life} are the yearly attributed cost, investment cost and lifetime respectivly. When combined with costs or revenue from an implementation the yearly attributed cost is the proportion of the total that accounts for the investment cost.

A similar method and often used term is payback time, t_{pb}, defined by

$$t_{pb} = \frac{I}{C}. \tag{6}$$

Where I is the investment in NOK, t_{pb} is the payback time and C is the saved cost per year. The payback is therefore the time an investment uses to pay for itself, if the payback time is lower than the lifetime of an investment it is profitable.

The benefit of finding yearly attributed costs is that it can be directly used to compare yearly costs between scenarios. Combined with operation cost or profits of implementations the yearly attributed cost directly reflects yearly costs.

2.1.3 Linear regression

Linear regression is a standard method to describe the linear relationship between data sets. Alpaydin (2020) pp.79-81 presents linear regression as follows: for a linear model $f(x)$, defined as

$$f(x) = \beta + \alpha x. \tag{7}$$

Where β and α are constants. The unknown function that is to be approximated, $g(x)$, is defined by

$$r = g(x) + \epsilon. \tag{8}$$

ϵ is random noise assumed to follow a Gaussian distribution with 0 mean and constant variance σ^2. Replacing the unknown function with the linear model $f(x)$, we have the probability, $p(r|x)$, with relation

$$p(r|x) \sim \mathcal{N}(f(x), \sigma^2). \tag{9}$$

Where σ^2 is the variance. The joint probability density, $p(x, r)$, can be written as

$$p(x, r) = p(r|x)p(x). \tag{10}$$

Applying the log likelihood function, $log\, \mathcal{L}(\mathcal{X}) = log \prod_{t=1}^{N} p(x^t, r^t)$, to the given independent and identical sample $\mathcal{X} = \{x^t, r^t\}_{t=1}^{N}$ results in

$$\mathcal{L}(\mathcal{X}) = log \prod_{t=1}^{N} p(r^t|x^t) + log \prod_{t=1}^{N} p(x^t). \tag{11}$$

The second term is independent from r and can be neglected. Writing out the first term and neglecting independent terms and factors results in

$$\mathcal{L}(\mathcal{X}) = -\frac{1}{2} \sum_{t=1}^{N} \left(r^t - g(x^t|\beta, \alpha)\right)^2. \tag{12}$$

The error function, $E(\mathcal{X})$, defined as

$$E(\mathcal{X}) = -\mathcal{L}(\mathcal{X}) \tag{13}$$

can be minimized to find the parameters β and α which are best adapted to the dataset which is to be approximated.

For linear regression, taking the derivative of the error function with respect to β and α results in

$$\sum_t r^t = N\beta + \alpha \sum_t x^t \tag{14}$$

and

$$\sum_t r^t x = \beta \sum_t x^t + \alpha \sum (x^t)^2. \tag{15}$$

Written in vector-matrix results can be written as

$$\boldsymbol{A} = \begin{bmatrix} N & \sum_t x^t \\ \sum_t x^t & \sum_t (\mathrm{x}^\mathrm{t})^2 \end{bmatrix}, \tag{16}$$

$$\boldsymbol{w} = \begin{bmatrix} \beta \\ \alpha \end{bmatrix} \tag{17}$$

and

$$\boldsymbol{y} = \begin{bmatrix} \sum_t r^t \\ \sum_t r^t x^t \end{bmatrix}. \tag{18}$$

Now it is possible to calculate

$$\boldsymbol{w} = \boldsymbol{A}^{-1}\boldsymbol{y}. \tag{19}$$

Using the resulting parameters β and α in the model $f(x)$ returns the linear approximation of the data which has the lowest error function. The derivation of linear regression is based on Alpaydin (2020) pp.79-81.

For a dataset with values y_1, y_2, x_1 andx_2 this condenses down to finding the slope

$$\beta = \frac{y_2 - y_1}{x_2 - x_1}, \tag{20}$$

then find the intercept:

$$\alpha = y_1 - \beta \cdot x_1 \tag{21}$$

resulting in

$$\hat{f}(x) = \alpha + \beta x. \tag{22}$$

This makes for an easy way to interpolate values between two data points.

2.1.4 Logarithmic regression

Logarithmic regression can be done in a similar fashion, based in the steps from 2.1.4, the coefficients for a logarithmic model, $h(x)$, is identified. The logarithmic model is defined as

$$h(x) = \beta\, ln\,(x) + \alpha. \tag{23}$$

It is beneficial to use logarithmic regression when it is reasonable to assume that the growth of the modelled value would decrease with an increase to its dependent variable.

2.1.5 R^2-value

R^2-values can tell how good a performed regression of data is. Based in Walpole et al. (2012, p.461) it is defined as

$$R^2 = 1 - \frac{SSE}{SST}. \tag{24}$$

Where SSE is the error sum of squares and SST is the total corrected sum of squares. SSE and SST are defined as

$$SSE = \sum_{i=1}^{n} (y_i - \hat{y_i})^2 \tag{25}$$

and

$$SST = \sum_{i=1}^{n} (y_i - \bar{y})^2. \tag{26}$$

Where $\hat{y_i}$ is the i'th predicted value of the regression model, and $\bar{y}$ is the mean of the original data. In words it is a measure of proportion of variability explained by the regression model. This makes it suitable as parameter for deciding whether sets of data relate enough on each other to be used in further estimations.

2.1.6 Relative change

Comparing estimations with altered parameters provides a measure of how sensitive the results are to altering that parameter. The relative change, R_c, from one set of data to another is found using the formula:

$$R_C = \frac{\widehat{y_2} - \widehat{y_1}}{\widehat{y_1}} \quad (27)$$

Where R_C is the relative change, β is the new estimate and α is the old estimate. This method isolates one variable. To analyse the dynamic of multivariate estimations the relative change for each variable must be done separately and then compared with each other.

Relative changes are valuable when analysing how impactful changing parameters are, while still indirectly reporting the new estimates for the parameter change, which is done by simply multiplying the base case estimate with the factor $(R_C + 1)$.

2.2 Electricity, space heating and direct hot water

Electricity is an important aspect of this thesis, both as a parameter to measure energy technologies against each other, but also incorporated in the estimations. Two key assumptions are used for most of the estimations in the thesis. First that 1kW of electricity can be converted to equivalently 1kW of heat with radiation heating (Forsberg et al., 2017). Secondly that all buildings are assumed to have an already installed electricity heating system, so that the cost of that is not included in the estimations in this thesis.

Norway has a history of delivering cheap and renewable energy, which both industry and households have been reliant on (Hansen & Moe, 2022). This means that incentives might have been fewer to reduce electricity dependency, as it has been both cheap and sustainable.

The mechanisms for heat loss from buildings is a governing factor in the variation of building heat losses between location, weather, hour of the year and building materials. Rasmussen (2021) lists the most important mechanisms as the transmission of heat from the building's materials, ventilation, and transmission of heat in infiltration. To reduce building heat losses these mechanisms should be minimized. Walker and Pavía (2015) shows that 10% - 45% is a commonly reported amount of heat loss through walls. For water-borne space heating Bojić et al. (2013) uses $37°C$ for water-borne heating systems, and Hesaraki et al. (2015) defines $55°C$, $45°C$ and $35°C$ as respectively medium, low, and very low temperatures for water-borne heating.

As direct hot water (DHW) use is a major part of a buildings total needs it can be separated as its own category. The use of hot water is larger when the building is in use, differing from regular space heating demands. In other words, the hourly demands of space heating and

direct hot water heating is separable. DHW temperatures in Sweden and Finland are $55°C$, and typically used temperatures in Norway are $60°C$ (Meireles et al., 2022), (Ivanko et al., 2020).

2.3 Climatic impacts

2.3.1 Established literature on climatic impact of energy technologies

For assessing the climatic impacts of the estimates that are created in this thesis the climatic impact of alternative and traditional technologies should be used as a comparison. A common measure of climate impact is global warming potential (GWP), which equates the total emissions to a corresponding sum of CO2- equivalents (CO2e). As discussed in Lynch et al. (2020) GWP based in CO2e falls short to describe all impacts of pollutants, for instance because of different breakdown times of greenhouse gases. The most common practice is to report the GWP over 100 years, and as it is the most common within the literature to report the GWP it is a suitable basis for this thesis. Table 2.1 show the GWP for different technologies from various life cycle assessment (LCA) studies.

Table 2.1 - GWP of various energy technologies from established LCA literature

Technology	kgCO2e/kWh	Source
GSHP	0.010	Finnegan et al. 2018
GSHP	0.015	Blum et al. 2010
ASHP	0.276	Finnegan et al. 2018
ASHP	0.234	Naumann et al. 2022
Solar thermal	0.026	Finnegan et al. 2018
Solar thermal	0.023 – 0.036	Masruroh et al. 2006
PV	0.080 – 0.120	Laleman et al. 2011
PV	0.079	Alam & Xu 2022
PV	0.047 – 0.069	Santoyo-Castelazo 2021
Natural gas	0.584	Agrawal et al. 2013
Coal	1.127	Agrawal et al. 2013
Wind	0.018 – 0.031	Raadal et al. 2014

Wind	0.0083 – 0.0338	Raadal et al. 2011
Wind	0.00863	Xu et al. 2018
Wind	0.0032 – 0.0286	Wang et al. 2019
Wind	0.007 – 0.010	Garret & Rønde 2012
Hydropower	0.0004 – 0.0035	Wang et al. 2019
Hydropower	0.0029 – 0.0049	Raadal et al. 2011
Nuclear	0.0015 – 0.0124	Wang et al. 2019
CHP	0.00792 – 0.01836	Havukainen et al. 2018
Biomass electricity	0.1375	Muench & Guenther 2013
Biomass heat	0.0295	Muench & Guenther 2013
Biomass CHP	-0.0907	Muench & Guenther 2013

Electricity in Norway overall is calculated to have a GWP of 0.019 kgCO2e/kWh (Tuset, 2020). This is calculated based on the energy production in Norway and any imported power. As the grid is interconnected all over Europe this a natural way of reporting what the emissions attributed to electricity is.

2.3.2 Comparative basis for climatic impacts

For comparisons between energy technologies and the locations where they are installed a common basis for reported climatic impact should be established. As the LCA field uses GWP, often in kgCO2e/kWh, as a measure of climatic impact and is suitable our research for two reasons. First, as the performance of a technology will vary between locations, resulting in varying total energy production over the systems lifetime it is a measure of which location is the most suitable for reducing climatic impact for the same technology investment. That is, the climatic impact is attributed to every single kWh produced. Secondly, creating estimates in the same unit allows for direct comparisons to results from literature without conversion.

One concern with using GWP is that it might give the wrong impression for technologies where the climatic impact is not directly tied to the use phase. For PV systems and central heating systems the climatic impact should be attributed to the kWh that have been produced over the lifetime of the system. Using GWP directly, as a description of the total emission of

kgCO2e/kWh, could for instance lead to a misrepresentation of the climatic impact of identical systems at different locations. If two PV systems with the same total emissions, but different total energy production, a faulty conclusion of the total climatic impact of the two systems could occur if the lifetime production of the systems were multiplied with the same GWP. The system with the lowest production would seem like the most option with the least emissions, while in reality it would not be. In other words, GWP results are fixed to their given local-specific conditions. To circumvent this problem, the climatic impact of the technologies should be calculated from first finding the system-specific lifetime emissions and then attribute the emissions to each kWh produced. For heat pumps and bioenergy central heating systems, which requires fuel, electricity and biomass, the total emission of kgCO2e will increase with increased kWh production, but the emission factor, kgCO2e/kWh, might decrease. The emission factor is for heat pumps and bioenergy central heating dependent on the emission factor of the fuel and the total use of fuel.

A general formula for the emission factor of a location-specific technology implementation, e_f, is:

$$e_f = \frac{e_{life}}{E_{life}}. \tag{28}$$

Where e_{life} and E_{life} are the total lifetime, - emissions and energy production in kgCO2e and kWh respectively.

The defined emission factor is a measure of the same units as GWP, and is comparable to it, but preserves local-specific variations.

2.4 Photovolatic panels

2.4.1 Earth – Sun orientation

The performance of PV panels is limited to the amount of solar irradiance at the panel's location. Total solar irradiance is the total power in W striking from the sun upon 1 unit area at 1 astronomical unit (distance from the Sun to the Earth) from the sun (Solanki et al., 2013). Naturally, the power reaching the Earth varies by the Earth's rotation around the Sun and around itself. Iqbal (1983) describes these relations as follows. The plane which the Earth revolves around the Sun is called the ecliptic plane, and the axis which the Earth rotates around itself is called the polar axis, these dynamics causes respectively seasonal changes and

daily changes of irradiance. Solar declination is the angle between a line from the centre of the Earth to the centre of the Sun and the equatorial plane. Variation in this also causes seasonal changes, specifically the length of day and night. This cycles between the vernal and autumnal equinoxes, i.e. summer and winter solstice. The effect of changing solar declination is larger at higher latitudes, resulting in polar nights and midnight sun. That is, higher latitudes have periods of no sunlight, and periods of sustained sunlight. Closer to the equator this effect diminishes, resulting in less seasonal effects.

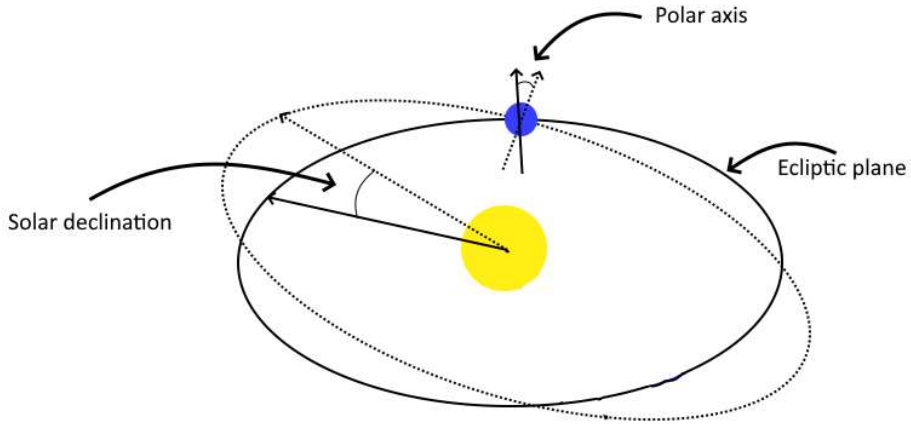

Figure 2.1 - Sun-Earth astronomical relationships impacting solar energy modelling

Figure 2.1 shows the most important Earth-Sun relationships impacting solar energy production potential.

2.4.2 Atmospheric effects

The content of the atmosphere also limits performance of PV panels. Solanki (2015) p.326, p.337 describes many of these effects and is the basis for the terms presented in this paragraph. The length of atmosphere the solar radiation must travel through varies with latitude. This is important since the radiation is subjected to absorption and scattering within the atmosphere. As the length increases more of the irradiation is absorbed and scattered. This measure is described by Air Mass (AM) and is in its simplest form described by the following equation:

$$AM = \frac{1}{cos\,\theta}. \tag{29}$$

With θ being solar zenith angle, defined as

$$\theta = 90° - \delta. \tag{30}$$

Where δ is the solar altitude, i.e. the angle to the sun from a horizontal plane, ranging from 0° to 90° where 0° occurs at sunrise and 90° when the sun is overhead. AM0, AM1.5 and AM2 are common values in the solar energy field, and corresponds to solar irradiations of $1376W/m^2, 1000W/m^2$ and $894W/m^2$ referring to no atmosphere, ground-level with a 48° solar zenith angle and 60° solar zenith angle respectively.

Typically, 16% of extra-terrestrial solar irradiation is absorbed in the atmosphere, and 6% is reflected from the atmosphere. The proportion of radiation that reaches the earth directly is called direct radiation. The radiation which is scattered within the atmosphere is called diffuse radiation. Some of the direct and diffuse radiation is reflected on the ground, known as albedo radiation. The sum of direct, diffuse and albedo radiation is called global radiation, and is the potential for collecting solar energy. The amount of direct, diffuse and albedo radiation varies with local conditions. Cloudy weather reduces the direct radiation while the amount of diffuse radiation could be relatively high. High albedo surfaces will naturally increase the albedo radiation.

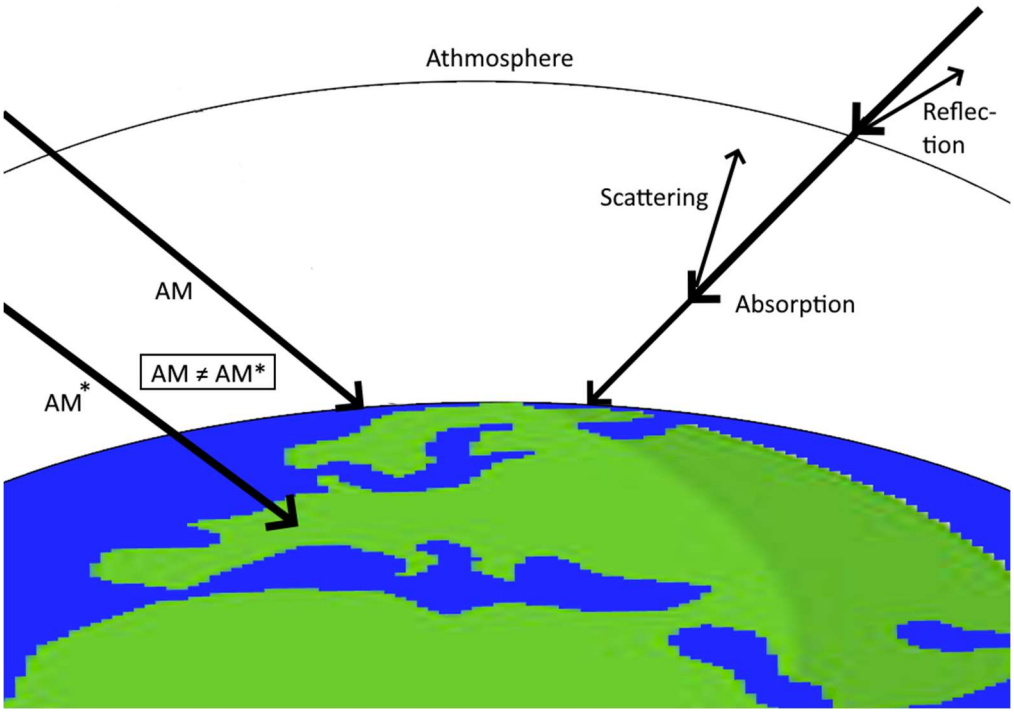

Figure 2.2 - Atmospheric effects impacting solar radiation

Figure 2.2 shows some of the most important processes sunlight undergoes before reaching the Earth's surface where it can be utilized by PV panels.

2.4.3 PV panel working principle

Photovoltaic panels work by exploiting the atomic structure of silicon (Si). It has an ability to be doped with other elements. Doping materials means adding other substances in clean materials (Stokkan, 2020).

An elementary explanation of elements characteristics includes the electron structure - eight electrons in an atoms outer electron shell makes for a stable atom, except for the inner shell which only has room for two electrons. Si has 4 electrons in its outer shell, these electrons are called valence electrons. Elements with this property (elements in period table group 14) have a lattice shaped structure, which allows for electrons to move around from atom to atom (Andersen, 2019). By doping Si with elements with 3 and 5 valence electrons (period table group 13 and 15) the material then contains atoms with 1 and 7 valence electrons. The consequence of this is that only a small amount of energy is needed to free the one valence electron from the material doped with elements of the 15 periodic group and the material doped with 13 periodic group only needs one extra electron to be stable. These materials are called p and n type semiconductors, respectively doped with group 13 and group 15.

Sunlight has enough energy to generate the electron flow when shining upon the semiconductive material, this is known as the photovoltaic effect (Hofstad, 2023). Whether or not photons are able to excite electrons is dependent on the materials band gap energy. Different materials match with different wavelengths of light to generate electron excitation, and their efficiencies are restricted to the Shockley-Queisser limit (Sutherland, 2020). The most commercially available material is crystalline silicon, which have a relatively high efficiency.

When these materials are connected with a conductor electrons can flow from the n-type material to the p-type material. That is, electric charges travelling through the conductor. The definition of electrical current is "The current (in amperes) through a given area is the electric charge passing through the area per unit time" (Sadiku, 2015, p. 176). Which means that the electron transfer between the materials by definition is electric current.

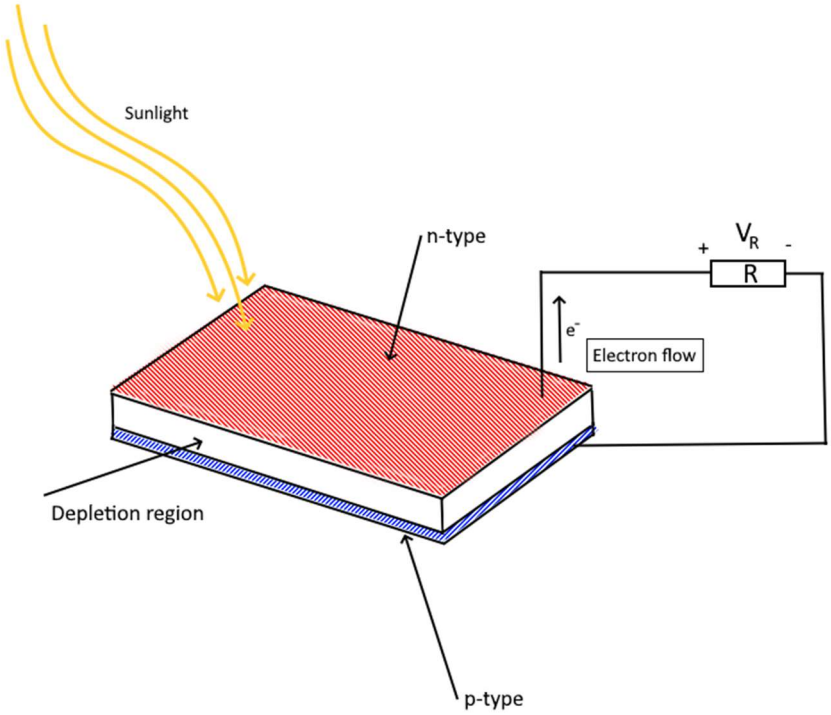

Figure 2.3 - Illustration of workings of photovoltaic panels generating electricity from sunlight.

Figure 2.3 shows the fundamental concept of how special material properties is able to generate electricity. R and V_R refers to resistance and voltage over the resistance respectively.

2.4.4 PV panel sizes

Different PV panels on the market have different kWp to area relationships, and a set value should be established to be used in estimations later. Table 2.2 shows key data retrieved from PV producers.

Table 2.2 - PV panels kWp under STC, panel area and area/kWp

Product	kWp	area	area/kWp	Source
Ulica 455W	0.455	2.17	4.78	Ulica 455, n.d.
JASOLAR 365W	0.365	1.87	5.12	Jasolar 365, n.d.
LONGI Hi-MO 410W	0.41	1.95	4.76	Longi 410, n.d.
TONGWEI 415W	0.415	1.99	4.79	Tongwei 415, n.d.
Mean	0.41	1.99	4.86	N/A

The kWp is reported under standard testing conditions (STC) which is set at $25°C$, $1000W/m^2$ and AM 1.5 (Solanki, 2015, p.123). In contrast to the market data Finnegan et al. (2018) uses $0.14kWp/m^2$, corresponding to $7.14m^2/kWp$, in their review article, however the studies and other sources within it used are relatively old.

2.4.5 PV panel investment cost

With larger PV panel investments, the cost per kWp decreases, as shown in Figure 2.4. The figure is based on offers from Otovo and Solenergi Norge in addition to acquired data from Asplan Viak Tromsø (Solenergi Norge, n.d.), (Otovo, n.d.), (Asplan Viak, personal communication, September, 8 2023).

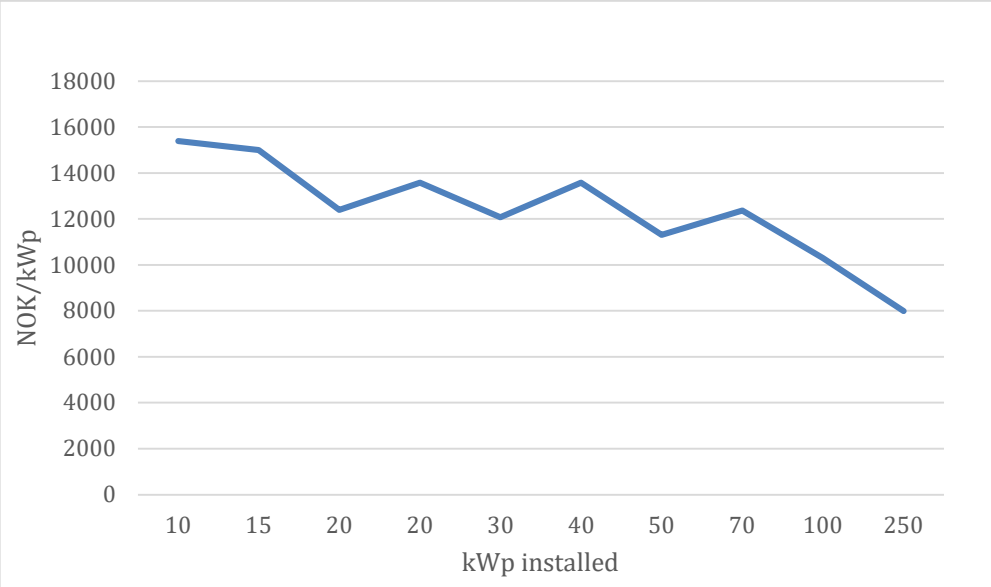

Figure 2.4 - PV system prices in NOK/kWp based in kWp installed

Figure 2.4 shows that the price per kWp between suppliers are not similar, thus creating the jagged shape of the plot. The majority of price estimates includes all panels, mounting system and inverters, but excludes installation and transport.

2.4.6 PV panel climatic imapcts

The climatic impact of PV panels is an important aspect and should be covered. Most of Norway is also considered as areas with low solar irradiation in accordance with Laleman et al. (2011), despite being an old study it is a complete LCA of PV systems in low solar irradiation areas. Laleman et al. (2011) reports that for a typical 3kWp system results in a GWP of 0.080 kgCO2e/kWh – 0.120 kgCO2e/kWh over lifetimes of respectively 30 and 20 years. A newer study based in Canada reports a GWP of 0.079 kgCO2e/kWh for 3kWp

Mono-Si PV panels with a 30 year lifetime (Alam & Xu, 2022). It is also reported that it is especially the panels themselves, excluding inverters and mounting system etc. which contributes the most to the GWP. While the reported GWP is low, the assumption of lifetimes might not hold, Libra et al. (2023) reports that in an analysis of 85 PV plants the actual lifetime of the systems was closer to 10-12 years than 20-30 years as declared by manufacturers. A significant decrease which has implications for the GWP of PV systems.

To find an emission factor which is specific to the parameters set for the calculations in this thesis the total emissions related to the PV system structure itself should be attributed to the produced electricity by an installation of that size at that location, as described in 2.3.2. In other words, the results should be adjusted to a kWp basis.

Laleman et al. (2011) reports 5000-6000 kgCO2e for 3 kWp system which results in 1666 to 2000 kgCO2e/kWp. Santoyo-Castelazo et al. (2021) attributes 47.16 gCO2e to a functional unit of 1kWh for a 3kWp system, where they expect 1156 kWh/kWp over a 30 year lifetime. As a PV panel will not produce emission during use, the 4906 kg CO2e assumed emissions are all attibuted to the 3 kWp system itself. That is 1635 kgCO2e/kWp. Alam & Xu (2022) uses 1060 kWh/kWp for a 3kWp system, 0.0791 kgCO2e/kWh, 30 year lifetime and a functional unit of 1kWh. Resulting in 7546 kgCO2e for the 3 kWp system, equivalent to 2515 kgCO2e/kWp. For all LCA reports the considerable majority of emissions are related to the production of the system, neglecting emissions related to transport etc. ensures transferability to a Norwegian scenario.

2.5 Heat pumps

2.5.1 Heat pump working principle

The concept of a heat pump is to retrieve heat from one reservoir and deposit the heat somewhere else. The process requires some work but allow for efficient heat transfer. Heat pumps can retrieve heat from low-temperature zones and deposit that heat somewhere useful. Heat pumps can retrieve heat from the outside surroundings and deposit that heat inside buildings. This process is possible due to the physical characteristics of refrigerants and altering aggregate states. Refrigerants in heat pump cycles are materials with boiling points dependent on the pressure they are subjected to. When fluids evaporate, they bind heat and when a gas condenses it releases heat (Lorentzen, 2018). Closed systems with heat exchangers, compressors and expansion valves allows the process to be exploited for heating.

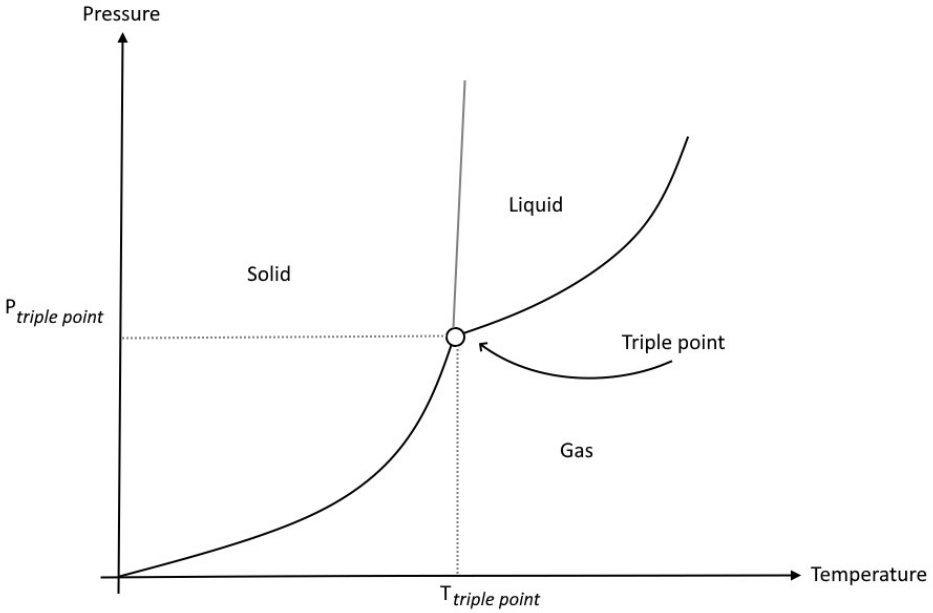

Figure 2.5 - PT diagram of an arbitrary material and aggregate phases which heat pumps exploit

Figure 2.5 shows how an arbitrary material changes aggregate phases under different pressures and temperatures. At the triple point marked, each state of the material can occur. The vaporization and condensation which happens between the liquid and gas phase is what allows heat pumps to retrieve and deposit heat.

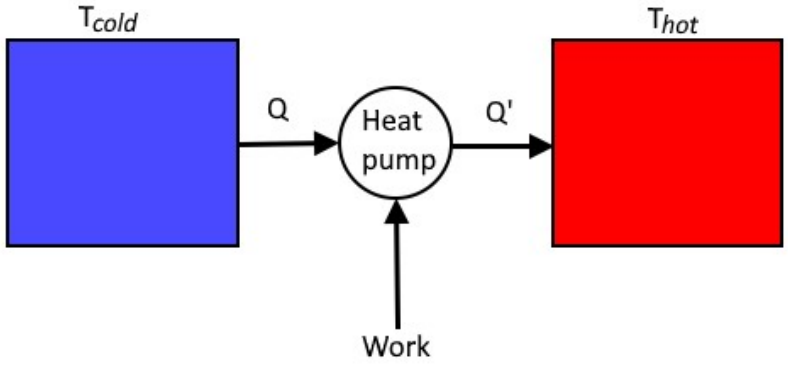

Figure 2.6 - Conceptual macroscopic illustration of how heat pumps work

Figure 2.6 shows the concept of a heat pump retrieving heat from a cold reservoir and depositing it in a hot reservoir, with Q indicating heat.

The processes which run the heat pump cycle requires some power to work, for instance a compressor. The ratio between work and deposited heat is known as the coefficient of performance (COP) and its formula is:

$$COP = \frac{Q}{P} \tag{31}$$

Where Q is the heat deposited from the heat pump and P is the work required to deliver the heat (Hofstad, 2021). Assuming maximum theoretical efficiency the formula for COP of a heat pump can be written as:

$$COP = \frac{T_{hot}}{T_{hot} - T_{cold}} \tag{32}$$

With temperatures in Kelvin the formula illustrates the temperature dependency for heat pumps, as T_{cold} approaches T_{hot} the COP increases.

Air source heat pumps (ASHP) are a simple form of HPs which uses the outside of a building as the cold reservoir and the inside as the hot reservoir. Compared to ground source heat pumps (GSHP), which facilitates drilled holes in the ground to collect heat, ASHPs are uncomplicated implementation but are naturally more subjected to changing temperatures.

2.5.2 ASHP COPs

Ruhnau et al. (2019) presents a relation of COP outside temperatures based in manufacturer data. The data for ASHPs are presented in Figure 2.7.

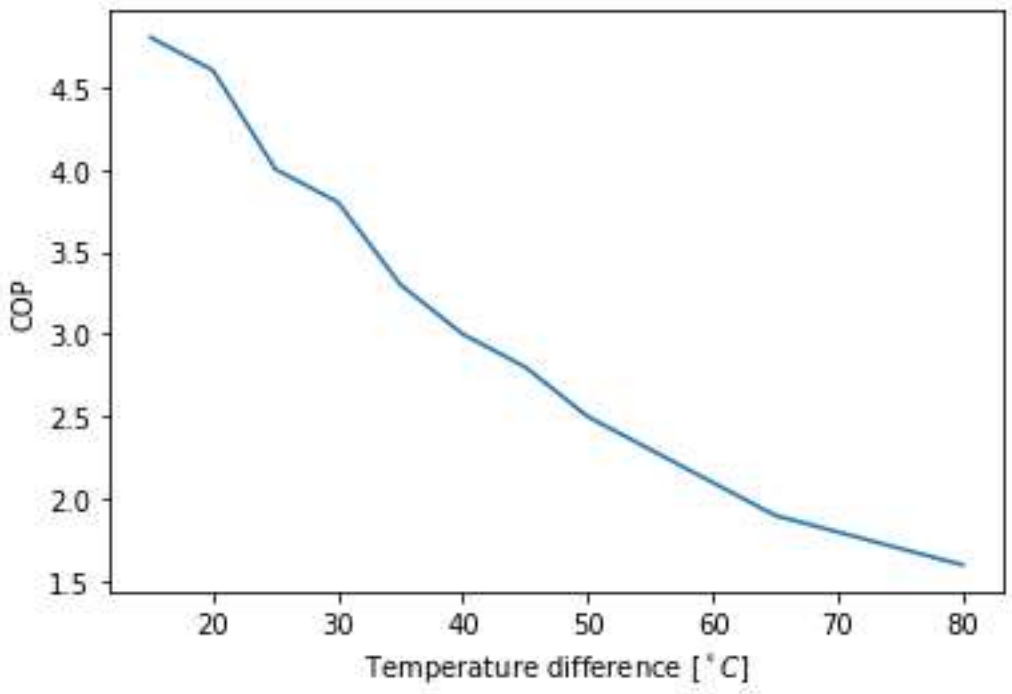

Figure 2.7 - ASHP COP corresponding to outside temperature from Ruhnau et al. (2019)

Figure 2.7 shows a steady decrease of performance as temperature differences increases.

As manufacturers probably reports data from ideal conditions it is likely that the actual COP is too high. Li et al. (2024) reports modified COP values based in outside temperature. With lower outside temperatures ASHPs will gather frost on the outside heat exchanger coil. As this reduces performance the heat pumps have built-in defrosting mechanisms which reduces the efficiency and the total operating hours of the heat pump. Varying degrees of frost correspond to a outside temperature and a COP reduction.

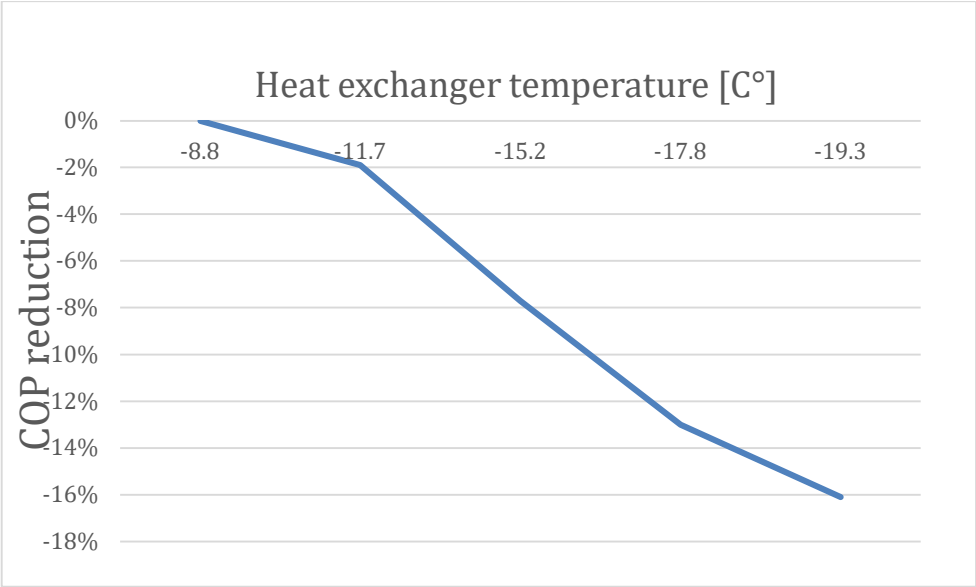

Figure 2.8 - COP reduction from icing of heat exchanger based in outdoor temperature, recreated from results from Li et al. (2024)

As shown in Figure 2.8 the COP steadily decreases with lower outside temperatures. Ideally the temperature range would extend even lower. Precisely how the relation behaves in lower temperatures is not necessarily obvious. The discussion of how even colder temperatures and humidity relates is beyond the scope of this thesis, and a 16% reduction in COP is assumed for all temperatures lower than what Li et al. (2024) is based on.

2.5.3 ASHP climatic impacts and investment cost

ASHPs offer a more efficient way of supplying heat, instead of using electrical resistive heating directly. With low GWP for the electricity Norway is climatically well suited for the use of modern ASHPs which are efficient in very cold conditions.

According to Naumann et al. (2022), an LCA done for German conditions, 81% of the GWP of ASHPs in the operation phase are attributed to the electricity use, while 19% is due to leakage of refrigerants. With 78% of the total GWP being attributed to the use phase, and the GWP of the Norwegian power mix being significantly lower than the German, a higher proportion of GWP should be attributed to refrigerant leakage in Norwegian conditions.

The type of refrigerant used in heat pump systems have varying environmental impacts. The impact of chlorofluorocarbons (CFC) became clear to world during the 1980-1990s as atmospheric ozone were being depleted, as a global ban on CFCs was put in place other refrigerants was commercially adopted (Keeble et al., 2020). The replacement for CFCs, refrigerants such as R134a and R410A poses their own problems with high GWP and are

currently being phased out. Human health considerations are also an aspect of finding suitable refrigerants. R32 is widely used for ASHPs and has a GWP of $677\frac{kg\ CO2e}{kg\ R32}$ while other refrigerants such as R134a, R404A and R410A have GWPs $1300\frac{kg\ CO2e}{kg\ R134a}$, $3942\frac{kg\ CO2e}{kg\ R404A}$ and $1924\frac{kg\ CO2e}{kg\ R410A}$ (Yang et al., 2021).

The literature of the climatic impact of ASHPs specifically in a Norwegian setting is scarce. However, adapting relevant literature allows for calculating the emission factor.

Naumann et al. (2022) reports that 3% of the total refrigerant mass leaks during manufacture and 6% leaks annually. The total refrigerant leakage is therefore dependent on the total filled mass of refrigerant, implicitly installed size, and lifetime. Calculating the required electricity to run the ASHP and the refrigerant leakage will account for the majority of total emissions.

Table 2.3 - Air-to-air heat pump manufacturer data

	Power input [W]	Nominal power input [W]	Listed heat output – lowest T_{out} [W]	Nominal COP	Nominal heat output [W]	Refrigerant mass [kg]	Price [NOK]	Source
Toshiba Daisekai 25 LL	150 – 1800	N/A	2900 $(-30°C)$	5.42	N/A	1.15	26990	Toshiba Daisekai 25, (n.d.)
Toshiba Daisekai 35 LL	160 – 2600	N/A	3200 $(-30°C)$	5.06	N/A	1.20	29990	Toshiba Daisekai 35, (n.d.)
Toshiba Polar 25 LL	200 – 2400	N/A	2600 $(-25°C)$	4.92	N/A	0.76	19990	Toshiba Polar 25, (n.d.)
Toshiba Polar 35 LL	200 - 2500	N/A	2700 $(-25°C)$	4.57	N/A	0.76	22990	Toshiba Polar 35, (n.d.)
Toshiba Signatur 25 LL	200 – 2400	N/A	2600 $(-25°C)$	4.92	N/A	0.76	26490	Toshiba Signatur 25, (n.d.)
Toshiba Signatur 35 LL	200 - 2500	N/A	2700 $(-25°C)$	4.42	N/A	0.76	28990	Toshiba Signatur 35, (n.d.)
Toshiba Seiya Nordic 25	210 – 1400	N/A	1600 $(-25°C)$	4.27	N/A	0.67	15490	Toshiba Seiya Nordic

LL								25, (n.d.)
Toshiba Seiya Nordic 35 LL	270 - 1800	N/A	2200 $(-25°C)$	3.89	N/A	0.80	16990	Toshiba Seiya Nordic 35, (n.d.)
Mitsubishi Kaiteki 6300	N/A	600	2300 $(-25°C)$	5.33	3200	0.85	21100	Mitsubishi Kaiteki 6300, (n.d.)
Mitsubishi Kaiteki 6600	N/A	820	3100 $(-25°C)$	4.87	4000	0.85	25800	Mitsubishi Kaiteki 6600, (n.d.)
Mitsubishi Kaiteki 8700	N/A	1480	4700 $(-25°C)$	4.05	6000	1.45	27900	Mitsubishi Kaiteki 8700, (n.d.)

Table 2.3 shows a range of techno-economic data for ASHPs from market data. All entries used R32 as the refrigerant. A large range of COPs, prices and power ranges are represented.

2.6 Combined heat and power

Combined heat and power (CHP) refer to a method which cogenerates heat and power. As this thesis seeks out to analyse the implementation of renewable energy sources all fossil fuel-based CHP plants are disregarded, and CHP refers to bioenergy CHP unless otherwise specified.

2.6.1 CHP potential

Using bioenergy-based solutions have the potential to be beneficial renewable investment. The theoretical potential of sustainable bioenergy production in Norway is around 39TWh (Trømborg, 2011). According to Ranta et al. (2020) biomass availability in Norway is not a limiting factor for increased bioenergy use. Torvanger (2021) reports that the total production of bioenergy in Norway in 2019 was 11.9TWh. While there is a potential of exploiting bioenergetic resources more other factors such as biodiversity, conservation and intrinsic value of nature is also important to discuss.

Bioenergy demands more land area than most other energy sources according to Núñez-Regueiro and Siddiqui (2020), which could point to Norway for greater exploitation of the resources in a global perspective.

Keeping all these factors in mind, some literature backs up the idea that exploiting bioenergetic sources can be done both environmentally friendly and supporting other societal interests (Donnison et al., 2021), (Torvanger 2021).

2.6.2 CHP working principle

The general way a bioenergetic CHP works is by exploiting the chemically potential energy in biomass sources. In its simplest form this process can be expressed by the chemical equation:

$$aFuel + bO_2 \rightarrow cCO_2 + dH_2O, \Delta H < 0. \quad (33)$$

Where the fuel is an organic compound comprised of carbon, oxygen, and hydrogen, ΔH is the enthalpy change, and a, b, c and d are arbitrary coefficients. The negative enthalpy change indicates exploitable heat from the reaction.

In a CHP plant the heat from the reaction is exploited both directly and in a power producing process. Small scale CHPs are often based on a Rankine cycle (Savola & Fogelholm, 2007). The Rankine cycle is a heat engine design, which operates between a high-temperature heat source and a heat sink to convert heat to mechanical energy (Badr et al., 1991). A CHP exploits the heat the Rankine cycle produces to allow for conversion to mechanical energy. In other words, the Rankine cycle produces mechanical energy which requires a certain share of heat loss, and the CHP exploits both the mechanical energy and heat.

The resulting mechanical energy can then generate electricity by driving a generator. A generator exploits the electromagnetic nature of certain materials to induce an electric field from a magnetic field. Known as Faraday's law, it describes how "… a time-varying magnetic field would produce an electric current" (Sadiku, 2015, p.408).

A CHP works by exploiting the concepts described and continuously supplying fuel to produce heat and power, the steps involved are illustrated in Figure 2.9.

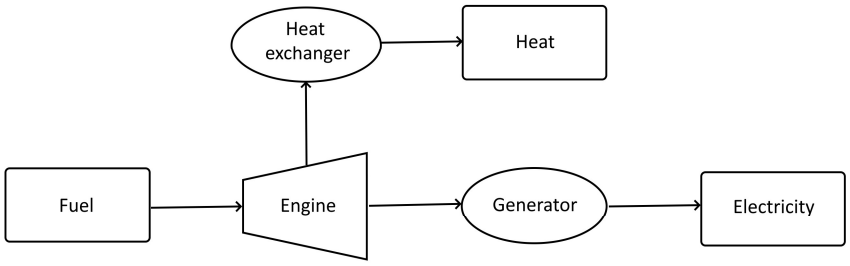

Figure 2.9 - Conceptual working scheme with most important concepts of a CHP

The Rankine cycle produces heat in excess, the heat from the process can be facilitated directly by using heat transferring appliances such as heat exchangers and water borne heating systems. The heat in excess is inevitable to drive the Rankine cycle. Ideally one would like to utilize all chemically potential energy in the fuel. Qiu et al. (2012), which the next paragraphs are based on, defines a thermal and electrical efficiency, and a total CHP efficiency, respectively as $\eta_h, \eta_{el}$and η_{CHP}. This is defined with a basis of the content of energy in the fuel and the biomass consumption for the Rankine cycle by the following:

$$Q_f = \dot{m} \cdot q_f \tag{34}$$

where Q_f is the potential heat, $\dot{m}$ is the fuel rate in kg/h and q_f is the energy content in Wh/kg. Using this, the efficiencies are defined as:

$$\eta_{el} = \frac{W_{el}}{Q_f}, \tag{35}$$

$$\eta_h = \frac{Q_{abs}}{Q_f} \tag{36}$$

and

$$\eta_{CHP} = \eta_{el} + \eta_{\mathrm{h}}. \tag{37}$$

W_{el} and Q_{abs} is the delivered electricity and absorbed heat. In the biomass micro-CHP experiment by Qiu et al. (2022) the η_{CHP} resulted in 78.8%.

Common fuels for bioenergy CHPs are either wood chips or pellets, larger more unprocessed wood scraps can be facilitated in larger biomass burning systems since system size, efficiency and fuel moisture are related (Holmberg, 2007). In this thesis only small-scale wood chip-based CHPs are considered, which demands fuel of specific quality.

2.6.3 CHP fuel and unit cost

With biomass fuel costing 62 $øre/kWh$ and the fuel having an energy content of 4.8 kWh/kg, the fuel has a price of 12.9 $øre/kg$ (Energioversikt [Energy overview], 2024). As the output of the CHP is a function of the mass of fuel the price per kg is the most suitable value to use. This fuel price assumes loading in the eastern area of Norway, and in real life some variations would be natural to assume.

2.6.4 CHP climatic impacts

The climatic impacts of biomass-based CHPs are a more complex subject than it is for PVs and ASHPs. The biomass fuel is part of the carbon cycle, which demands a discussion of biogenic and fossil carbon in addition to lifetime of greenhouse gases in the atmosphere and differences for biogenic and fossil carbon sources. The key issue of current climate change is the addition of fossil carbon into the atmosphere, while releases of biogenic carbon belonging to the carbon cycle would in the absence of fossil carbon emissions not alter the climate. While biomass such as trees, crop residue etc. should be viewed as biogenic carbon, it is not necessarily unproblematic to release it into the atmosphere. The sustained additions of fossil carbon will also be a part of the carbon cycle. In other words, the actual proportion of greenhouse gases in the atmosphere is what matters, not its source (Sterman et al., 2018). To be clear, if the atmosphere was not subjected to fossil emissions, the natural release of biogenic carbon would be unproblematic, and necessary for the carbon cycle. Partly due to this, it is possible to view greenhouse gases as having varied global warming potentials over time periods as the molecules will naturally decay, as mentioned in 2.3.2, or be sequestered into a non-impacting form. Many other factors, which falls outside the scope of this thesis, play into how this should be regarded; but if the CO2 content in the atmosphere continues to rise, the release of biogenic carbon might not be regarded as completely neutral and unproblematic. This discussion is central for how biogenic carbon emissions should be regarded in the LCA field, and any conclusive consensus is not established (Liu et al., 2017), (Van Fan et al., 2020). LCA results are central for the estimations in this thesis and makes CHP climatic impacts more complex than climatic impacts of PVs and ASHPs.

The established literature of LCAs on bioenergy small scale CHP seems to be scarce, especially sources which declares the emissions of each life cycle phase isolated.

For natural gas Meng & Dillingham (2018) reports that 0.5% of the relative contribution of greenhouse gas emissions can be attributed to construction and decommissioning of a 1 MW natural gas CHP plant. The relative contribution is however sensitive to the emissions of all the phases, and one would expect the relative contribution of the use-phase for a natural gas CHP to be much higher than for a biomass-based CHP, given the data in Table 2.1. This, with the lack of specifically small-scale CHP LCAs, complicates using LCA data for suitable emission estimations for small-scale biomass CHPs.

3 Method

3.1 External data sources

3.1.1 PVGIS

PVGIS is an interactive tool delivering solar energy related data. Developed by the European Commission's Joint Research Centre it is tool delivering up to date data. A detailed description of how it is created is done in Amillo et al. (2014). PVGIS 5.2 is based on the ERA-5 dataset produced by the European Centre for Medium-range Weather Forecast. In addition to this cloud interactions, theory of radiative transfer and aerosol content is included in the final estimations delivered to the user (European Commision, n.d.)

PVGIS allows for API connections and system output estimations of hourly resolution. With some fixed parameters such as using crystalline silicon PV panels, output per 1kWp installed and a loss percentage of 14, general local-specific PV outputs are retrieved by changing coordinates and optionally angles. Important to note is that for the use in this thesis clear-sky conditions are not an option, i.e. all data retrieved from PVGIS have weather conditions implemented, unless otherwise specified. In addition, horizon shadows can be retrieved from PVGIS and used, with a resolution of 3 arc-seconds which corresponds to a unique values for each 12^{th} second of the day.

With PVGIS delivering estimates based in up-to-date quality research and with API connectivity it suits the modelling method for this thesis perfectly.

Azimuthal directional parameters in PVGIS are between $-180°$ and $180°$, with $0°$ being south, and $-90°$ and $90°$ is east and west respectively. Others might use the range where north is $0°$ and $360°$, but for consistency PVGIS's range is used throughout the thesis.

3.1.2 Frost

Frost is an API service delivering historical observed weather and climate data from the Norwegian Meteorological Institute (MET). It delivers data based on requests from users.

In the MET database new stations are added and old ones removed. Stations record weather measurement at different intervals. For this thesis it is required that the air temperature measurements are recorded at least each hour and that measurements exist in the time period which is analysed. In addition to this it is needed to retrieve data from the closets weather station to the analysed location. To achieve this multiple steps are used to retrieve usable data.

First, all stations with, maximally hourly, air temperature measurements in the wanted time period is retrieved. Then, the closest station is determined by calculating the Euclidean distance between the weather stations and the location with the following formula:

$$Ed = \sqrt{(\lambda_{st} - \lambda_{loc})^2 + (\phi_{st} - \phi_{loc})^2} \quad (38)$$

Where λ_{st}, ϕ_{st}, λ_{loc} and ϕ_{loc} are the longitude and latitude of the station and the longitude and latitude of the location respectively.

The closest station is the station with the least Euclidean distance.

The air temperature measurement in the time period of the closest station is then retrieved. As all other data in this thesis is in hourly resolution the data that is in a format less than one measurement per hour needs to be transformed to represent the hourly temperatures. As measurement intervals are not standardized by MET a somewhat rough approach is used to achieve hourly resolutions. The number of measurements is divided by the number of wanted hours, that is, a number of measurements per hour. Now the wanted number of values (one value per hour) is retrieved from the measurement data with a spacing of the number of measurements per hour.

During testing of this method some shifting of results occur, if for instance one measurement is not recorded or any other malfunction occurs the data which is to represent the air temperature is not one-to-one with the temperature which did occur. This effect has significance over periods of multiple years. However, over a one-year period the data is not shifted so much that the temperatures will not represent a plausible value.

3.1.3 PROFet

PROFet is a tool developed by SINTEF from the work by Karen Byskov Lindberg to estimate energy needs for buildings given the local temperature. The estimates are based in measured data from a range of buildings. The background of the model is thoroughly described in Lindberg et al. (2019) and Andersen et al. (2021).

Using PROFet with an API connection involves setting the correct parameters and including a temperature file. The results are separated into the needs for space heating, direct hot water needs, and electricity needs based in building type and the temperature file. Only space

heating and direct hot water needs are affected by the temperature file. The temperature file used is retrieved from the Frost data.

3.1.4 Nord Pool electricity prices and energy fees

Nord Pool is power exchange which buyers and sellers of electricity in the Norwegian price zones uses. Prices changes per hour, which suits the aim of this thesis. To access historical power prices an Excel file of the power prices from 1st of January 2018 to 1st of January 2023 for all Norwegian price zones are downloaded from Forbrukerrådet ["Norwegian Consumer Council"] (Spotpriser, n.d.).

As the Nord Pool prices are listed with summer and winter times, in contrary to other sources in the thesis which uses UTC+1, it is important to insure that prices corresponds to other datasets. Summertime is practically UTC+2, and the price list skips the value for 0200 when switching to summertime, to convert the list to UTC+1 the value for timestamp 0100 is duplicated and set as the value for 0200. When the price list switches to wintertime the value at timestamp 0200 is duplicated, the duplicated value must then be deleted for the data to be in UTC+1. This is not too strenuous to do manually and insures compatibility.

To use the Norwegian power grid users must pay energy fees. Price models vary between regional grid leasers, but it is common to pay for the actual consumption. As described in Lindberg & Inderberg (2023), the price is mainly composed of volumetric fees and a moderate fixed charge. While not entirely correct the same energy fee model is applied for all areas. Differing between nightly and daily consumption is also common, and therefore the energy fee model used in this thesis is set to 0.20NOK/kWh in the daytime and 0.10NOK/kWh in the nighttime without any fixed fees, as they will not compose a majority of the cost.

3.2 Estimation methods

3.2.1 PV system estimations

To construct economic estimates for a certain square meter of housing, with 2 stories and rectangular gable roof, the steps presented below was used. All PV estimates are based in modelled values for 2015 from PVGIS.

A standard roof would extend beyond the outer walls of the house. PV systems are rarely installed so there is no extra area remaining on the roof, due to technical reasons. It is assumed that these two effects will counteract each other.

The PV estimations will only account for electrical needs of the house.

For a given location:

- The local temperature file is retrieved using FROST, and the corresponding hourly electrical needs are retrieved with PROFet for $1m^2$ of regularly efficient housing area.
- Wanted electricity prices are initialized and energy model applied in accordance with 3.1.4.
- Location specific hourly PV system output, $kWh_{out}(h, azi)$, is retrieved from PVGIS for a range of azimuth angles with increments of $15°$ degrees, covering all directions and a fixed slope angle set as the roof angle of $22°$.
- A set of system outputs for opposite configured roof instalments, $kWh_{out*}(h, \Theta)$, is constructed by adding half of the output facing in one azimuthal direction and half of the output facing the opposing direction, that is

$$kWh_{out*}(h, \Theta) = kWh_{out}(h, azi) + kWh_{out}(h, azi + 180°)$$

Where Θ is the set of configurations.

For a certain house size, the electrical needs are scaled by the size and all available kWp instalment sizes are used to produce a cost for covering electrical needs with an on-grid PV system:

- A value for the kWp available for installation on the roof is calculated with the formula:

$$kWp_{max} = \left[\frac{0.5 \cdot A}{cos(22°) \cdot \psi}\right] \quad (39)$$

  - Where A is the area, ψ is the area/kWp, and square brackets indicate rounding to nearest integer, with a roof angle of $22°$ the roof area will be

larger than the footprint of the house, and with the assumption of a 2-story house the area used for calculating roof area needs to be reduced to half.

For all available system sizes the following is calculated:

- The investment cost, $I(kWp)$ is calculated, see 4.2.1.
- Ranging from 1 to kWp_{max}, with increment 1, the hourly production, $P(kWp, h, \Theta)$ is determined by

$$P(kWp, h, \Theta) = kWp \cdot kWh_{out*}(h, \Theta). \quad (40)$$

- The yearly attributed cost is calculated as a function of the system size:

$$C_{year,PV}(kWp) = \frac{I(kWp)}{t_{life}}. \quad (41)$$

- For all configurations Θ:
  - The electrical needs are incrementally gone through to determine if the PV system production covers the electrical needs.
    - The deficit, i.e. the proportion the PV system does not provide for, is compensated for by buying electricity.
    - The surplus is sold to the grid.
  - The sum of bought electricity, sold electricity and the system specific yearly attributed cost is added together.
- The least costly azimuthal angle configuration is returned as the least costly alternative for the kWp system size.
- The least costly kWp system size option is returned as the least costly system for the fixed house size.

This method is then repeated over the wanted range of house sizes. Total cost of a specific house size is attributed to each square meter.

The alternative south-facing method is different as it only checks for southern facing modules. This method with the south facing system is configured for only one roof, i.e. the north facing roof does not have PV arrays. Effectively the method only checks different kWp sizes of a south-facing system for the house sizes and returns the best configuration for each house size.

3.2.2 ASHP estimations

To construct estimates for ASHPs the temperature dependent hourly COP is used to calculate the required power input to supply the needed heating in accordance with PROFet. To identify the performance of ASHP space heating for local-specific conditions the following algorithm is used.

For a given location:

- The local temperature file is retrieved using FROST, and the corresponding hourly space heating estimates are retrieved with PROFet for $1m^2$ of regularly efficient housing area.
- The temperature adjusted hourly COP in accordance with Li et al. (2024) and Ruhnau et al. (2019) is calculated, see 4.3.1.
- Location specific electricity price scenario and energy fee model is initialized.
- Relationship between price and maximum power output is initialized, see 4.3.1.

For all ASHPs in the price range of 15000 to 30000 NOK with increments of 2500 NOK:

- Yearly attributed cost is calculated in accordance with (5)
- The possible heating output as a function of the hourly COP is calculated for all hours of the year.
- For house sizes between $50m^2$ to $300m^2$ with increments of $10m^2$:
    - The hourly space heating demand is scaled with house size.
    - The space heating demands are incrementally gone through to determine if the ASHP covers space heating needs.
        - Deficits are covered by buying back-up electricity.
        - The cost of electricity required to deliver the ASHPs heat output is calculated.
    - The total cost, i.e. the sum of cost of required electricity and yearly attributed cost is calculated.
    - The total cost is attributed to each square meter of the certain house size.
    - The share of uncovered heating is calculated by dividing the delivered space heating energy from the ASHP with the size dependent space heating needs.

All combinations of ASHP size and house sizes are returned. For clarity's sake, the ASHP only covers space heating demands.

3.2.3 CHP estimations

For this thesis the data for the specific CHP module Walter from the Volter company is used. As concrete technical data was hard to acquire and attempted correspondence with other producers and suppliers were unanswered, Volter supplied necessary technical data and prices for the estimations. The module is restricted to a maximum production of $50kW$ and $130kW$ electricity and heat respectively (Volter, 2023). Additional relevant data includes $47kg/h$ fuel consumption at full power level and maximum annual run time of $7800h$ (Volter, personal communication, October, 31 2023).

Volter declares a maximum operational time of the Walter module to 7800 hours a year. A concrete maintenance schedule was provided after inquiring with the company, adding up all the required service and downtime in accordance with the schedule resulted in a number higher than 7800. Volter answers that they take into account unforeseen events which requires downtime of the module in an email-correspondence.

As the producer reports that some randomness should be included in the dimensioning of the module randomness is included in the estimation by picking random numbers between 0 and 1 and checking if they are larger than a set probability of the module being operational, and if the number is larger than the set probability 5 service/downtime hours is assumed. To ensure a plausible scenario of up uptime, each instance of downtime is set to 5 hours, with 5 following hours guaranteed uptime. Due to this the initial probability of $7800/8760$ is too low to be used as a threshold. To compensate a threshold of $7800/8760 + 0.08$ is used. Testing this procedure 100 times produce an average produced uptime of 7735 hours.

Estimations for CHP are limited to only one certain module and no relationship between investment cost and system size can be established. Economically optimal configurations based in house size cannot be identified as it can for the PV and ASHP estimations. An optimal building size for the specific module at the location analysed can be determined.

As the system size of the Walter CHP module is relatively much larger than the PV and ASHP systems, certain other assumptions must be used. For instance, suitable housing sizes. The total sizes used for estimations for CHPs will be larger, and it could be imagined that the

module supplies a neighbourhood of houses, or a very large building such as storage facility or office building.

Additionally, a CHP can act as a complete energy need supplier of space heating, direct hot water and electricity needs, and is estimated in this thesis as a provider of all needs.

For all CHP estimations 2022 electricity is used for hourly pricing of back-up heating.

The CHP algorithm is as follows, for a given location:

- A random uptime schedule is generated.
- The local temperature file is retrieved using FROST, and the corresponding hourly electrical, space heating and DHW needs are retrieved with PROFet for $1m^2$ of regularly efficient housing area.
- Space heating and DHW needs are added to one total heating need.
- Location specific electricity price scenario and energy fee model is initialized.
- The yearly attributed cost of the module is calculated in accordance with (5)

For all analysed house sizes:

- The hourly demands are scaled with the house size.
- For all hourly needs over the year it is checked if the CHP covers the need in accordance with maximum supply of heat and electricity and downtime schedule.
    - If the module cannot supply for a need the needs are covered with electricity from the grid
    - The fuel cost of supplying the needs is calculated, see 4.4.1.
- The total cost of electricity, fuel and yearly attributed cost is attributed to the house size.
- The share of uncovered heating and electricity needs are respectively calculated by dividing the delivered energy of the CHP by the size dependent building needs.

For the two CHP modules configuration additional steps include:

- Independent generated uptime schedules are assigned to each module.

- For each hour of the year, it is checked whether both modules, only one or no module is running, and total possible supply capped accordingly.

To determine the degree of covered needs the share of delivered energy is divided by the total energy demand of the specific configuration.

3.3 Model flowchart

The steps used to create estimates are illustrated. Frost, PVGIS and PROFet are API compatible, which allows for all data retrieval and handling to be done in Python. As the flowchart shows PV estimates are the only energy technology specific retrieved data, estimates for heat pumps and central heating appliances are based in the results from PROFet in conjunction with scientific literature and other technology specific retrieved data.

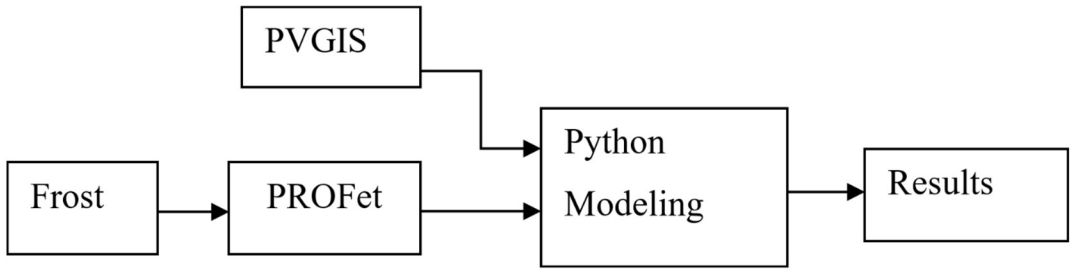

Figure 3.1 - Model flowchart visualizing processes included in modelling

Figure 3.1 shows the model flowchart described.

3.4 Main cases

All estimations are based in building type house of regular efficiency from PROFet and assuming no additional cost of the system other than the investment and potential fuel.

The performance of the technologies is judged indirectly on how a configuration is able to meet the specific building needs compared to a base case electricity only scenario. This is reflected in the total cost and degree of coverage of needs. Both the potential in production and the building needs are a function of local-specific conditions, and performance is measure of a how well a technology meets a building's needs and the cost of meeting them.

Five main cases are used, chosen because they are the biggest cities within their price zone. Norway has 5 different power price zones: NO1, NO2, NO3, NO4 and NO5. The price varies

from zone to zone and price-dynamics are unique for each zone. The cause of this is a large and highly debated topic, and main the focus of this thesis is the results the price-dynamics induce.

NO1 is the price zones for the south-eastern region of Norway, including Oslo, NO2 is the southernmost region, including Stavanger, NO3 is the middle of Norway, including Trondheim, NO4 is the northernmost region, including Tromsø and NO5 is the western region, including Bergen.

The climate of each region is also interesting features, whilst the NO1 region being very large it is the region with largest variation in daily sunlight duration and generally a cold region. The western regions will naturally have more cloud coverage.

Hellström et al. (2012) lists that price volatility is tied together with capacity constraints of the power market, and price jumps are often caused by temperature shocks and production breakdowns. This indicates that temperature is an important variable when analysing performance of grid-connected energy technologies. The capacity of the power grid is dependent on the network of transmission lines, which are shown in Figure 3.2.

Figure 3.2 - Transmission lines in the Nordic countries, from (Svenska Kraftnät, 2023, September 29)

Figure 3.2 shows that there are more transmission lines in the southern part of Norway, and only one main line cover parts of Northern Norway. Additionally, there are transmission lines from Southern Norway to Denmark, Netherlands, Germany and Great Britian. Power production, and demand within regions are also central to what the resulting capacity constraints are.

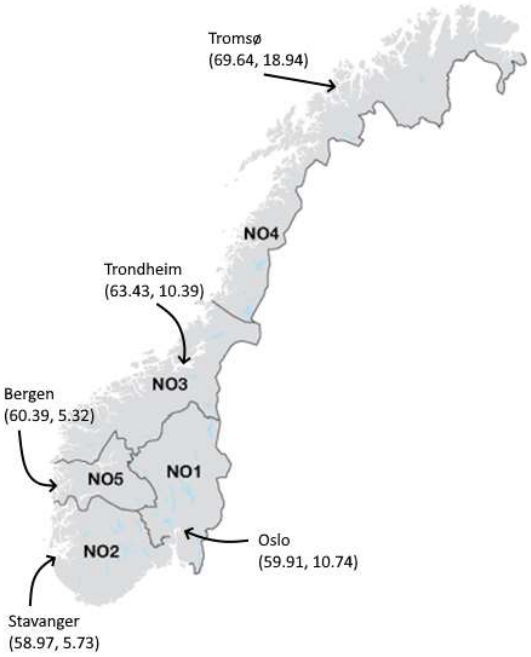

Figure 3.3 - Overview of Norwegian price zones with main cases marked, adapted from (Statnett, 2022, October 3)

As Figure 3.3 shows the area of price zones varies a lot, and in reference to Figure 3.2, the majority of 275kV transmission lines are between NO1, NO5 and NO2.

In addition to the main cases, Karasjok (69.68, 25.51) is used as an example for extreme temperature conditions in estimates concerning heating. As it is an example of a very cold location. The ocean west of Tromsø (69.811, 17.169), Storfroa (66.463, 11.951) and Slettingen (57.962, 7.494) are used for some supplementary cases for preliminary PV results.

4 Results and discussion

4.1 Preliminary results

4.1.1 Solar conditions

Naturally solar conditions will vary based on geography. In Figure 4.1, the global tilted irradiance (GTI) for an optimally sloped angle is presented for the main case cities.

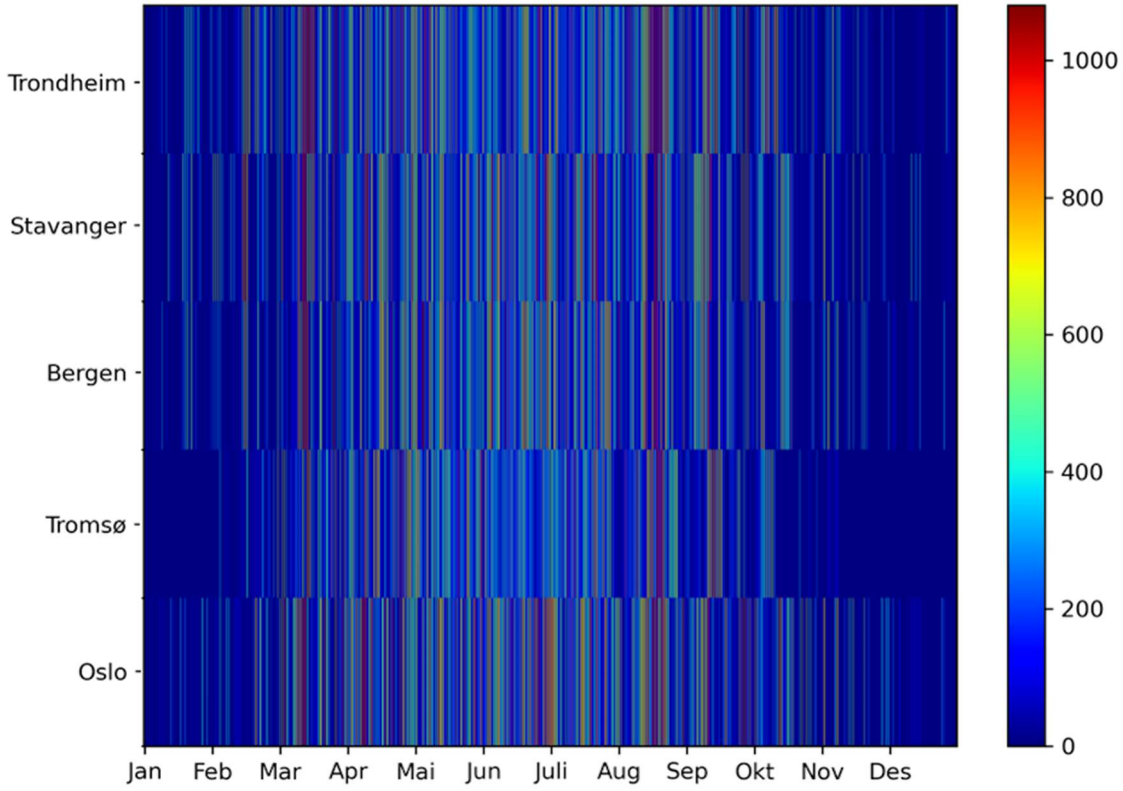

Figure 4.1 – GTI from 2015 on optimally directed sloped plane of main case cities in W/m2

The most noticeable difference in Figure 4.1 is that Tromsø have periods of no irradiance, this is because only Tromsø have polar nights, where the sun is below the horizon from November 27th to January 15th. Another noticeable difference is the degree of even spread of irradiance for the regions, Oslo and Stavanger have more even coverage than Bergen and Trondheim, especially in the beginning and the end of the year. Most likely due to Oslo and Stavanger being located south of Bergen and Trondheim.

The total GTI over 2015 for the locations is given in Table 4.1.

Table 4.1 - Total GTI of main case cities based in 2015

Location	**Total GTI** [$\boldsymbol{kWh/m^2}$]
Oslo (59.91, 10.74)	1160
Tromsø (69.64, 18.94)	867
Bergen (60.39, 5.32)	892
Stavanger (58.97, 5.73)	990
Trondheim (63.43, 10.39)	1050

Oslo receives the most global irradiance with $1160 kWh/m^2$ and Tromsø receives 75% of that. Trondheim receives second most, despite being further north than Bergen and Stavanger, which might be a consequence of the weather conditions being less beneficial.

4.1.2 Slope and azimuth relations

Slope and azimuth angles are important when dimensioning PV arrays. Depending on location different configurations will receive varying amount of irradiance. Figure 4.2 shows how slope and azimuth angle are codependent.

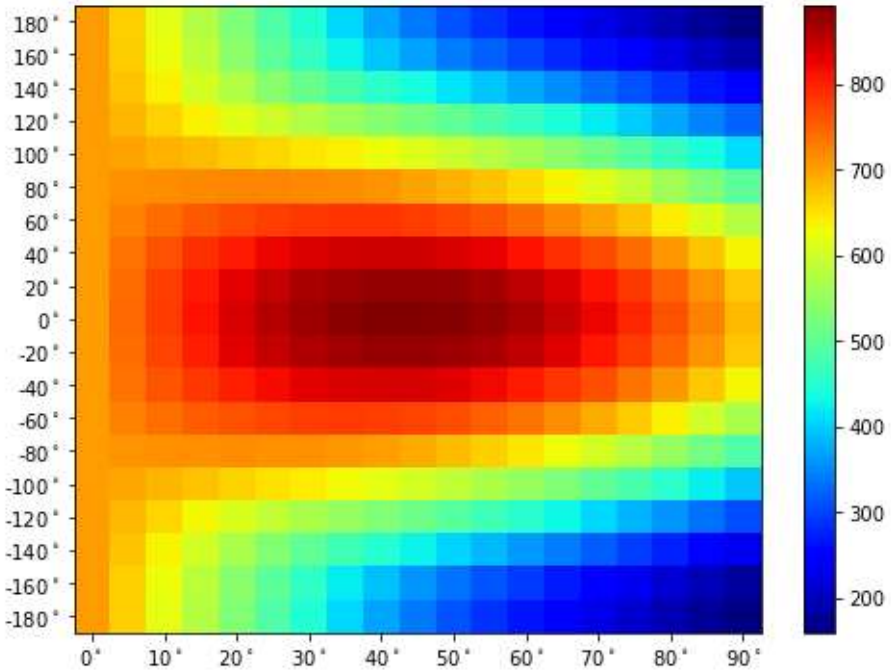

Figure 4.2 - Total yearly production of different azimuth and slope relations in Oslo for 1kWp [kWh/kWp]

Figure 4.2 illustrates the dependency between azimuth angles and slope angles and highlights the configurations which produce the most energy over a year. The highest total production values are centred around angles facing south; 0° azimuth. The slope angles have less severe effects in the south facing range, while its impact is noticeable in other directions. For example, for arrays facing North the slope angle has a severe impact in total energy production.

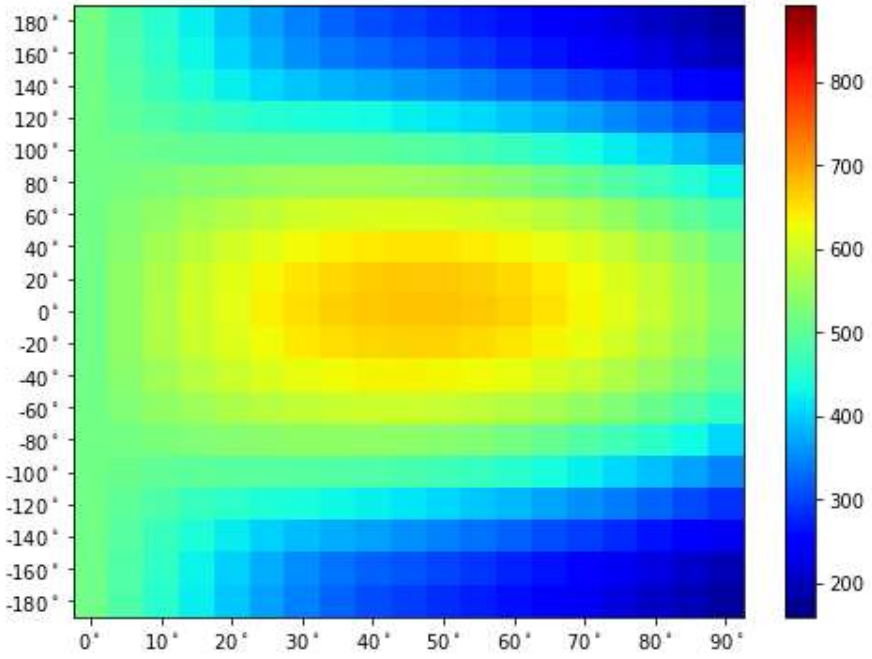

Figure 4.3 - Total yearly production of different azimuth and slope relations in Tromsø for 1kWp [kWh/kWp]

Comparing Figure 4.2 and Figure 4.3 shows that Tromsø have less potential production across configurations. The trend between azimuth and slope angles is however the same between Tromsø and Trondheim.

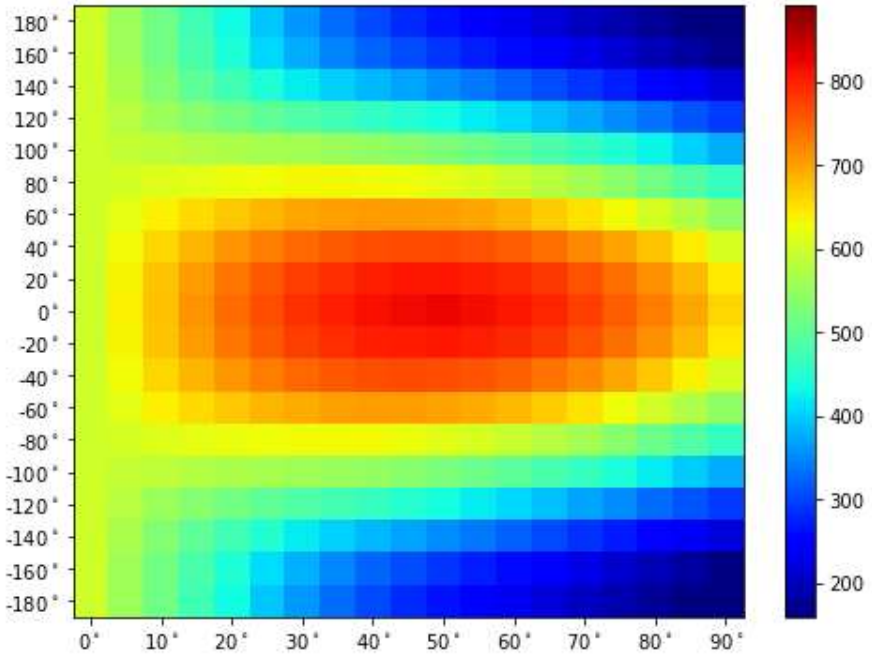

Figure 4.4 - Total yearly production of different azimuth and slope relations in Trondheim for 1kWp [kWh/kWp]

Comparing Figure 4.3 and Figure 4.4 shows that Trondheim has generally higher production than Tromsø, while the trend between slope and azimuth angles are the same. In other words,

the change alternatively configured PV systems have for yearly production potential is not unique to locations. Similar figures for Bergen and Stavanger are reported in Appendix A.

Differently configured solar arrays will have their peak production at various times of day. This concept is what is indented to be exploited to configure a solar array system to be as economical as possible. For instance, to configure solar arrays in an east west split instead of directly south. Figure 4.5 shows how 1kWp arrays facing south and two 0.5kWp arrays facing respectively east and west at summer solstice have different production patterns depending on their location.

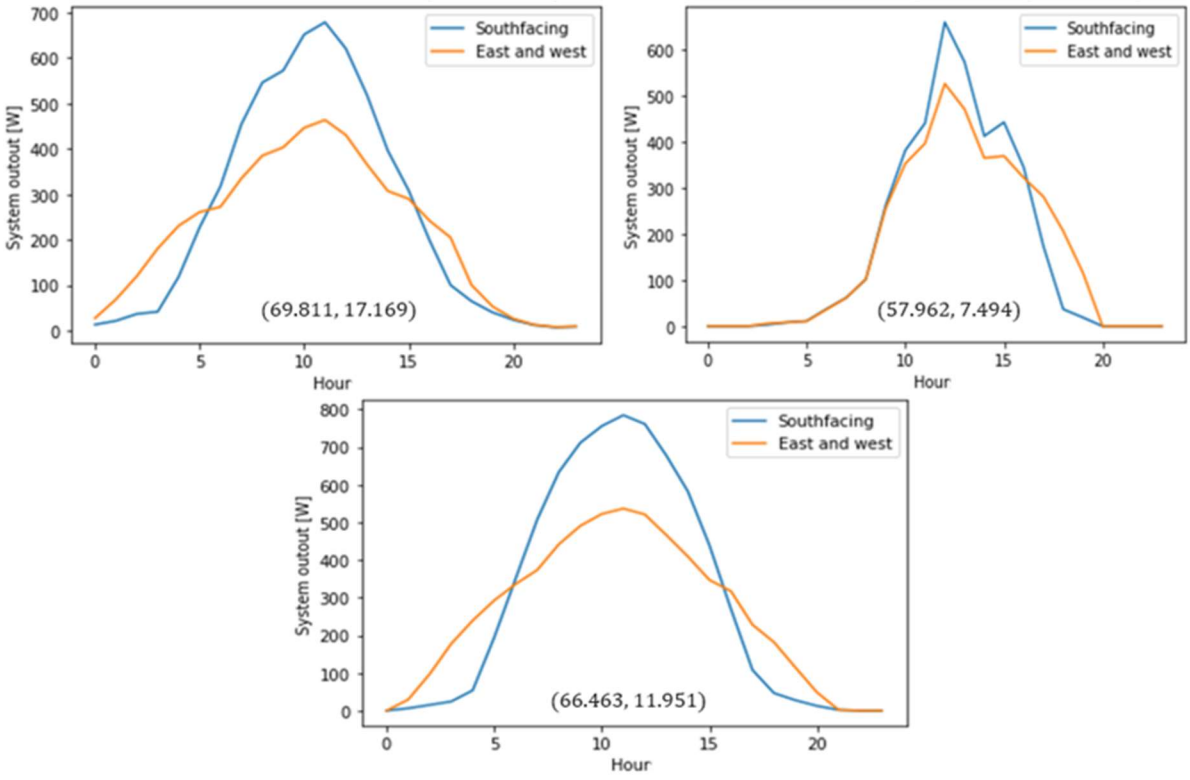

Figure 4.5 - 1kWp south facing and 0.5/0.5kWp east-west facing module outputs at summer solstice for 3 different locations

The locations used in Figure 4.5 were chosen to try to find locations unaffected by clouds at summer solstice. The second figure in Figure 4.5 might however be subjected to some clouds during the day. The degree of reduced total production and elongated production potential for east-west facing arrays varies between the locations. To illustrate, a threshold is set at 100W for useful production. Table 4.2 shows the reduction of total production and elongated production period for the locations.

Table 4.2 - Energy production and production periods of south facing and east-west facing modules

Coordinates	South [Wh]	East-west [Wh]	Differe-ce	South period	East-west period	Elongated period
69.811, 17.169	5982	5284	12.3%	14 hours	17 hours	3 hours
57.962, 7.494	3967	3884	2.0%	10 hours	12 hours	2 hours
66.463, 11.951	6964	6137	11.4%	13 hours	17 hours	4 hours

The elongated periods and reductions of total energy production does not follow some obvious pattern, especially considering that these metrics will vary for each day of the year. As opposed to the yearly production potential, these results point to that there are differences between locations in extending production periods over the day.

4.1.3 Electricity prices

The electricity prices for each price zone in 2022 is plotted in Figure 4.6

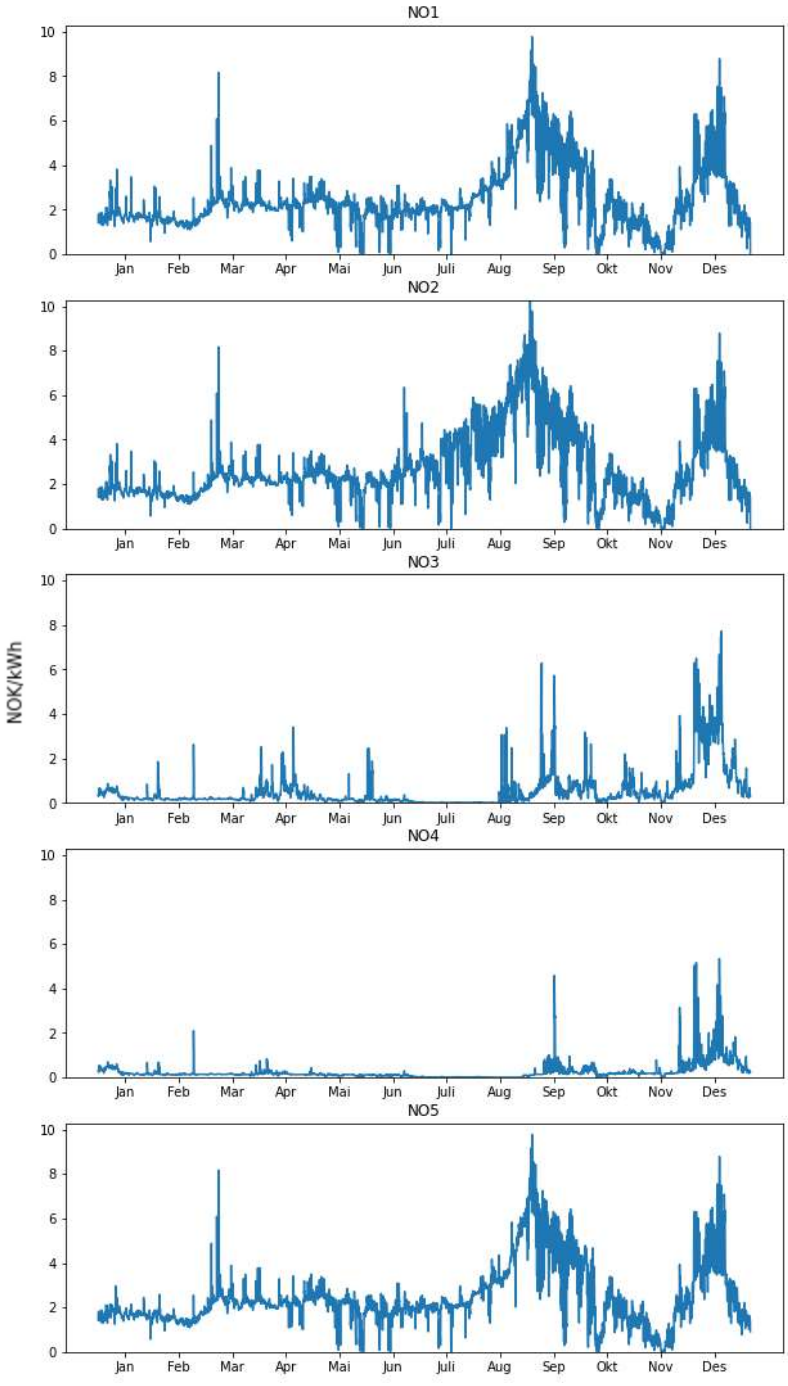

Figure 4.6 - Electricity prices in Norwegian price zones 2022

Figure 4.6 shows clearly how varied the prices are over seasons and compared to each other. All zones have dramatic spikes in the fall, with NO1, NO2 and NO5 reaching especially high prices. December is also an especially expensive month, probably corresponding to the temperature drop, in accordance with Hellström et al. (2012). Zones NO1 and NO4 is in high contrast to each other.

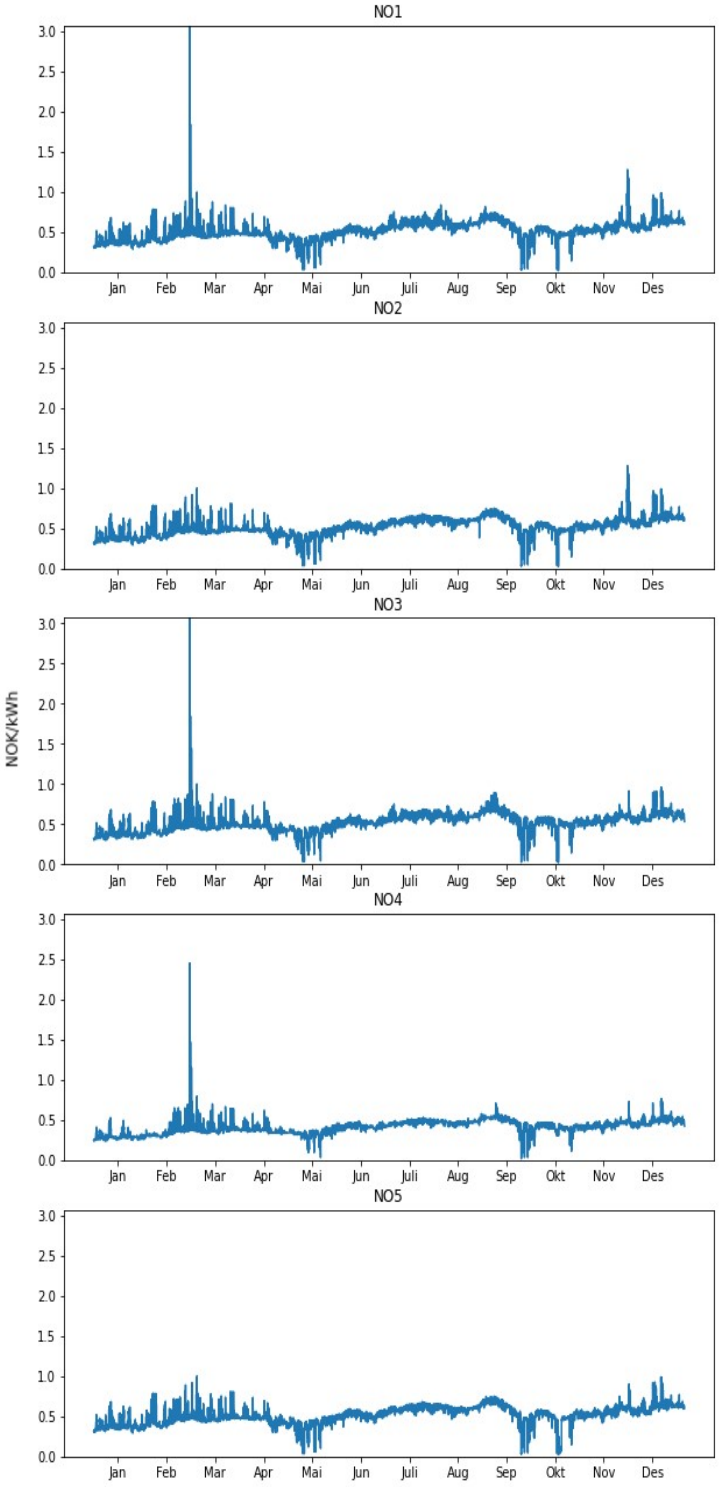

Figure 4.7 - Electricity prices for Norwegian price zones 2018

Figure 4.7 show that common for all regions is the rise of prices in December, similarly to the 2022 scenario in Figure 4.6. The most drastic spikes generally occur during cold periods.

Compared to 2022 prices the 2018 prices are quite similar between prices zones, with some irregularities between them. Again, the most drastic irregularity occurs during a cold period. Important to note is that the y-axis is formatted differently between Figure 4.6 and Figure 4.7, with the same scales the variations within 2018 would barely be visible.

In addition to clear variations over the year there are variations throughout the day. Figure 4.8 displays the electricity price for the ten days throughout the year which has the highest difference between lowest and highest cost during the day, showcasing the volatility.

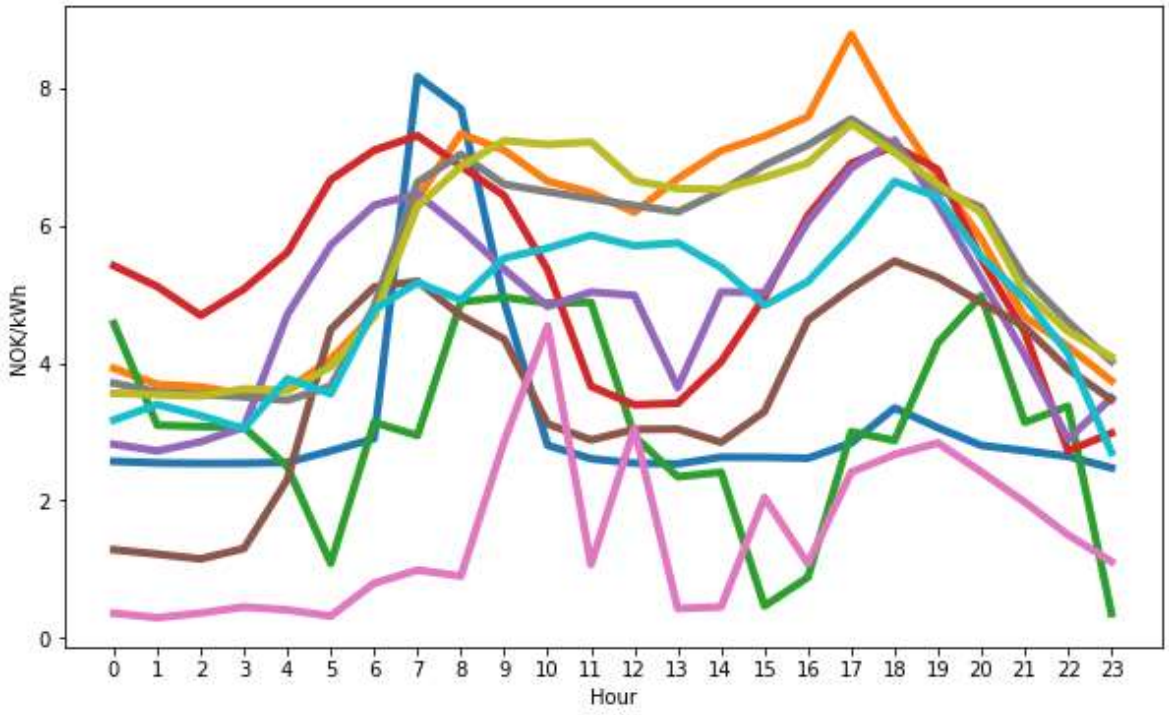

Figure 4.8 – Daily prices for the 10 days with biggest daily difference between maximum and minimum price over the day for NO1 in 2022

The periods throughout the day that varies the most is in the morning and the afternoon. Many days shows a clear rise in price in the morning and decline in the evening. For some of the days the high price is sustained over the day-time, while some have dips around noon.

As NO1 shows strong volatility over 2022 it is a natural comparison to find the ten most volatile days in NO4, as it is a more stable price zone over 2022.

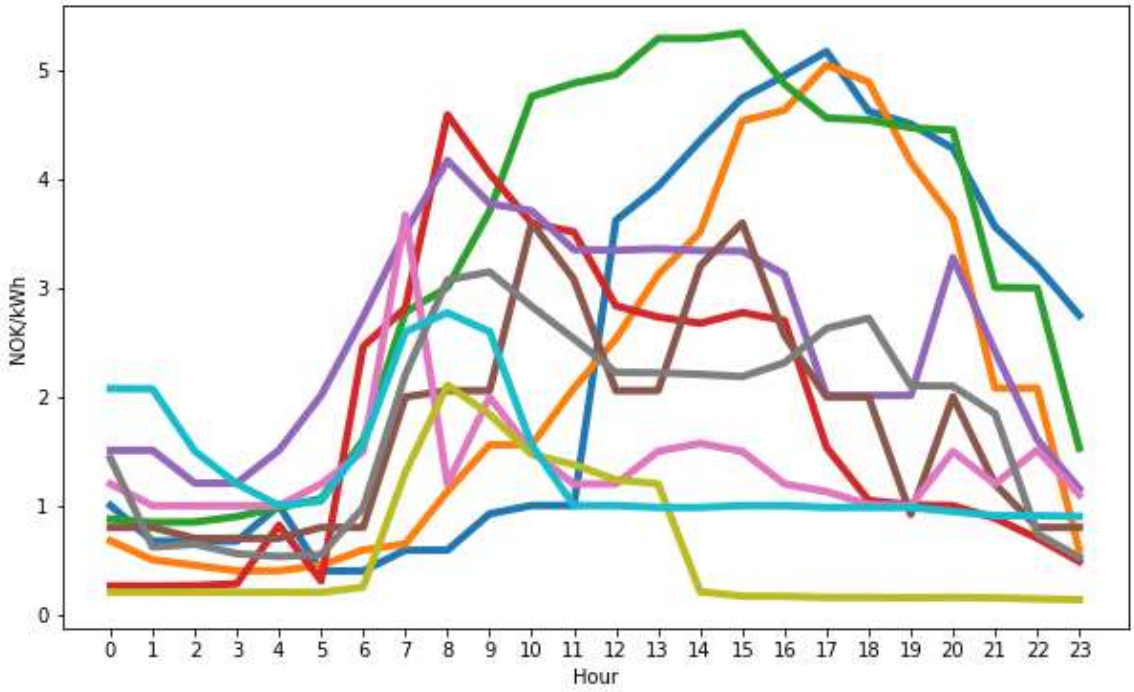

Figure 4.9 - Daily prices for the 10 days with biggest daily difference between maximum and minimum price over the day for NO4 in 2022

Peaks in Figure 4.9 occur either at morning or at the evening, with some having the same two-peak pattern as in Figure 4.8. None of the days shown in Figure 4.9 or Figure 4.8 have their daily peak price at noon. This differs from what Hartner et al. (2015) reported for German and Austrian conditions. This indicates that alternative configurations of PV systems could be more cost saving as higher production can match higher prices better.

For ASHPs and CHP there is no equivalent direct way which involves alternatively configuring the system to match prices. However, one could deliberately not cover space heating needs, to then later compensate for the temperature drop when the hourly prices are better, and in accordance with better hourly COPs for ASHPs. This is not covered in the thesis, but illustrates how PV and, ASHPs and CHPs are fundamentally different.

4.1.4 Electricity use exclusively

The costs of using only grid electricity to cover electrical needs, space heating and DHW are estimated by using actual electricity prices and PROFet building need estimates. To isolate the dynamics between electricity prices, 2022 temperatures are used for all electricity price scenarios.

Table 4.3 - Cost of covering 1m^2 of electrical needs, space heating and DHW with electricity exclusively for main cases based in 2018 prices in NOK

	Electrical needs	Space heating	Direct hot water	Total
Oslo	27.62	79.80	13.92	121.34
Tromsø	23.36	89.42	11.74	124.52
Bergen	27.3	74.08	13.74	115.12
Stavanger	27.42	74.26	13.8	115.48
Trondheim	27.84	95.02	14.02	136.88

With 2018 prices the costs are very similar between the locations. Space heating costs are naturally larger in Tromsø and Trondheim where it is colder. Space heating costs account for the majority of the total cost for all locations.

Table 4.4 - Cost of covering 1m2 of electrical needs, space heating and DHW with electricity exclusively for main cases based in 2022 prices in NOK

	Electrical needs	Space heating	Direct hot water	Total
Oslo	104.68	277.14	52.99	434.81
Tromsø	17.58	73.08	8.52	99.18
Bergen	104.42	270.33	52.83	427.59
Stavanger	113.00	276.95	57.88	447.83
Trondheim	29.70	123.38	14.40	167.48

Compared to 2018, costs between locations vary a lot. The southernmost regions have significantly higher prices than the northern ones. Tromsø has a lower total cost, while Trondheim has moderately higher cost.

Table 4.5 - Cost of covering 1m2 of electrical needs, space heating and DHW with electricity exclusively for main cases based in 0.40NOK/kWh fixed price in NOK

	Electrical needs	Space heating	Direct hot water	Total
Oslo	22.49	61.17	11.18	94.84
Tromsø	22.49	87.18	11.18	120.85
Bergen	22.49	59.83	11.18	93.51
Stavanger	22.49	59.08	11.18	92.75
Trondheim	22.49	79.60	11.18	113.27

From Table 4.5 it is clear that electrical needs and DHW only are functions of the square meters for houses. Based in 2022 weather Table 4.5 also shows how the temperature differences for the locations are reflected in higher space heating costs in a fixed price scenario.

Generally, this shows that for the electricity price scenarios used the temperature difference between locations are much less significant than the prices.

4.1.5 Building efficiencies

Key elements within building efficiencies and insulation properties are described in 2.2. Using PROFet to retrieve space heating demands for a cool day these differences and the consequential heat loss is clearly illustrated.

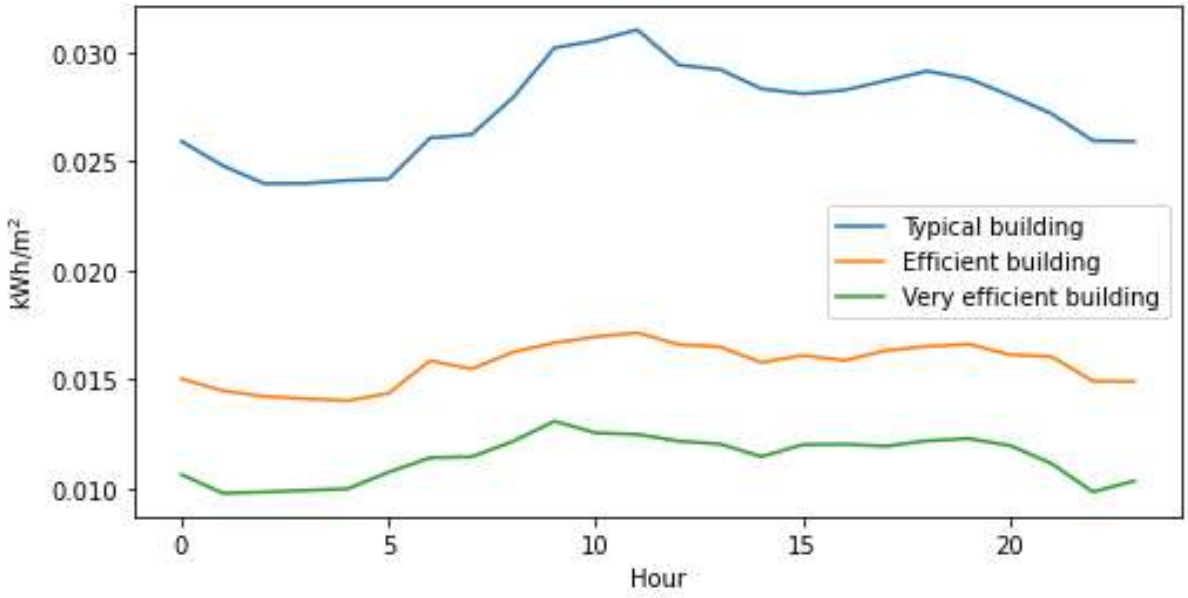

Figure 4.10 - Space heating demand for different efficiencies of 1st of January 2022 in Tromsø

Figure 4.10 shows that a building of the typical building stock loses up to triple the amount of heat then a building classified as very efficient.

Better insulation is a passive energy reducing measure unlike the energy technology implementations presented in this thesis. Whether or not investing in better insulation instead of an energy technology is more cost saving could be determined using the methodology used in this thesis if quality estimates of the varying square meter building price was retrieved. Comparing active and passive options or combinations of them could produce insightful results.

For the rest of the thesis only efficient housing is considered.

4.1.6 Load duration and coverage

At some point an incremental system size increase might not provide for a more economic configuration as the incremental addition of system size might be less useful and not cost saving anymore. In 3.2.1 and 3.2.2 and it is explained that all the available system sizes for all house sizes are estimated, and resultingly checking if configurations with the described dynamic occurs. As handling of CHPs are different, the same dynamic would occur when the building needs are larger than what the CHP will normally provide.

One could configure a system were 80% of heating should be provided by a ASHP and the rest by electricity. Figure 4.11 shows the load-duration curve of a house in the Tromsø area, and at which loads 80% of the heating demand over the year will be accounted for.

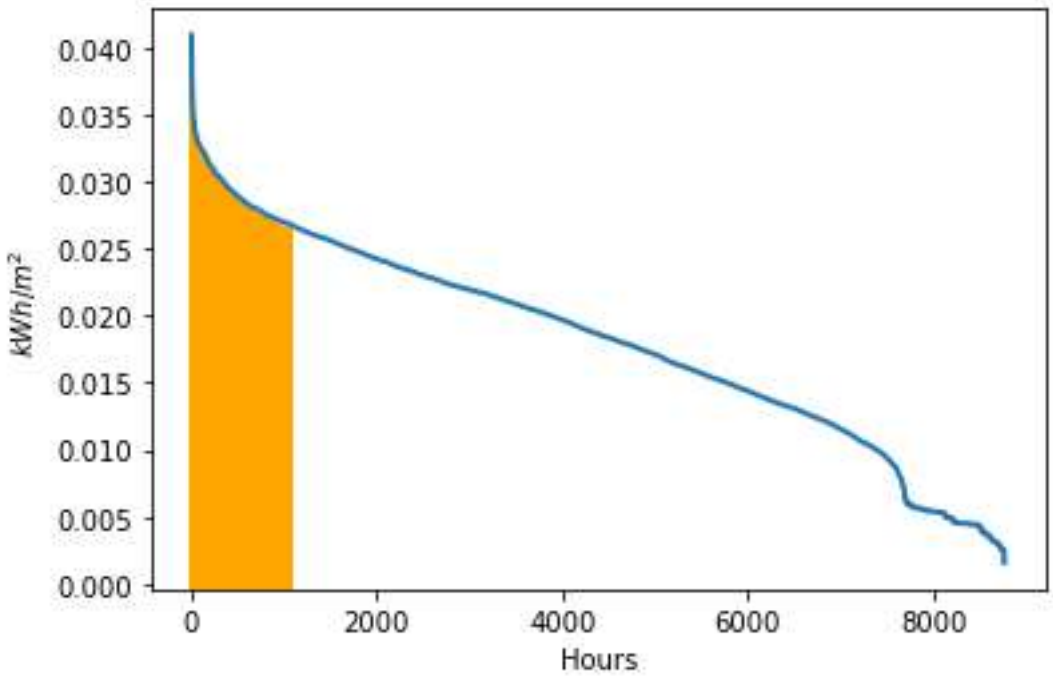

Figure 4.11 - Load duration curve for 1m² housing area based in Tromsø with 2022 weather.

Figure 4.11 shows that there is no need to provide heating for more than around $0.025\frac{kWh}{m^2}$ since 80% of the energy demand is covered beneath that. As the highest load is upwards to $0.040\frac{kWh}{m^2}$, but for a limited amount of hours, the additional investment required of a ASHP to deliver this might be too expensive relative to how much the ASHP is used at full capacity. The same example could be applied to a CHP investment.

Now it is interesting to mark which hours throughout the year the uncovered loads occur at. Figure 4.12 shows an example from Tromsø of which hours are the ones that is not needed to dimension for as they are within the last 20% percentile of heating demands.

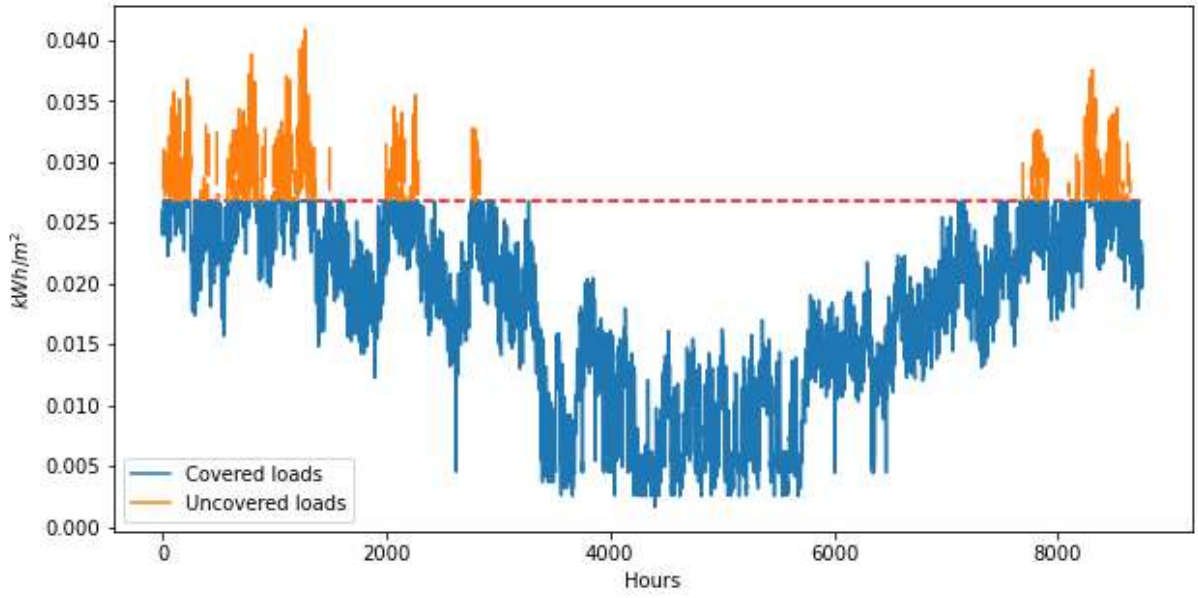

Figure 4.12 - Uncovered heating loads highlighted at the hours where they occur based in Tromsø with 2022 weather

Figure 4.12 shows loads that are uncovered occurs in the winter. Note that the limit at which the ASHP in the example can deliver at will also deliver at its maximum capacity when electricity must be used as back-up heating.

4.2 Photovolatic systems

4.2.1 PV system investment cost

With logarithmic regression on the investment costs per kWp listed in 2.4.5 the resulting cost per additional kWp, $\hat{I}_{kWp}(x_i)$, is

$$\hat{I}_{kWp}(x_i) = -2468 \log x + 16126. \tag{42}$$

with $\hat{I}_{kWp}(x_i)$ as the estimated investment cost in NOK/kWp for the concrete kWp size x_i. The total investment cost is the cumulated sum of all $\hat{I}_{kWp}(x_i)$ from 1kWp to the maximum size.

$$\hat{I}_{PV} = \sum_{i=1}^{kW\ max} \hat{I}_{kWp}(x_i)\,. \tag{43}$$

The advantage of using logarithmic regression is that it is natural that one would pay less per kWp installed when investing in a larger system, but this effect would not continue endlessly, the logarithmic regression limits the continuous reduction of kWp price.

The cost is attributed to each year of lifetime, which for PV systems are, unless otherwise specified, 12 years.

4.2.2 PV system configurations

The estimations do not show any reliable dependency on house size for which direction returns the economically optimal configuration, the configurations are therefore reported on their own.

Table 4.6 – Economically optimal PV system configurations of different pricing scenarios for the main cases

	Oslo	Tromsø	Bergen	Stavanger	Trondheim
2022 prices	$-90°, 90°$	$-100°, 75°$	$-90°, 90°$	$-90°, 90°$	$-100°, 75°$
2018 prices	$-90°, 90°$	$-90°, 90°$	$-90°, 90°$	$-90°, 90°$	$-90°, 90°$
Fixed price	$-90°, 90°$	$-90°, 90°$[1]	$-90°, 90°$	$-90°, 90°$	$-90°, 90°$

$-90°, 90°$ corresponds to an east-west configuration and is often the best configuration. Tromsø and Trondheim deviates from this when using 2022 prices. The reported configuration is the result which best aligns with the lowest cost combination of a buildings electrical need and the local-specific solar conditions. An analysis of why this differs between scenarios and locations are beyond the scope of the thesis but might be a consequence of the individual price zone dynamics. For clarity's sake it should be noted that all scenarios are based in a 2022 weather scenario.

All system sizes available are checked for all house sizes and no results indicate that dimensioning PV systems smaller than the maximal possible size is useful.

For a clear depiction of the potential for selling electricity is with the configurations the total revenue from selling all electricity produced to the grid is calculated.

[1] Smallest house sizes return the same configuration as in 2022 as economically optimal before it settles at $(-90°, 90°)$. Likely a consequence of the system size being in only integers.

Table 4.7 – Yearly revenue from selling all electricity produced by 1kWp PV system with slope angle 22° for 2022, 2018 and fixed electricity prices oriented south or east-west [NOK/kWp]

	Oslo	Tromsø	Bergen	Stavanger	Trondheim
2022 South	2128	88	1622	2111	276
2022 East-west	1713	63	1390	1788	202
2018 South	463	269	343	397	416
2018 East-west	378	222	297	335	330
Fixed South	338	246	257	296	300
Fixed East-west	276	204	222	248	238

For 2022 and 2018, the revenue is naturally highest when the electricity price is highest. Neither 2022, 2018 or the fixed price scenario stand out as especially different from each other when switching from south and east-west for any of the locations. Generally, the potential is lower per kWp. The revenue from a 2kWp system oriented east-west is significantly higher than for 1kWp south facing system.

4.2.3 PV systems in 2022 electricity price scenario

PV system results are presented as the total cost of covering all electrical needs with an on-grid PV system with the yearly attributed cost of the investment. First, the economically optimized results, in accordance with 3.2.1, are shown.

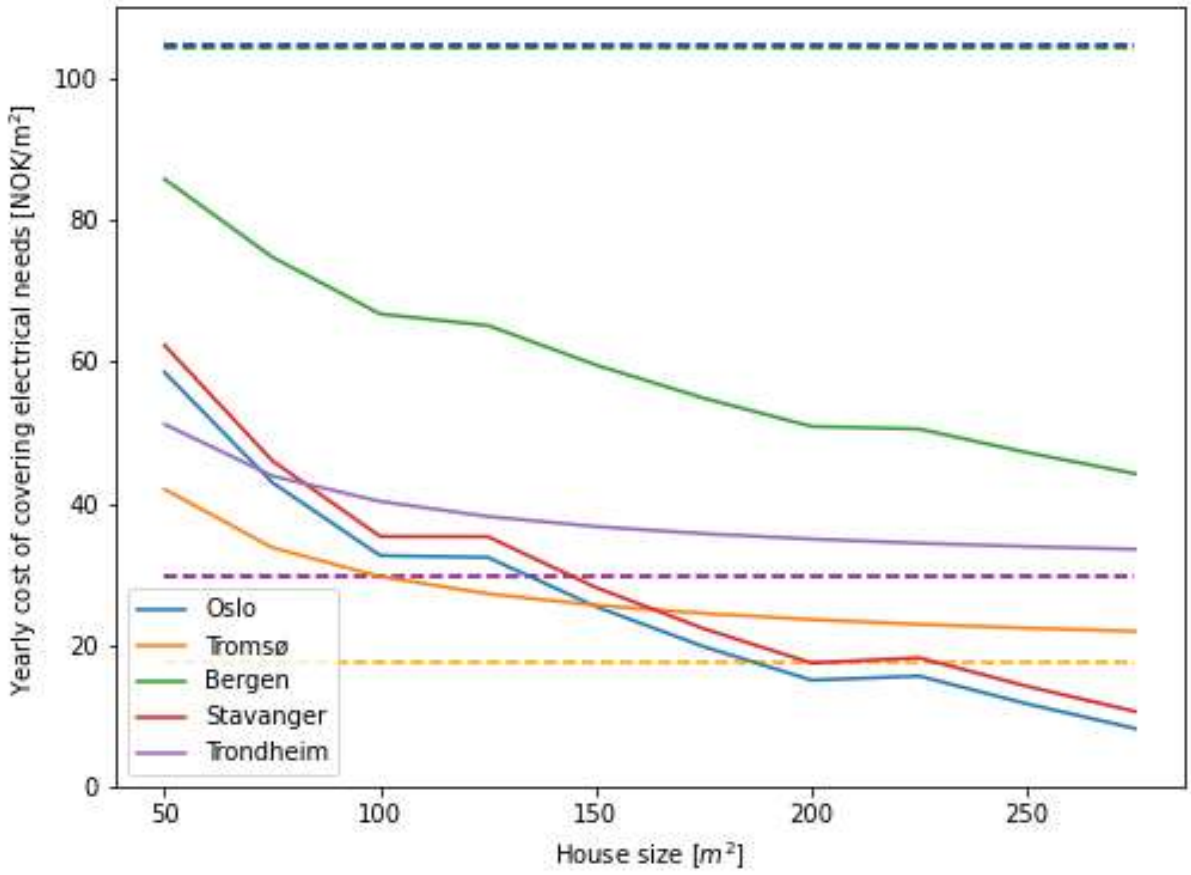

Figure 4.13 - Cost of covering electrical needs with economically optimized PV system implementation in NOK/m2 based in 2022 electricity prices, with grid electricity prices from Table 4.4 as dashed lines

Figure 4.13 illustrates how the dynamic of how costs change with house size are different between locations. The cost dynamic of Trondheim and Tromsø are similar, with steadily decreasing lines, as opposed to the other locations where changes are more abrupt. This is because of Tromsø and Trondheim being in more stable and lower priced price zones.

Table 4.8 - Cost of covering electrical needs with economically optimized PV system implementation in NOK/m2 based in 2022 electricity prices

	$50m^2$	$100m^2$	$150m^2$	$200m^2$	$250m^2$
Oslo	58.47	32.64	25.45	15.08	11.74
Tromsø	42.01	29.68	25.64	23.63	22.42
Bergen	85.71	66.7	59.51	50.85	47.17
Stavanger	62.29	35.34	28.15	17.5	14.22
Trondheim	51.17	40.28	36.74	34.98	33.92

In comparison to Table 4.4 the PV system implementations are only better than using electricity from the grid for the southernmost regions, which had the most volatile and highest electricity prices. Since the cost steadily decreases for Trondheim and Tromsø, PV system implementations could be cheaper than using electricity from the grid exclusively for larger house sizes. As shown in Table 4.1 Bergen has the second lowest global irradiance, and in combination with volatile and high electricity prices the resulting costs are bigger than for Tromsø and Trondheim.

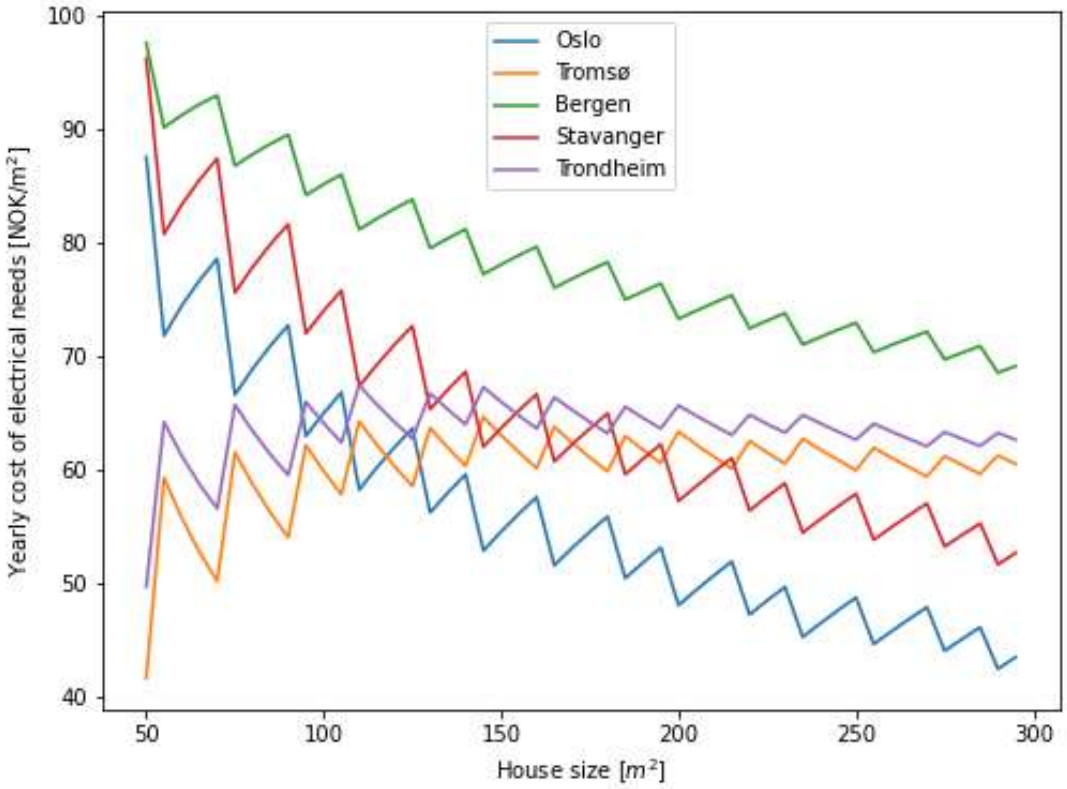

Figure 4.14 - Cost of covering electrical needs with south facing PV system implementation in NOK/m2 based in 2022 electricity prices

Figure 4.14 shows different dynamics for the south facing PV system. The jagged lines are a result of the method for south facing systems checking for more house sizes than the economically optimizing method, while system size only is in integers. Trondheim and Tromsø have the same cost for $50m^2$ in the economically optimized and south facing scenarios. In the south facing scenario costs increase as opposed to decreasing.

Table 4.9 - Cost of covering electrical needs with south facing PV system implementation in NOK/m2 based in 2022 electricity prices

	$50m^2$	$100m^2$	$150m^2$	$200m^2$	$250m^2$
Oslo	87.52	64.95	54.5	48.02	48.69
Tromsø	41.56	59.84	63.01	63.32	59.92
Bergen	97.59	85.14	78.06	73.26	72.93
Stavanger	96.23	73.97	63.63	57.2	57.84
Trondheim	49.62	64.06	65.95	65.64	62.61

Compared to using electricity from the grid, the conclusion is still the same for the locations. However, the economic performance is overall worse. Despite a larger investment cost for economically optimized systems, based in 2022 electricity prices it is a much better economical option than south facing only.

4.2.4 PV systems in 2018 electricity price scenario

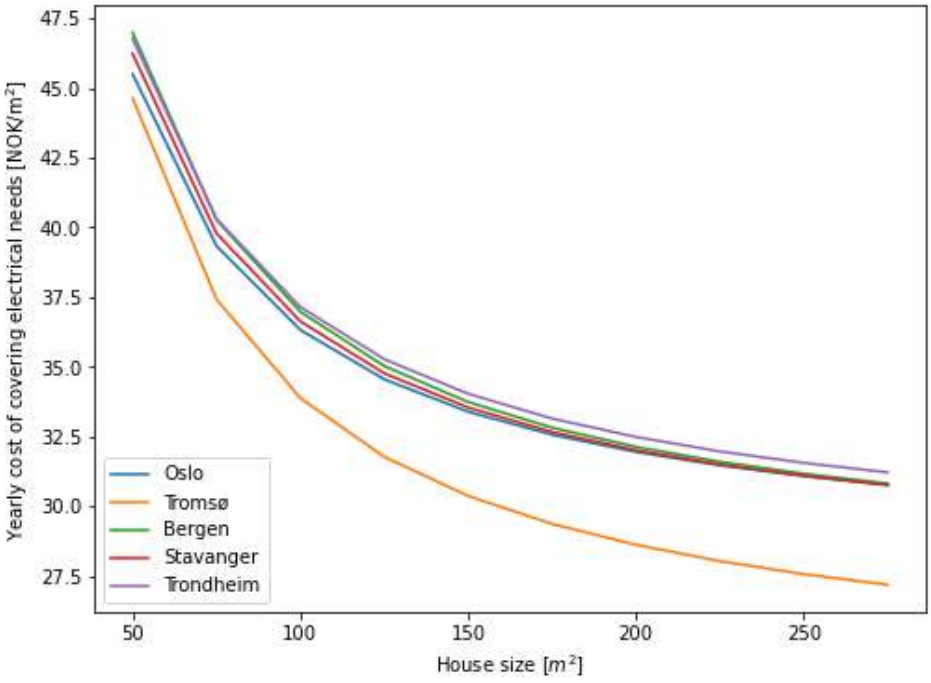

Figure 4.15 - Cost of covering electrical needs with economically optimized PV system implementation in NOK/m2 based in 2018 electricity prices

Figure 4.15 shows that there is no difference in change dynamics between locations. All have steadily decreasing costs per square meter as the investment cost per additional kWp

decreases. 2018 was unsuited to generate revenue from selling electricity for the locations with largest production potential. In reference to Table 4.3, the cost per square meter for Tromsø is 84.5% of that of Oslo. At $100m^2$ the total cost in Tromsø is 91.0% of that in Oslo. This indicates that the initial differences between cost of covering electrical needs in Table 4.3 is persevered in Figure 4.15.

Table 4.10 - Cost of covering electrical needs with economically optimized PV system implementation in NOK/m2 based in 2018 electricity prices

	$50m^2$	$100m^2$	$150m^2$	$200m^2$	$250m^2$
Oslo	45.50	36.33	33.4	31.96	31.09
Tromsø	44.63	33.88	30.38	28.63	27.57
Bergen	46.99	36.98	33.74	32.14	31.17
Stavanger	46.23	36.64	33.55	32.02	31.10
Trondheim	46.76	37.15	34.04	32.49	31.56

Table 4.10 shows that none of the locations provide for a cheaper total cost of covering electrical needs compared to electricity of the grid in the range of house sizes analysed. This indicates that in a cheap electricity price scenario the investment cost has a big impact.

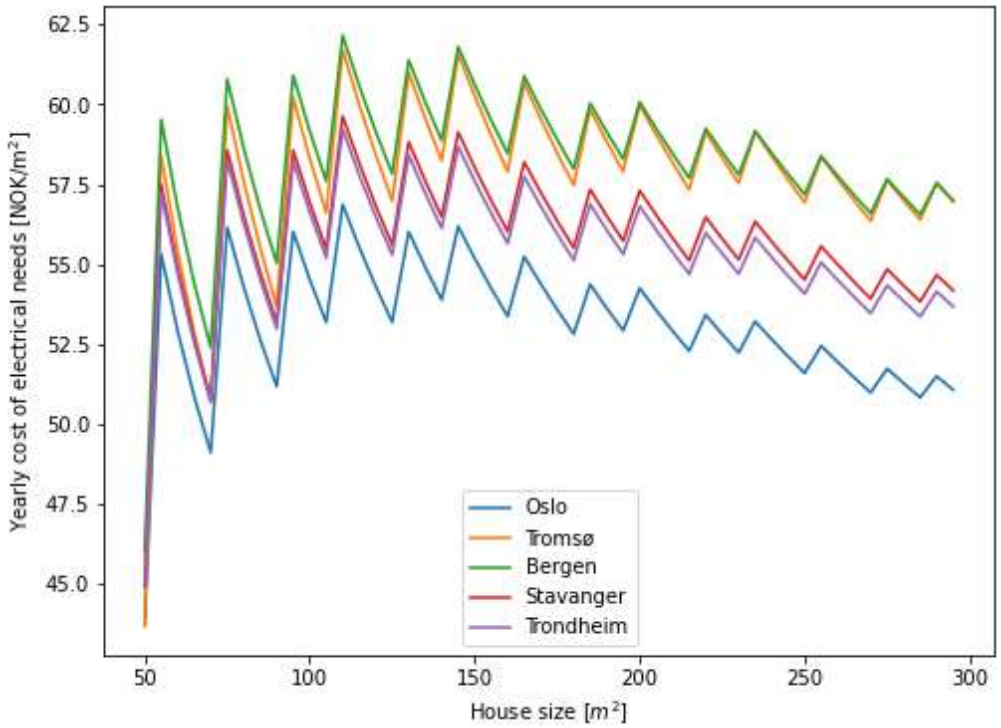

Figure 4.16 - Cost of covering electrical needs with south facing PV system implementation in NOK/m2 based in 2018 electricity prices

Figure 4.16 shows that for a south facing system in 2018, Tromsø is one of the lesser performers, and that the least costly location corresponds with highest global irradiance, see Table 4.1.

Table 4.11 - Cost of covering electrical needs with south facing PV system implementation in NOK/m2 based in 2018 electricity prices

	$50m^2$	$100m^2$	$150m^2$	$200m^2$	$250m^2$
Oslo	43.78	54.53	55.19	54.25	51.6
Tromsø	43.69	58.32	60.26	59.97	56.93
Bergen	46.05	59.17	60.61	60.07	57.18
Stavanger	44.94	56.94	58.02	57.3	54.52
Trondheim	44.98	56.63	57.6	56.82	54.07

All locations show worse economic performance than for an only south facing system. With Tromsø having the biggest relative change. Electricity demand and investment cost are only functions of the square meters, and the south configuration might not have the potential to

produce any considerable profits from selling surplus electricity. This results in the primary factors for costs being bought electricity and the attributed investment cost.

4.2.5 PV systems in fixed price scenario

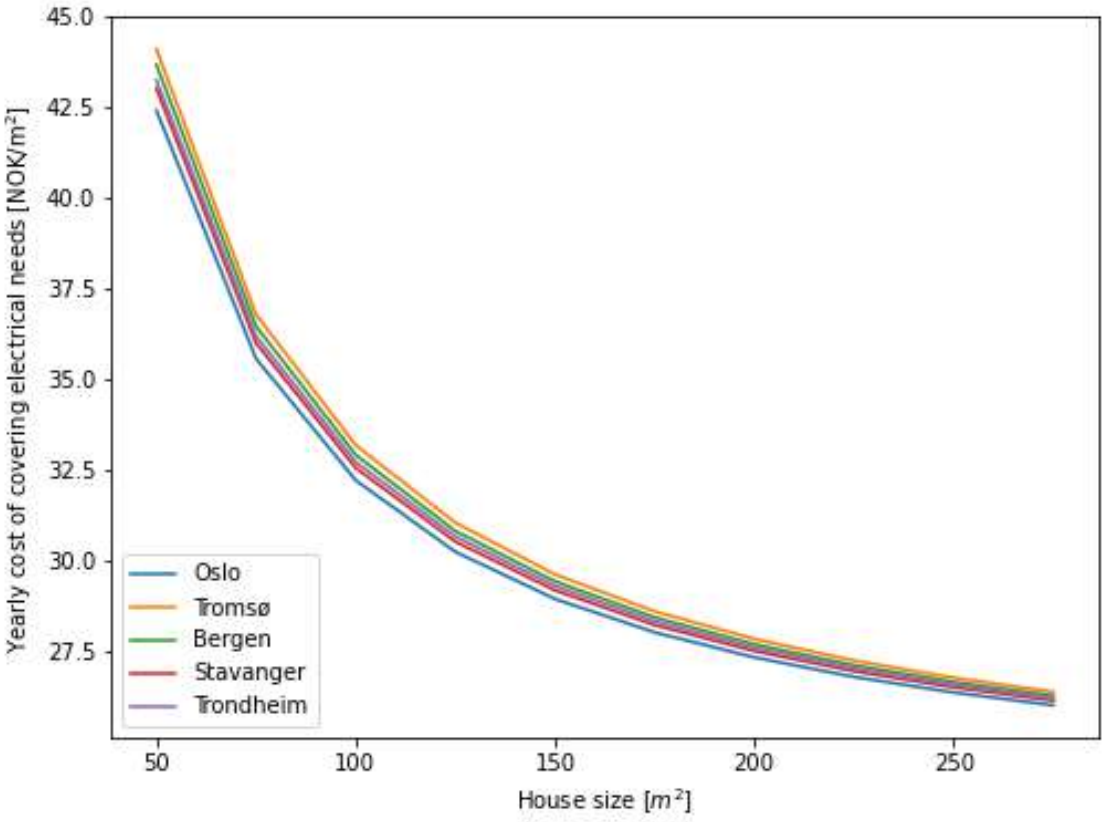

Figure 4.17 - Cost of covering electrical needs with economically optimized PV system implementation in NOK/m2 based in 0.40NOK/kWh fixed price

Figure 4.17 follows the same dynamic as Figure 4.15, but the least costly locations are ordered after their global irradiance. The arguments proposed in 4.2.4 apply for these results as well.

None of the systems are able to produce more energy in total than what is required to cover the electrical needs over the year. As the expected lifetime is low, a large part of the total costs is the yearly attributed investment cost. With this configuration and lifetime, differences are barely visible. The investment cost of 17 kWp PV system for a $150m^2$ house is 191451 NOK, attributed to a 12-year lifetime results in 15954 NOK/year. The potential yearly revenue in accordance with Table 4.7 ranges between 4692 – 3468 NOK/year. The cost of covering electrical needs is, in accordance with Table 4.5, 3373 NOK/year. Resulting in a difference in the range of 1318 – 94 NOK/year, which is miniscule in comparison to the yearly attributed cost. A higher lifetime will yield bigger differences between locations.

Neglecting any additional costs from electrical needs as they are constant between locations, the difference between locations is maximally around 9.8%.

Results for the south facing system does not differ much from Table 4.11 and the south facing results are similar to Figure 4.16 and does not provide any additional information, but are reported in Appendix B.

4.2.6 Sensitivity analysis – PV lifetime

As the assumed lifetime for PV systems in this thesis is low, it is reasonable to check what a higher lifetime, closer to what manufacturers might declare, would yield. As the economically optimized 2022 scenario is the scenario with lowest cost for some of the locations it is an interesting basis for the analysis.

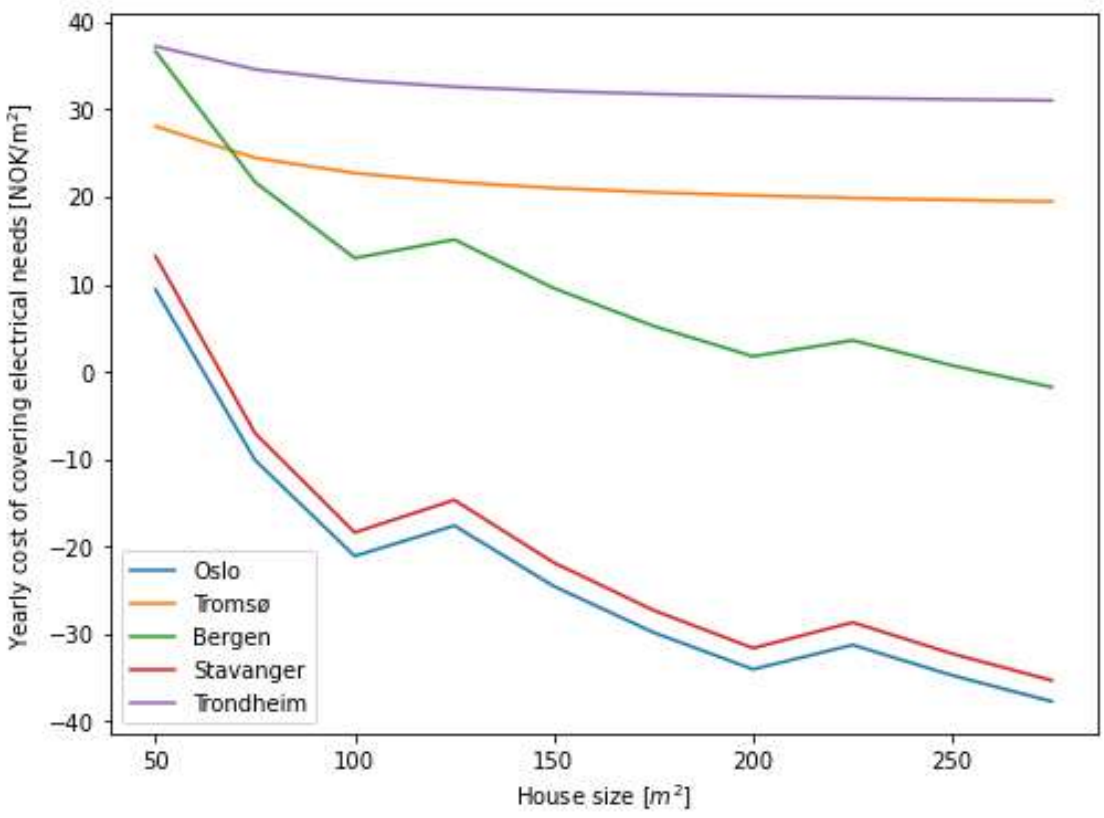

Figure 4.18 - Cost of covering electrical needs with economically optimized PV system implementation in NOK/m2 based in 2022 electricity prices with 25 year lifetime

Figure 4.18 shows that an extended lifetime is very impactful for Bergen, and as opposed to in Figure 4.13 Bergen is cheaper than Tromsø and Trondheim. The impact in Trondheim and Tromsø is moderate, but the revenue potential is low, as shown in Table 4.7. Oslo and Stavanger capitalize very well and generates profits.

To investigate whether the electricity price scenario or the lifetime is the most impactful it is interesting to see how impactful extended lifetime is for the results in Figure 4.17.

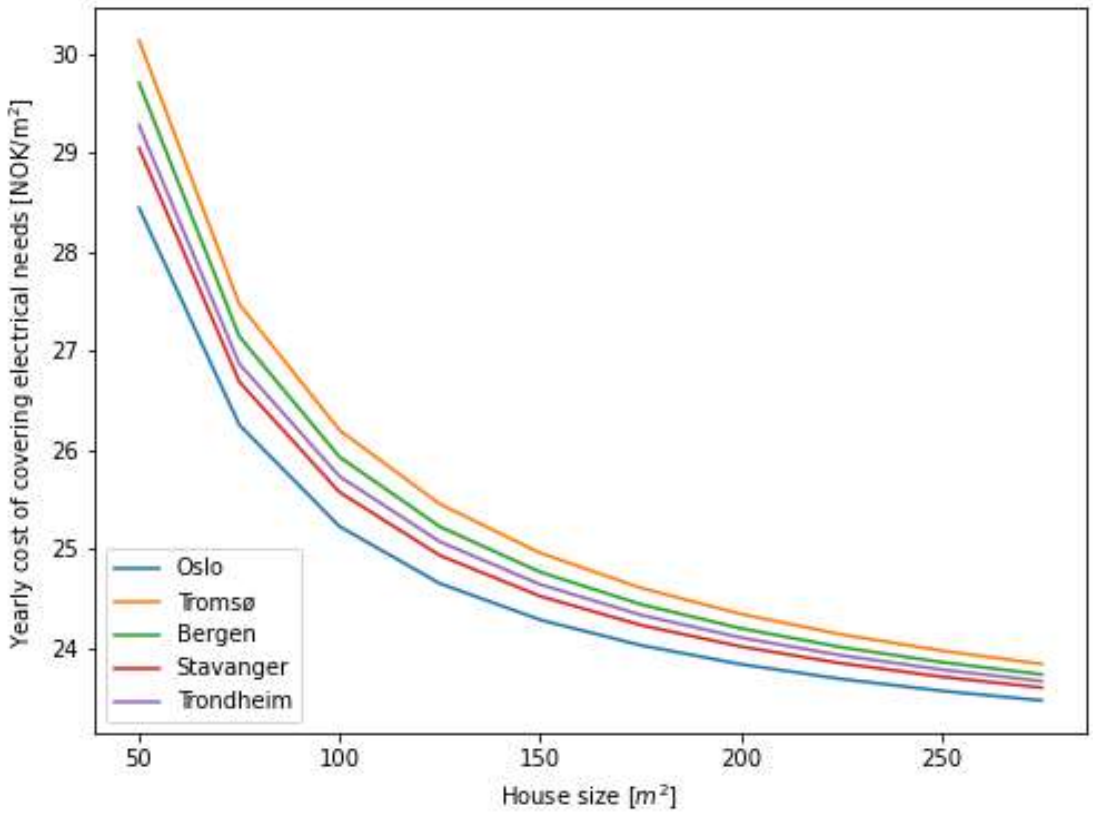

Figure 4.19 - Cost of covering electrical needs with economically optimized PV system implementation in NOK/m2 based in 0.40NOK/kWh fixed price with 25 year lifetime

While differences between locations are larger, as discussed in 4.2.5, the relative change is small compared to extending lifetimes for the 2022 scenario. Showing that electricity prices are very impactful for PV system implementation.

4.2.7 LCOE estimations

LCOE estimates will be reported for the standard parameter economically optimized 2022 configuration, as it contains alternative azimuthal configuration, and a south facing scenario. This is motivated by checking if a LCOE estimate, as they are constructed in this thesis, will give any insights between standard and alternative configurations.

Table 4.12 – LCOE in NOK/kWh for main cases and different house sizes with economically optimized configuration

	50 m^2	75 m^2	100 m^2	125 m^2	150 m^2	175 m^2	200 m^2	225 m^2	250 m^2	275 m^2
Oslo	1.66	1.55	1.47	1.43	1.38	1.33	1.29	1.27	1.23	1.21
Tromsø	2.24	2.09	1.99	1.93	1.86	1.79	1.74	1.71	1.67	1.63
Bergen	2.07	1.93	1.83	1.78	1.71	1.65	1.60	1.57	1.53	1.50
Stavanger	1.84	1.72	1.63	1.59	1.53	1.47	1.43	1.40	1.37	1.34
Trondheim	1.92	1.80	1.71	1.66	1.59	1.54	1.49	1.47	1.43	1.40

Table 4.12 shows LCOE estimations deviate somewhat from the pattern shown in total global irradiance from Table 4.1 with Stavanger and Trondheim changing place. Trondheim the only case where the economic optimal configuration deviates from east-west configuration, and the reduction in energy production increases the LCOE. Naturally the LCOE is decreasing for larger sizes as the investment cost of the system is cheaper per kWp.

Table 4.13 – LCOE in NOK/kWh for main cases and different house sizes for south facing configuration

	50 m^2	75 m^2	100 m^2	125 m^2	150 m^2	175 m^2	200 m^2	225 m^2	250 m^2	275 m^2
Oslo	1.36	1.27	1.20	1.17	1.12	1.09	1.05	1.03	1.01	0.98
Tromsø	1.86	1.74	1.65	1.60	1.54	1.49	1.45	1.42	1.38	1.35
Bergen	1.78	1.66	1.58	1.53	1.47	1.42	1.38	1.36	1.32	1.29
Stavanger	1.55	1.45	1.37	1.33	1.28	1.24	1.20	1.18	1.15	1.12
Trondheim	1.53	1.43	1.35	1.32	1.27	1.22	1.19	1.16	1.14	1.11

Table 4.13 shows that the LCOEs of the south facing PV system are lower than for the economically optimized one performing one. Also, Trondheim has the lowest cost in terms of

LCOE. LCOE is strictly a measure of lifetime cost and lifetime energy output, and the smaller installations in combination with south facing configuration minimizes this measure, but as previously shown it is not the most economical solution. This shows that the larger systems with alternative configurations benefit from the income potential they have compared to the systems with the lowest LCOE. In other words, a clear indication that being mindful of price dynamics and local-specific conditions is very important when configuring PV systems. The PV system size difference relative to electricity needs as a function of house size is also highly influential for the results. But, as shown the optimal configurations of this is almost always east-west, and installing a south and north facing PV system is not competitive with the other configurations, with the parameters set in this thesis.

Comparing these results to Zainali et al. (2023) where the LCOE of similar PV cases was reported to be 0.85 to 1.15 SEK/kWh, which per 16th of May 2024 is 0.85 to 1.15 NOK/kWh, the LCOE results in this thesis are generally higher. However, minimizing LCOE does not produce the economically optimal PV configuration, as discussed above. Finaly, note that Zainali et al. (2023) uses a more precise LCOE formula, accounting for more variables, and assumes higher lifetimes. Regardless of this, the estimates shown in this section falls reasonably close to Zainali et al. (2023).

4.2.8 PV panels climatic impact

Since the reported emissions discussed in 2.4.6 vary greatly it is suitable to declare a lower and upper estimate of total emissions. The lower limit for CO2e emissions is set to 1500 kg/kWp and the higher limit to 2500 kg/kWp.

As the emission factor only depends on the local-specific PV production, lifetimes and total emissions, the emission factors are simply calculated by dividing the total emission with the total energy produced over the lifetime.

Table 4.14 - Emission factor in kgCO2e/kWh for PV panels with configurations 12-, 20- and 30-year lifetime facing south or east-west based in Oslo

	South		**East-west**	
	1500 kg/kWp	2500 kg/kWp	1500 kg/kWp	2500 kg/kWp
12 years	0.1478	0.2464	0.1811	0.3018
20 years	0.0887	0.1478	0.1086	0.1811
30 years	0.0591	0.0985	0.0724	0.1207

Table 4.14 shows that the variations in emission factors are quite large, but none are as low as for Norwegian electricity. In reference to the established GWPs for PV from Table 2.1 the results in Table 4.14 do not reach the lowest value but exceeds the highest value. From Table 2.1 the results from Laleman et al. (2011) and Alam & Xu (2022) are the most applicable as comparisons and some of the 20 and 30 year lifetime results corresponds to their results.

The south facing configuration has the lowest emission factors as it produces the most energy, which is attributed to the total emissions.

Table 4.15 - Emission factor in kgCO2e/kWh for PV panels with configurations 12-, 20- and 30-year lifetime facing south or east-west based in Tromsø

	South		**East-west**	
	1500 kg/kWp	2500 kg/kWp	1500 kg/kWp	2500 kg/kWp
12 years	0.2029	0.3381	0.2443	0.4072
20 years	0.1217	0.2029	0.1466	0.2443
30 years	0.0811	0.1352	0.0977	0.1629

Table 4.15 shows that as the total energy production in Tromsø is lower the emission factors are larger. Only results with a 30-year lifetime falls within the range reported in Laleman et al. (2011) and Alam & Xu (2022).

Emission factors for the other main cases does not show any new insights which is not already discussed throughout 4.2 but are reported in Appendix C.

4.2.9 PV systems evaluation

Assumptions used includes no degradation of the PV systems, no change of inverter, no yearly changes in weather conditions, no maintenance costs, and no local-specific transportation costs. Implementation of these aspects would probably make the PV estimates more expensive. However, if the lifetime assumed is regarded as a relatively low, this might compensate for the lacking extra expenses when attributing yearly costs. Results in 4.2 are also only based in a 22° slope angle, and as shown in Figures 4.2, 4.3 and 4.4, the potential for other slope angles and how they relate to azimuthal angles might produce other results. Results are also based in the chosen electricity price scenario repeating over the lifetime of the system.

There is a clear correlation between economic performance of PV systems, local-specific conditions, and electricity prices. Electricity prices have a special high impact, and its impact also differ between locations. Figure 4.15 shows optimally configured PV systems and the total cost of covering electrical needs with Tromsø as the location with lowest cost, despite having the lowest potential production. For the locations with higher production potential the electricity prices in 2018 does not allow for any significant revenue from selling electricity. But as Figure 4.13 shows, the 2022 electricity price scenario induces different dynamics. In a low price scenario, the yearly attributed cost, which is the same for all locations, is the majority of total cost.

Norwegian electricity has a GWP of 0.019 kgCO2e/kWh (Tuset, 2020). Compared to this PV system perform poorly climatically. One could expect that implementing PV systems in Norway would result in higher emission factors, but comparatively, with the same basis as the literature used, the increase is not very large.

Although PV systems has a comparatively poor climatic performance, it does not mean that there is no place for small-scale PV systems in Norwegian power production. For prosumers small scale implementations can be, if configured wisely, profitable. There is a potential in exploiting this to construct incentives to alter the behaviour of prosumers. To clarify, as alternative configurations show economic promise, rewarding prosumers for certain beneficial production/consumption patterns which have benefits for the power grid or power market is certainly feasible. This would be an example of a cleverly designed power market with potential to mitigate intermittency and volatile electricity price problems.

These results show that on-grid alternative PV system configurations are potentially much more economic than energy maximizing ones, which in reference to Khatib and Deria (2022) illustrates that PV systems are highly sensitive to local-specific conditions and the power market it is dependent on. Which impact large implementations of such systems in the electricity production grid would have is not possible to say based on the results in this thesis. Hartner et al. (2015) reported in their analysis that electricity prices peaked at noon in Germany and Austria, and it is previously shown that in Norway in 2022 that is not the case, which leaves the question open as to the electricity price patterns in Norway might benefit from alternatively configured PV systems.

4.3 Air source heat pumps

4.3.1 ASHP relations

From the collected manufacturer data from 2.5.3 it seems that establishing some relationship between power input and listed heat output could be difficult. Using the values gathered, and assuming that to deliver the maximal heat output it requires maximum power input, the COP at lowest listed outdoor temperature ranges from 1.08 to 1.61 which for a temperature difference of $45°C - 50°C$ contradicts the values from Ruhnau et al. (2019) where the expected COP from a typical ASHP in that temperature range should be > 2.

To compare different installation sizes and which configuration is the best investment a variable which correlates to the performance of the heat output of the ASHP must vary with the price. Logical options from the collected data are the refrigerant mass and the listed power input. Figure 4.20 and Figure 4.21 shows respectively the refrigerant mass plotted against the price and maximum listed power input along with the linear regression line and the R-squared value.

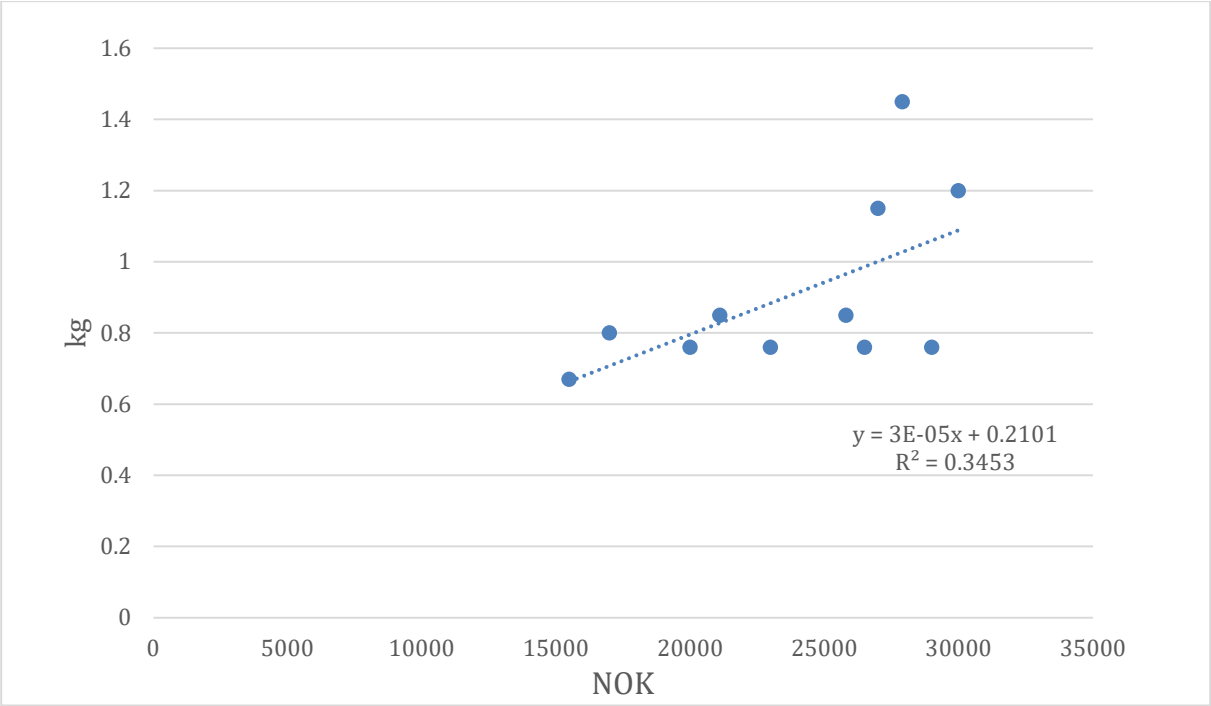

Figure 4.20 - Refrigerant mass plotted against ASHP price with linear regression results and R^2-value

Figure 4.20 shows that for the higher price ranges the amount of refrigerant mass varies a lot. Other factors such as design and additional features can be the cause of the large price variation.

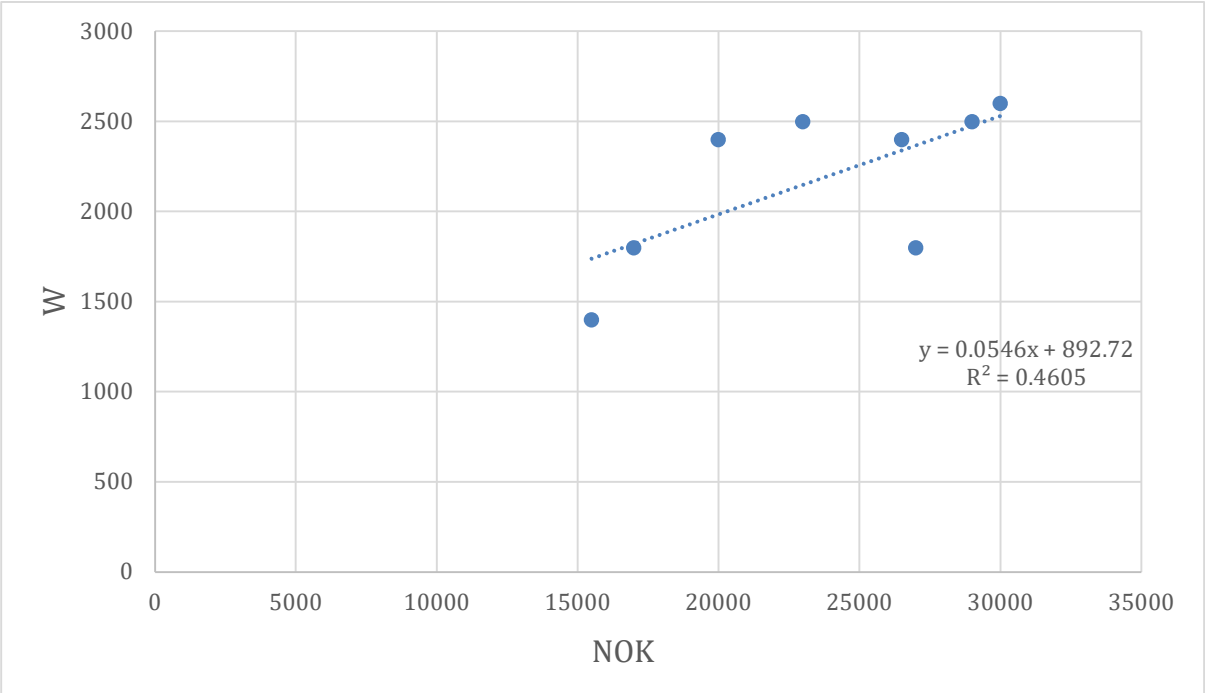

Figure 4.21 - Maximum listed power input plotted against ASHP price with linear regression results and R^2-value

Figure 4.21 shows that ASHPs in the lowest price range increases the slope of the regression line. Many of the ASHPs in the middle and higher price ranges have similar maximum powers. While the R-squared value is not very good, it is the best option to model performance after. An ASHP of a certain price has a maximum power input. It is a better option sticking to the linear regression results instead of fitting a polynomial or logarithmic model as the price of the ASHP varies with other factors than the performance. If the sample of ASHP data was larger, alternative regressions could be considered. An economic relationship to the performance is then established.

In addition to the economic relationship a relationship between installation size and refrigerant leakage must be established. Figure 4.22 shows the refrigerant mass plotted against the maximum listed power input.

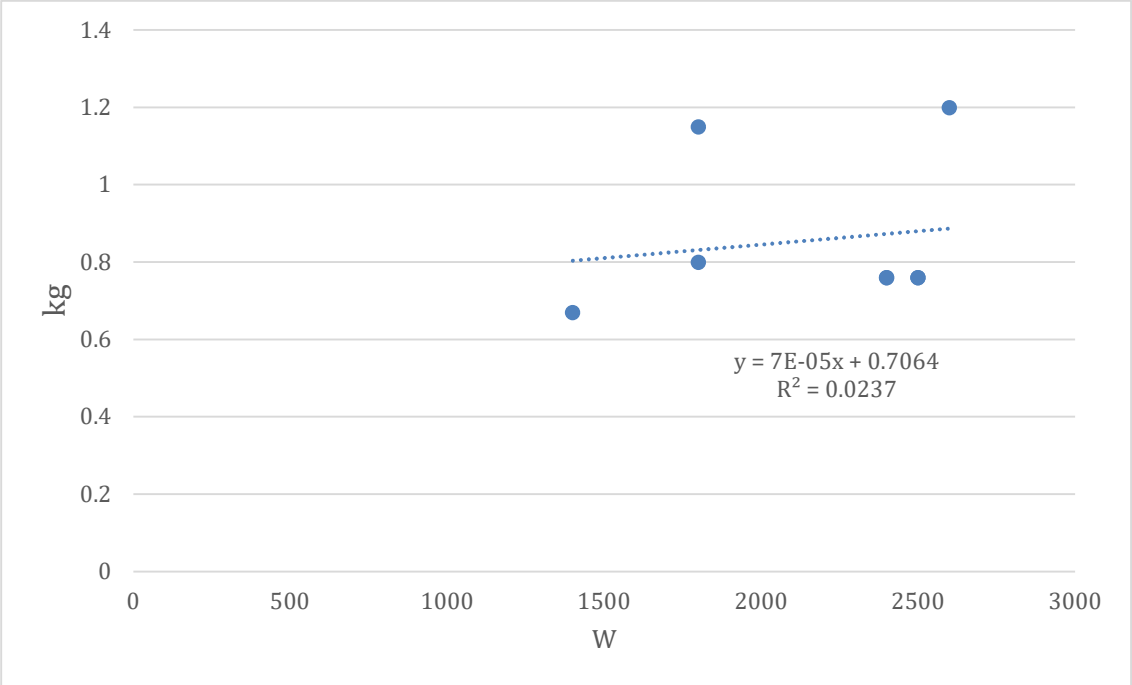

Figure 4.22 - Refrigerant mass plotted against maximum listed output with linear regression results and R^2- value

Figure 4.22 shows a very weak relationship between the variables and is not suitable for creating estimates. An alternative is setting a fixed refrigerant mass for the least costly and most costly ASHP option and use simple linear regression between those points. The refrigerant masses ranges between 0.67kg and 1.45kg and respective prices are 15490 NOK and 27900 NOK. Using linear regression:

$$\beta = \frac{1.45 - 0.67}{27900 - 15490} \cdot \frac{kg}{NOK} = 6.285 \cdot 10^{-5} \frac{kg}{NOK} \tag{44}$$

and

$$\alpha = 0.67kg - 6.285 \cdot 10^{-5} \frac{kg}{NOK} \cdot 15490NOK = -0.303kg \quad (45)$$

then

$$\hat{y} = -0.303 + 6.285 \cdot 10^{-5} x[kg]. \quad (46)$$

Now a relationship between price and refrigerant mass is established. The formula must be restricted to a sensible domain, since the refrigerant weight obviously cannot be 0 kg or under. A natural lower limit is set to 15000 NOK reflected in the acquired market data. Expanding the relationship far beyond the data it is based on might also produce unrealistic results. An upper limit of 35000 NOK can provide for some basis for analysis while not being totally unrepresentative of the price-refrigerant mass relation.

To determine a basis for estimating the climatic impact due to refrigerant leakage a relation between installed ASHP size and total filled mass of refrigerants must be established. With such a relationship established calculating the climatic impact is straightforward by using the same assumptions as in Naumann et al. (2022).

As the basis for COP for ASHP from Ruhnau et al. (2019) are manufacturer data, which reports the COP for actual operation time, and not adjusted for required downtime, the results from Li et al. (2024) are used to adjust the reported the initial COPs.

Table 4.16 – Linear regression for COP reduction corresponding to outside temperature based on Li et al. (2024)

Temperature ranges C°	$[-8.8, -11.7]$	$[-11.7, -15.2]$	$[-15.2, -17.8]$	$[-17.8, -19.3)$
Linear regression $[COP_{new}]$	-0.05766 $-0.006552x$	-0.1749 $-0.01657x$	$-0.2328 - 0.02038x$	-0.2379 $-0.02067x$

Table 4.16 is constructed by linear regression from the used temperature ranges and corresponding percentage of reduced COPs previously shown in 2.5.2.

4.3.2 Economically optimized ASHP heating

Figure 4.23 shows the results of how much you must expect to pay each year when investing a certain amount in an ASHP, which will dictate its performance, for house sizes ranging from $50m^2$ to $290m^2$. The investment cost of the ASHP is attributed to each year of its 20-year lifetime and electricity is used as backup heating when the ASHP will not meet the heating requirements on its own.

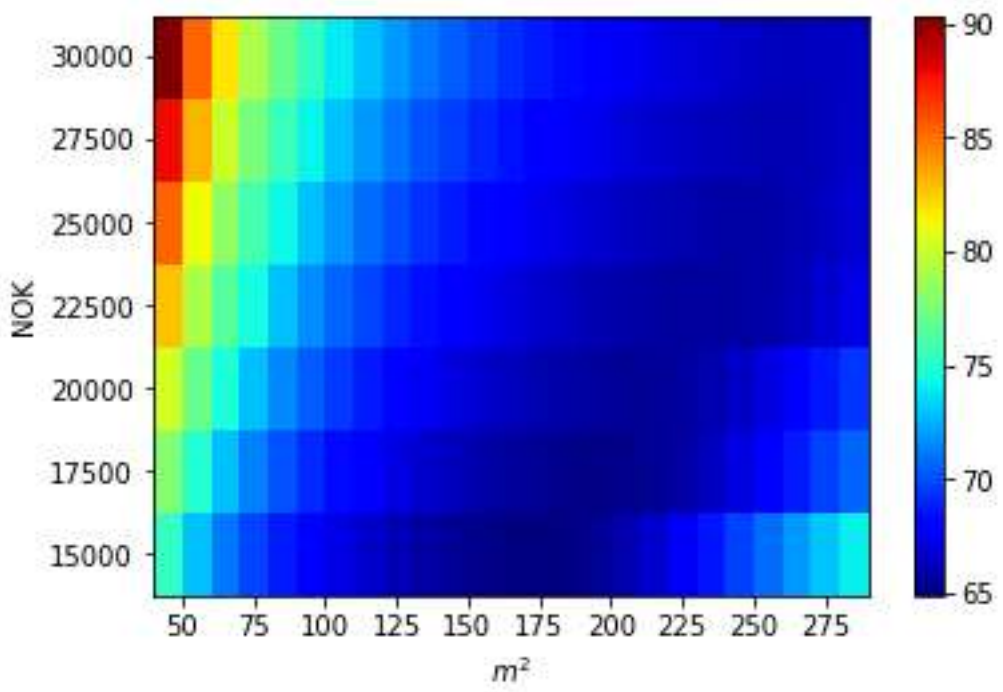

Figure 4.23 - Total yearly prices in NOK of covering a house's heating demand with ASHPs of various sizes using electricity as back up, with electricity prices and temperature from 2022 in Oslo/NO1 per square meter

For the 15000 NOK ASHPs with the lowest maximum power input the price per square meter rises for the largest house sizes. This indicates that a lower degree of coverage of heat by ASHPs for larger houses is less economical than investing in a larger and more expensive one. Comparing Figure 4.23 and Table 4.4 shows that ASHPs significantly reduces costs.

The dark blue area indicates that there is a clear house size to price relationship.

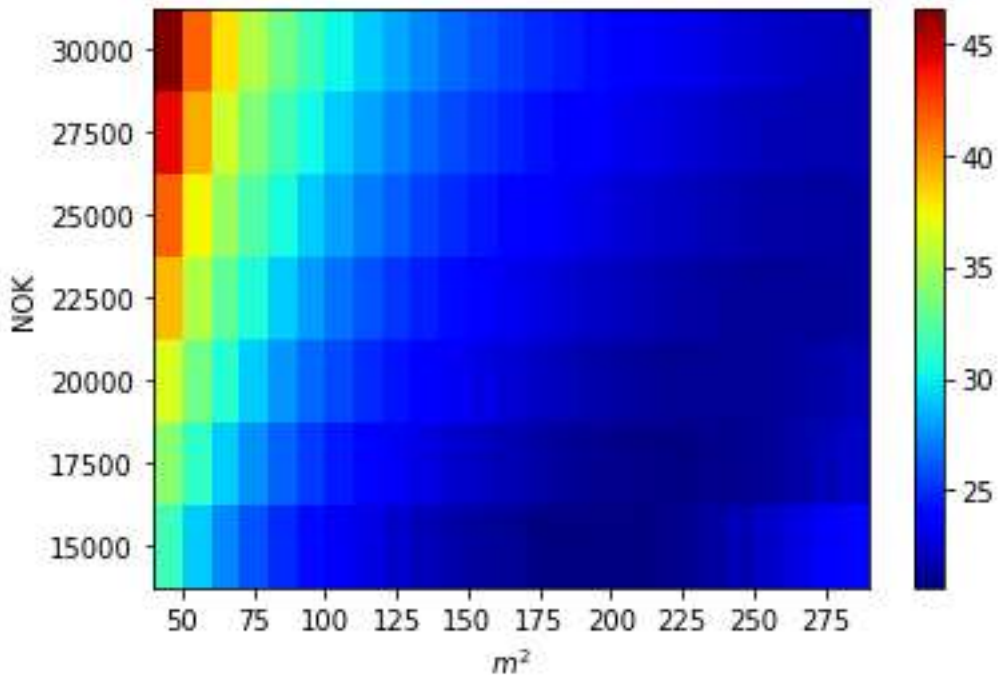

Figure 4.24 - Total yearly prices in NOK of covering a house's heating demand with ASHPs of various sizes using electricity as back up, with electricity prices and temperature from 2022 in Tromsø/NO4 per square meter

As in the Oslo estimates the most economical option for higher square meterage is larger ASHPs but the location in the plot where the dynamic is shifted towards higher square meterage. In comparison to Figure 4.23, the overall costs are significantly lower.

The two most important variables for ASHPs are the electricity price and the outdoor temperature. To analyse the relation between those two variables, Figure 4.25 shows a scenario with Oslo temperatures and NO4 electricity prices.

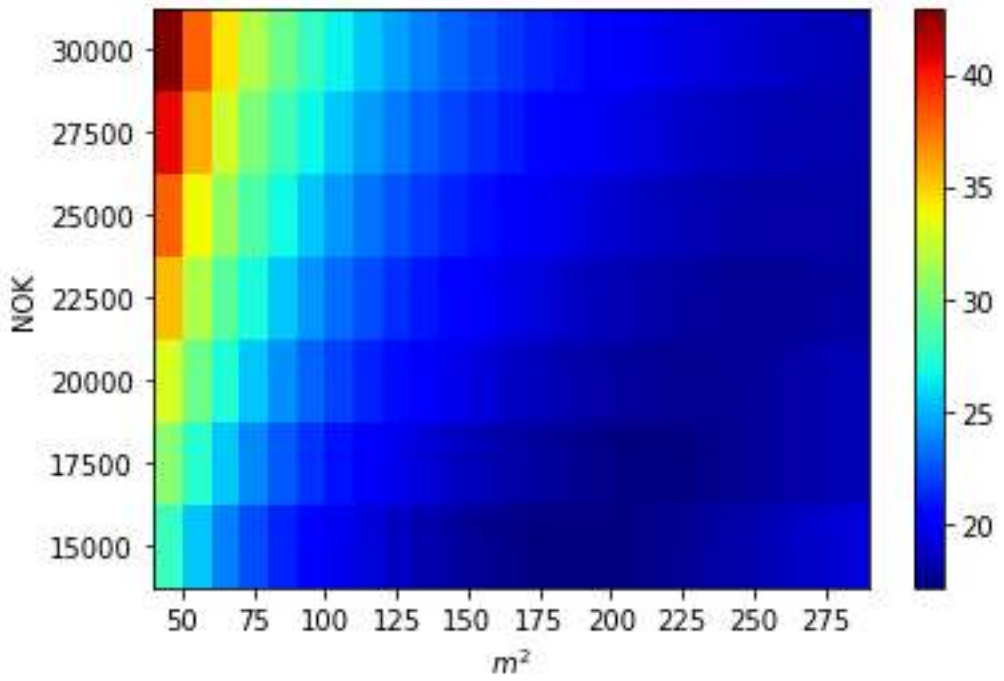

Figure 4.25 - Total yearly prices in NOK of covering a house's heating demand with ASHPs of various sizes using electricity as back up, with electricity prices and temperature from 2022 in Oslo with NO4 prices per square meter

Figure 4.24 and Figure 4.25 are very similar, with slightly lower prices in Figure 4.25, while the ASHP price – house size dynamic is barely shifted. This indicates that the electricity price is very important for ASHP configurations.

With the produced estimates it is now possible to identify the economically optimal heating-coverage for the ASHP configuration. Basing this in the heating cost per square meter data only the index of the least costly option needs to be identified, since a heating-coverage is calculated for all configurations.

The heating-coverage could be the initial parameter to dimension ASHPs, and the results produced here are based in the least costly configuration, making the heating-coverage a secondary result. In other words, the least costly location-specific configuration is already identified when the heating-coverage is estimated making it somewhat redundant. However, finding the heating-coverage for many locations might produce some insight into which degree of heating-coverage is generally suitable.

The results of the main cases with electricity prices from 2022 is shown in Table 4.17.

Table 4.17 - Coverage percentage and cost per square meter of least costly option regardless of size for main case cities for 2022 electricity prices

	Coverage in %	Cost per m^2 [NOK/ m^2]
Oslo	99.9	64.9
Tromsø	99.8	20.6
Bergen	99.9	60.5
Stavanger	99.9	60.6
Trondheim	99.8	35.8

The coverage percentage is so high that the small share of uncovered heating by the ASHP might as well be a consequence of the discrete data the estimations are based in. Specifically, the jumps between maximum heat outputs might be too large, meaning that the ASHPs can not provide for all the heating need. An incrementally larger ASHPs might cover the heating need and also be cheaper. In other words, the lack of continuity of the used data could be the reason the coverage percentage is not 100%.

Table 4.18 - Coverage percentage and cost per square meter of least costly option regardless of size for main case cities for 2018 electricity prices

	Coverage in %	Cost per m^2 [NOK/ m^2]
Oslo	99.3	19.9
Tromsø	99.5	23.7
Bergen	99.5	18.1
Stavanger	99.8	17.4
Trondheim	98.6	26.4

Comparing Table 4.17 and 4.18 shows that when using 2018 electricity prices the results are similar for the coverage percentage, while the cost per square meter is lower.

The results show that lower and less volatile electricity prices naturally produce lower cost per square meter while the coverage percentage is essentially unchanged. In contrast to the

other cities the price in Tromsø was higher in 2018 than in 2022, due to the electricity price being lower.

These results indicate that there is no reason to dimension ASHPs lower than the total space heating needs are in the main case regions. This is based in a simplified simulation where there are no other costs than the initial investment of the ASHP. The dynamic proposed in 4.1.6 is essentially none-occurring in these estimations.

4.3.3 ASHP in extreme conditions

It is highly interesting to analyse the performance of ASHPs in low-temperature environments, using Karasjok as an example is suitable for this as it is one of the coldest locations in Norway.

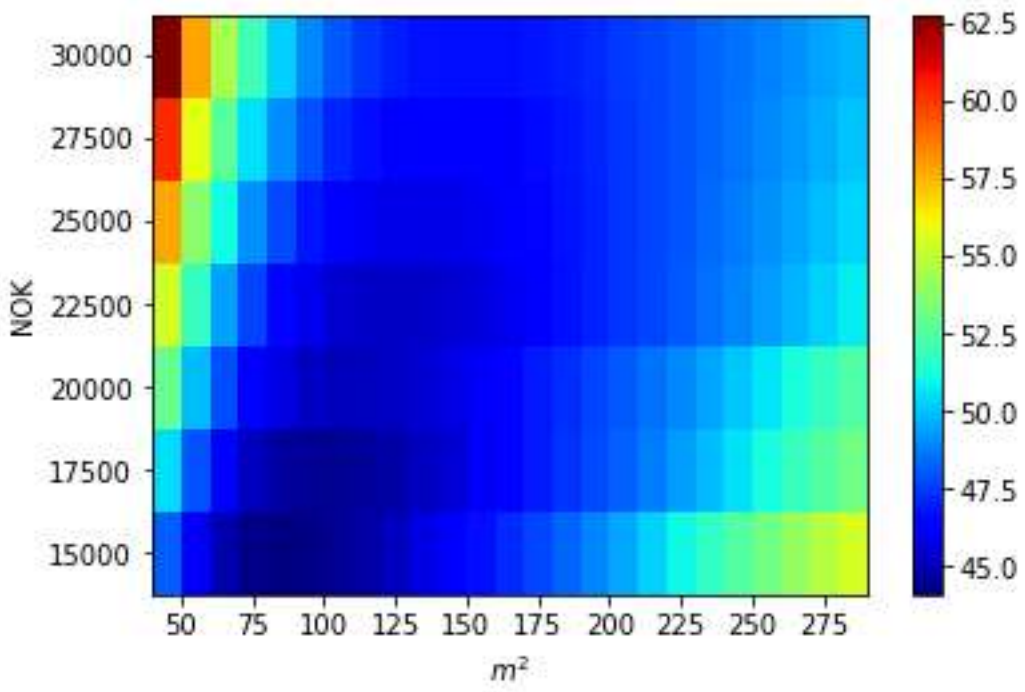

Figure 4.26 - Total yearly prices of covering a house's heating demand with ASHPs of various sizes using electricity as back up, with electricity prices and temperature from 2022 in Karasjok/NO1 per square meter

Figure 4.26 shows that the cold conditions in Karasjok indicates that bigger investments in ASHPs should be done even at very low square meterage. Additionally, the clear dynamic between house size and larger investments is smoothed out in Figure 4.26.

As ASHPs are less efficient in low temperature a worry could be that the investment cost of an ASHP could be too high. In Table 4.19 the total cost of using an ASHP costing 15000 NOK as described earlier is compared to the cost of using only electricity.

Table 4.19 - 15000 NOK ASHP and electricity, and only electricity total cost for space heating in Karasjok scenario in NOK

	$50m^2$	$100m^2$	$150m^2$	$200m^2$	$250m^2$	$300m^2$
ASHP/electricity	2409	3968	6396	9175	12414	16075
Only electricity	3351	6702	10054	13405	16757	20108

The ASHP option clearly outperforms the electricity scenario, even though the region has low electricity prices and being one of the coldest areas in Norway. This backs up the claims in Gibb et al. (2023) and shows that ASHP are efficient even in extreme cases.

As for the degree of heating-coverage for ASHPs in Karasjok the least costly configuration of installed size and house size have a coverage of 86.6%, a significant deviation from the least costly configuration of the results from the main cases. Under dimensioning ASHPs could be an economical optimal option in extreme conditions following the example from 4.1.6.

4.3.4 Sensitivity analysis - ASHP and electricity price

To do a sensitivity analysis for the ASHPs the most economical option per square meter option should be isolated and used as the basis. Table 4.20 shows the lowest cost per square meter configuration with 2022 electricity prices, and Table 4.21 shows the corresponding ASHP size.

Table 4.20 – Cost in NOK of lowest cost ASHP option per square meter in 2022, compared to cost using electricity, in accordance with Table 4.4

	$50m^2$	$100m^2$	$150m^2$	$200m^2$	$250m^2$	$300m^2$	Electricity
Oslo	75.4	68.7	65.7	65.0	65.5	66.4	277.14
Tromsø	31.6	25.0	22.0	20.7	20.8	21.3	73.08
Bergen	71.9	65.3	62.3	60.9	60.7	61.0	270.33
Stavanger	72.5	65.8	62.9	61.4	60.7	60.7	276.95
Trondheim	44.5	37.8	35.8	36.6	37.4	38.6	123.38

As Table 4.20 shows the price variations between the main cases are considerable. Clearly the high electricity prices in southern regions have a substantial effect which completely

counteracts the lower heating demands. Additionally, for all locations the costs reach a minimum before it grows again.

Table 4.21 – Optimal ASHP size in max power input in kW based in 2022 prices

	$50m^2$	$100m^2$	$150m^2$	$200m^2$	$250m^2$	$300m^2$
Oslo	1.72	1.72	1.72	1.85	2.13	2.54
Tromsø	1.72	1.72	1.72	1.72	1.85	2.13
Bergen	1.72	1.72	1.72	1.72	1.85	2.13
Stavanger	1.72	1.72	1.72	1.72	1.72	1.85
Trondheim	1.72	1.72	1.72	1.85	2.13	2.54

Table 4.21 shows that larger investments in ASHPs in Oslo and Trondheim for large house sizes are economically beneficial. Although prices for Oslo and Trondheim are in opposite sides of the spectrum the same size of ASHP is optimal. Comparing this to Tromsø, which has considerably larger heating demands than both Oslo and Trondheim but with a lower optimal ASHP size, illustrates the unique dynamics for each region. As Tromsø had the lowest electricity prices each incremental increase of ASHP size requires larger house sizes to be the economically optimal option. For Oslo the saved electricity cost due to the incremental ASHP size increase justifies the larger investment.

Table 4.22 - Optimal ASHP sizes in max power input in kW based in 2018 prices

	$50m^2$	$100m^2$	$150m^2$	$200m^2$	$250m^2$	$300m^2$
Oslo	1.72	1.72	1.72	1.72	1.72	1.85
Tromsø	1.72	1.72	1.72	1.72	1.85	2.13
Bergen	1.72	1.72	1.72	1.72	1.72	1.72
Stavanger	1.72	1.72	1.72	1.72	1.72	1.72
Trondheim	1.72	1.72	1.72	1.72	1.85	2.13

Again, the smallest ASHP dominates as the best option, with size increases in the larger house sizes in colder regions.

The relative change between each size and location configurations is shown in Table 4.23.

Table 4.23 - Relative change in % of lowest cost per square meter configuration from 2022 to 2018

	$50m^2$	$100m^2$	$150m^2$	$200m^2$	$250m^2$	$300m^2$
Oslo	-58.85	-64.56	-67.48	-69.11	-69.42	-69.41
Tromsø	9.94	12.59	14.29	15.04,	14.16,	13.58
Bergen	-58.28,	- 64.24	-67.31	-68.87	- 69.92	-70.21
Stavanger	-59.04	- 65.02	-68.1	-69.66	-70.62	-71.33
Trondheim	-17.72	-20.85	-24.14	-27.79	- 29.03	-29.98

Table 4.23 shows that the relative changes increase in magnitude with increased size for almost all cases regardless of whether the scenario is cheaper or more expensive. As previously shown the most economical option for all cases both in 2022 and 2018 is to maximize coverage. The continuous change increases are due to changed electricity cost. For most of the sizes and locations the configuration with the lowest costs included the smallest ASHP. Since the investment cost does not change, but electricity consumption does, prices continue to increase as a larger ASHP is still not more economic. Oslo and Tromsø reaches a local maximum change, where a bigger ASHP is more economic, stopping the increase in changes. This occurs between $250m^2$ and $300m^2$ for Oslo.

Change increases might stop when it is more economic to invest in a larger ASHP. However, as reported for Trondheim, increases of system size still results in change increases. For $250m^2$and $300m^2$ size increases were more economic than smaller sizes. As these estimates are based in both investment cost and local-specific electricity prices the dynamic of these variables is not easy to discern. However, it is apparent that the results are sensitive to their local-specific conditions.

For a fixed price scenario, the relative change results are the shown in Table 4.24.

Table 4.24 - Relative change of lowest cost per square meter configuration from 2022 to fixed price of 0.40 NOK/kWh

	$50m^2$	$100m^2$	$150m^2$	$200m^2$	$250m^2$	$300m^2$
Oslo	-62.67	-68.75	-71.86	-73.59	-74.22	-74.3
Tromsø	8.76	11.09	12.6	13.21	12.27	11.72
Bergen	-61.77	-68.08	-71.33	-72.99	-74.12	-74.61
Stavanger	-62.43	-68.75	-72.0	-73.66	-74.67	-75.43
Trondheim	-26.67	-31.37	-35.44	-39.39	-40.67	-41.4

Only Tromsø reaches a local maximum of growth in change. Otherwise, the results are similar to the change from 2022 to 2018.

Table 4.25 - Optimal ASHP sizes in max power input in kW based in fixed 0.40 NOK/kWh price scenario

	$50m^2$	$100m^2$	$150m^2$	$200m^2$	$250m^2$	$300m^2$
Oslo	1.72	1.72	1.72	1.72	1.72	1.85
Tromsø	1.72	1.72	1.72	1.72	1.85	2.13
Bergen	1.72	1.72	1.72	1.72	1.72	1.72
Stavanger	1.72	1.72	1.72	1.72	1.72	1.72
Trondheim	1.72	1.72	1.72	1.72	1.85	2.13

The ASHP sizes for the fixed price scenario are almost identical to the 2018 price scenario. However, in reference to the relative changes between sizes in Table 4.24 and results in Table 4.25 an ASHP size increase is not the only cause of maximized changes as this does not occur in Oslo and Trondheim. Indicating that there are varying unique location-specific conditions affecting the economic performance including weather and price dynamics.

The results show that ASHP are almost always a good economic investment. Additionally, aiming for a 100% heating load coverage is often the best economically performing option.

4.3.5 ASHP climate impacts

To estimate location-specific climatic impacts of ASHPs the emission factor based on all related emissions and supplied energy of the technology is found. For ASHPs this specifically includes the emissions of using electricity and emitted refrigerants and the supplied heat from the ASHP. The emissions are attributed to the actual performance of the ASHP. Emissions related to the back-up heating is not attributed to the ASHP. However, as he coverage for these scenarios are close to 100% this is no issue for the estimations.

As shown in 2.5.3 the variation of cooling agents of a sample of ASHPs were between 0.67 kg and 1.45 kg of R32. Naumann et al. (2022) uses a lifetime of 20 years in their LCA and as previously noted, 3% of cooling agent is emitted under manufacture and 6% leaks annually. Assuming that the cooling agent is topped of annually the total cooling agent emissions for the ASHPs in the sample ranges between 0.824 kg and 1.784 kg of R32. Which can be regarded as equivalent to 577 kg of CO2e and 1208 kg of CO2e. 20 year lifetime is assumed for the ASHP results.

In addition to being location-specific the emission factor varies with the price of the heat pump and the square meters to be heated. This way a figure can be constructed to directly compare against the cost per square meter figures.

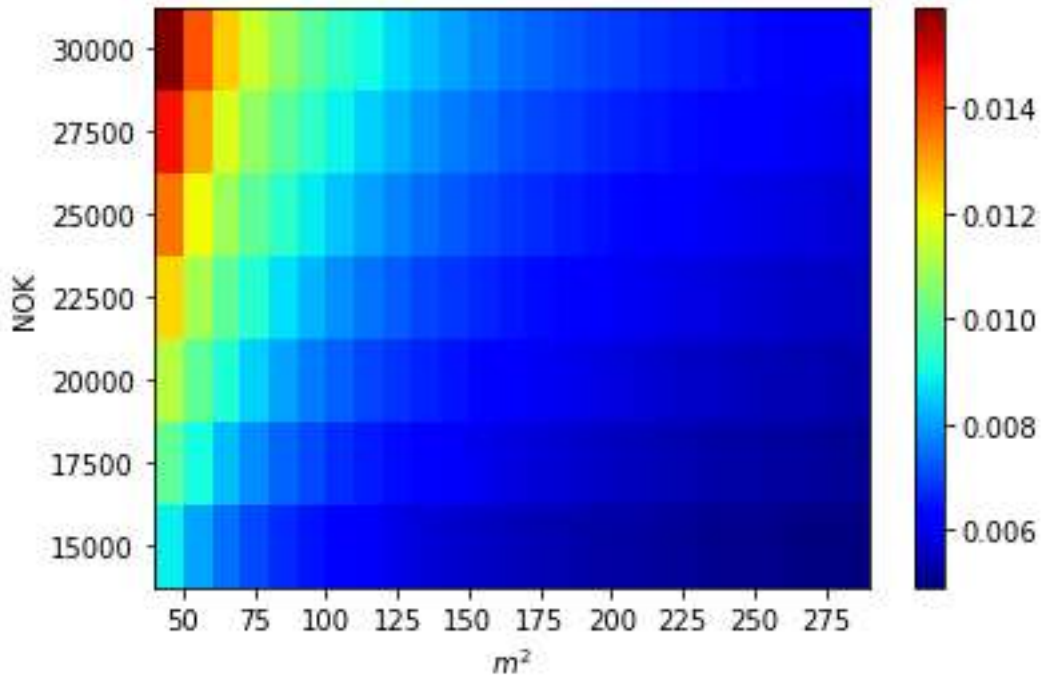

Figure 4.27 - Emission factor of ASHP implementation with 20 year lifetime in Oslo for different ASHP and house sizes in kgCO2e/kWh

Figure 4.27 shows that the emission factors are regardless of the house sizes and ASHP prices are lower than the GWP of electricity, which is 0.019 kgCO2e/kWh, as presented in 2.3.1. Results for other locations are similar to those reported in Figure 4.27. The same dynamic between house sizes and ASHP sizes is present for all locations. Locations with higher heat demands such as Tromsø have lower emission factors, since a larger number of kWh is attributed to the total emissions.

The most interesting aspect of estimating climatic impact of ASHPs is to identify under which parameters an ASHP would be regarded to have higher climatic impacts than using electricity only. The obvious parameter to investigate first is the lifetime.

Table 4.26 - Emission factor for ASHP in Oslo with lifetime of 10 years and 2022 weather in kgCO2e/kWh

House size / NOK	$50m^2$	$150m^2$	$250m^2$
15000	0.0090	0.0057	0.0051
20000	0.0114	0.0065	0.0055
25000	0.0138	0.0073	0.0060
30000	0.0162	0.0081	0.0065
35000	0.0186	0.0089	0.0070
40000	0.0210	0.0097	0.0075
45000	0.0234	0.0105	0.0080
50000	0.0258	0.0113	0.0084

Table 4.26 shows that only the configurations which are over dimensioned, based on the results in 4.3.2, reaches and surpasses the GWP of Norwegian electricity.

Table 4.27 - Emission factor for ASHP in Tromsø with lifetime of 10 years and 2022 weather in kgCO2e/kWh

House size / NOK	$50m^2$	$150m^2$	$250m^2$
35000	0.0145	0.0076	0.0063
40000	0.0162	0.0082	0.0066
45000	0.0179	0.0088	0.0070
50000	0.0196	0.0093	0.0073

As Table 4.26 and Table 4.27 shows the emission factors for the largest investments for the lowest house size are larger than 19 grams per kWh. In addition, the emission factors for Tromsø are better than in Oslo, likely due to the ASHP providing more kWh of heat to attribute the emission to. Based on previous results, there is no reason whatsoever to invest in so large ASHPs for small house sizes.

The estimations only consider the use-phase and the leakage of refrigerants which Naumann et al. (2022) reports as the most significant contributors to emissions for ASHP. The motivation for the results above is to identify the threshold where ASHPs are marginally better than electricity, but with the assumptions used the threshold will not be entirely correct. When the margins are so small the contributions which are disregarded becomes relatively more important. That is, ideally all contributions to emissions of the ASHP should be regarded if the threshold is to be set with confidence. Despite this, the results are precise enough to conclude on a more general basis that ASHPs do reduce climatic impacts considerably.

4.3.6 ASHP evaluation

There is no doubt to the economic benefits of ASHP implementation. For modern ASHPs the low-temperatures and even extreme conditions within Norway is not impactful enough to render ASHP implementations as bad implementations. Specifically in reference to the Oslo and Karasjok results with 2022 electricity prices, see Figure 4.23 and Figure 4.26, the results are more sensitive to electricity prices than to low temperatures. In very low temperature zones, combined with cheap electricity dimensioning ASHPs lower than what the maximum heating loads are, as described in 4.1.6, can be more economical.

The temperature dependent COPs in this thesis might be high as they are based in manufacturer data, and one modification, in accordance with Li et al. (2024). The temperature ranges used in Li et al. (2024) do not cover sufficient ranges to be completely applicable for Norwegian conditions, as many locations in Norway will have temperatures lower than $-19.3°C$ for significant periods of the year. How COP is affected in lower temperatures is not sufficiently modelled. No degradation of performance or maintenance cost is assumed and would certainly make the final estimates more expensive.

ASHPs are implementations with very low emission factors. Compared to Table 2.1, results in this thesis point to much lower emissions in a Norwegian setting. This is due to the very low GWP of electricity from the grid.

The share of heating required for direct hot water is not supplied by ASHP in these estimations. To directly heat water using only ASHP the temperature difference is very high compared to space heating, which would reduce performance. This leaves potential for other technologies to perform better than ASHPs when regarding all heating needs.

4.4 Combined heat and power

4.4.1 CHP relations

A linear relation between fuel consumption for the CHP and heat and power output is assumed for the module. This assumption does probably not hold true in a real life, as an engine will demand some minimum input. The reason for using the assumption is due to Volter only supplying max load fuel consumption. However, using linear regression, the relationship is as follows:

$$\hat{g}_c(\phi) = 0.2611 \cdot \phi, \phi \in [0,180]. \quad (47)$$

With $\hat{g}_c$ the consumed fuel, and ϕ is the combined output.

As for the efficiency of the module, the module produces 180kWh over one-hour, consuming 47kg of fuel, corresponding to 226kWh. This results in an electrical, thermal and total efficiency of 22.1%, 57.5% and 79.6% respectively using the method introduced in 2.6.2.

Volter reported a price for the walter unit of 2603609 NOK, based in 227720£ and exchange rates of October 31, 2023 (Volter, personal communication, October 31, 2023). This is

without VAT, transportation, or any additional required costs. To account for this a 20% increase is used on top of the reported price, amounting to 3124331 NOK.

The CHP option differs from the ASHP and PV scenarios as it probably requires more maintenance and service. The cost of this is not included in the estimations and might have a significant impact. As maintenance cost is not included at all for both PV and ASHP estimations, the basis for comparing the technologies could still be reasonable.

Additionally, a completely automated system is assumed which ensures production is not lower or higher than the demand. While not completely unrealistic it is an assumption that might not be true for many actual implementations of CHPs. With that in mind, the results are viable as an initial indicator as to what could be possible to save of costs if compared to a less demand-responsive system.

4.4.2 CHP estimations

Results for CHPs are presented for each location with both 1 CHP and 2 CHP configurations and location-specific price for covering all building needs – electrical needs, space heating and direct how water, with grid electricity for 2022, 2018 and fixed price scenario.

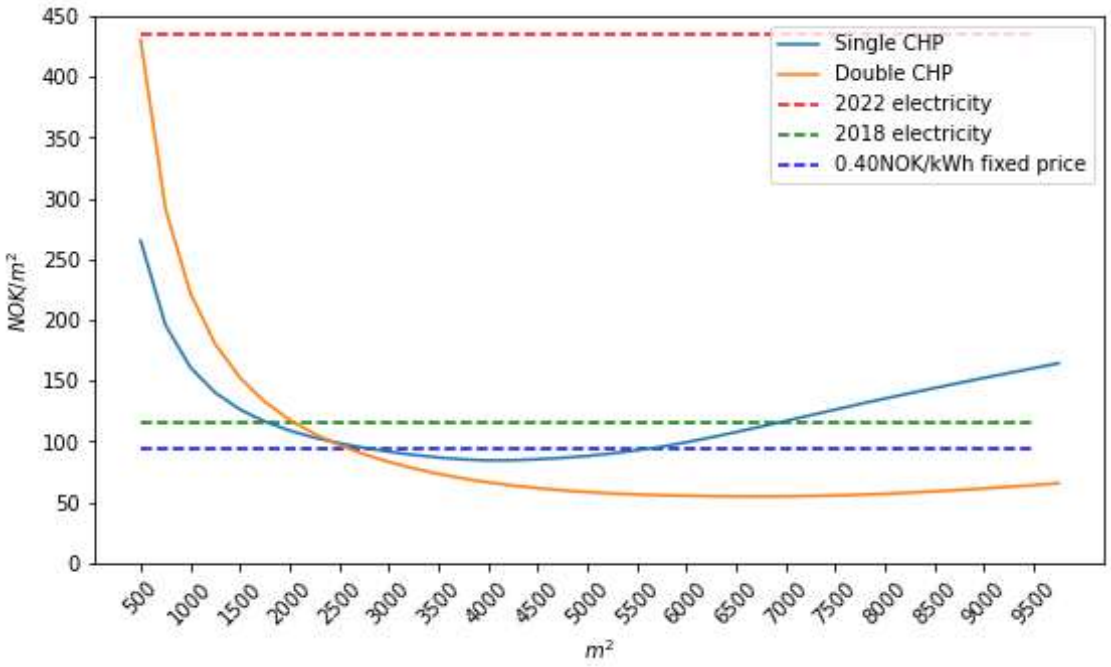

Figure 4.28 - Cost per square meter of 1 and 2 CHP module configuration, and 2018, 2022 and fixed electricity price scenarios for Oslo

As Figure 4.28 shows that compared to the least costly electricity scenario a single CHP configuration is only better over a limited range, while the double CHP configuration is cheaper from $2500m^2$ and throughout the analysed range.

For the single CHP the least costly possible option is 84.55 NOK/m^2 which corresponds to a coverage of heating of 88.0%[2]. Considering that the module will not provide for more than 88.3% it shows that the high back-up electricity price is the cause of the cost increase after reaching the least costly option. The maximum heat load over the year for the configuration resulting in 84.55 NOK/m^2 is 180.6kW, which is marginally higher than the maximum heating output of the CHP module. This strongly indicates that in a high electricity price scenario there is no reason to under dimension CHPs. The double CHP configuration also provide better reliability, as e.g. maintenance can be done sequentially unit by unit.

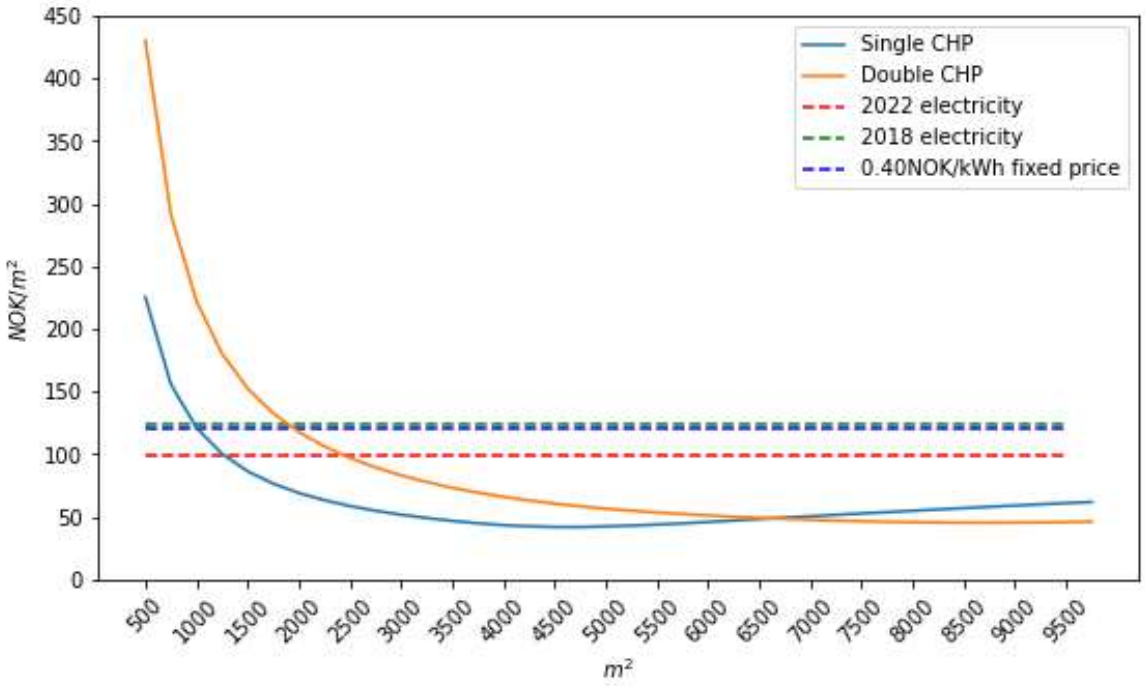

Figure 4.29 - Cost per square meter of 1 and 2 CHP module configuration, and 2018, 2022 and fixed electricity price scenarios for Tromsø

As Tromsø had low prices in 2022, the results in Figure 4.29 show other dynamics. The single CHP outperforms the double CHP over a larger range. Additionally, the least costly option for

[2] The maximum coverage of heating for CHPs is reduced compared to ASHPs due to the required down-time, i.e. not capped by the potential system output, as described in 4.1.6. This plays in additionally later when building needs exceed potential system outputs.

single CHP is reached before the double CHP configuration is cheaper, unlike in Figure 4.28. Similarly to Oslo, more reliance on back-up electricity increases cost. As Tromsø is a colder region the heating coverage is slightly lower, 87.9%. The least costly option has a heating coverage of 85.6% and a maximum heat load of 211kW. Compared to Oslo, the least costly option relies slightly more on back-up electricity. The maximum heating coverage and maximum possible heat supply still suggest a very low reliance on back-up electricity.

The electricity price scenarios in 2022 are very different between Oslo and Tromsø, but both scenarios perform best when only very low shares of delivered needs are covered from back-up grid electricity. This is due to the price of fuel per kWh being much cheaper than electricity in both scenarios. Implicitly, this shows that the temperature difference have relatively low impact on costs.

Table 4.28 – Cost in NOK per square meter of 1 and 2 CHP module configuration for Tromsø and Oslo

	$500m^2$	$1750m^2$	$3000m^2$	$4250m^2$	$5500m^2$	$6750m^2$	$8000m^2$	$9250m^2$
1 CHP Oslo	265	117	92	85	93	112	135	156
2 CHP Oslo	430	133	83	64	57	55	57	63
1 CHP Tromsø	225	77	52	43	44	50	55	60
2 CHP Tromsø	430	133	83	63	54	49	46	46

As Table 4.28 shows the least costly option in Oslo uses the double CHP option, but in Tromsø a single CHP is used. The range where this option is least costly is small and shows that one should be mindful of local-specific conditions when implementing CHPs.

As for the coverages for the double CHP configurations, Oslo has maximally 99.1% heating coverage and Tromsø has 98.9%. The least costly option in Oslo the coverage is 96.4% and in Tromsø 90.9%. Due to the larger investment cost the least costly options require a larger area to attribute total cost to, this results in lower degrees of coverage as the required area to minimize cost of the investment also requires larger needs than the double CHP configuration

can supply. For the double CHP in Tromsø the coverage is significantly lower than for one CHP, in contrast to Oslo.

The load coverage might be sensitive to the randomly generated down-time schedules as periods of larger building needs occur at different times in the year. That is, the majority of heating demands occur at winter. The double CHP configuration only have 97 hours with no operation, and 1796 hours with only one module being available. It is interesting to identify the operating schedule for the configuration.

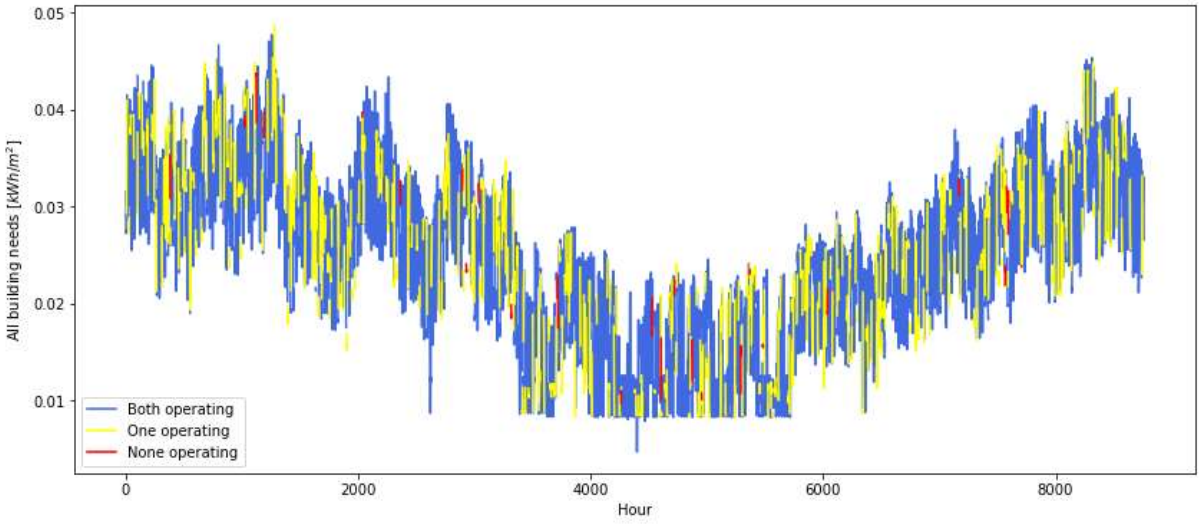

Figure 4.30 - All building needs in Tromsø and operation schedule of double CHP configuration

Figure 4.30 shows that a considerable portion of the instances where none of the CHPs are operating occur during summer when building needs are low. For the biggest load peak during the year only one module operates. Downtime of only one module is spread evenly throughout the year. Because of this it is reasonable to argue that the effect of different operating schedules is not as impactful as other factors.

The configurations are limited by their heating capacity before reaching the modules electricity generating capability. Electricity needs surpassing electricity supply has a minor impact on the total costs, compared to heating needs.

Results for Bergen and Stavanger are very similar to those of Oslo, and Trondheim similar to Tromsø, thus providing for no other insight other than CHP cost estimates sensitive to price zones. The figures for Bergen, Stavanger and Trondheim are reported in Appendix D.

4.4.3 CHP in extreme conditions

Using Karasjok as an example of extreme conditions, similarly as for the ASHP case in 4.3.3, results in the following figure:

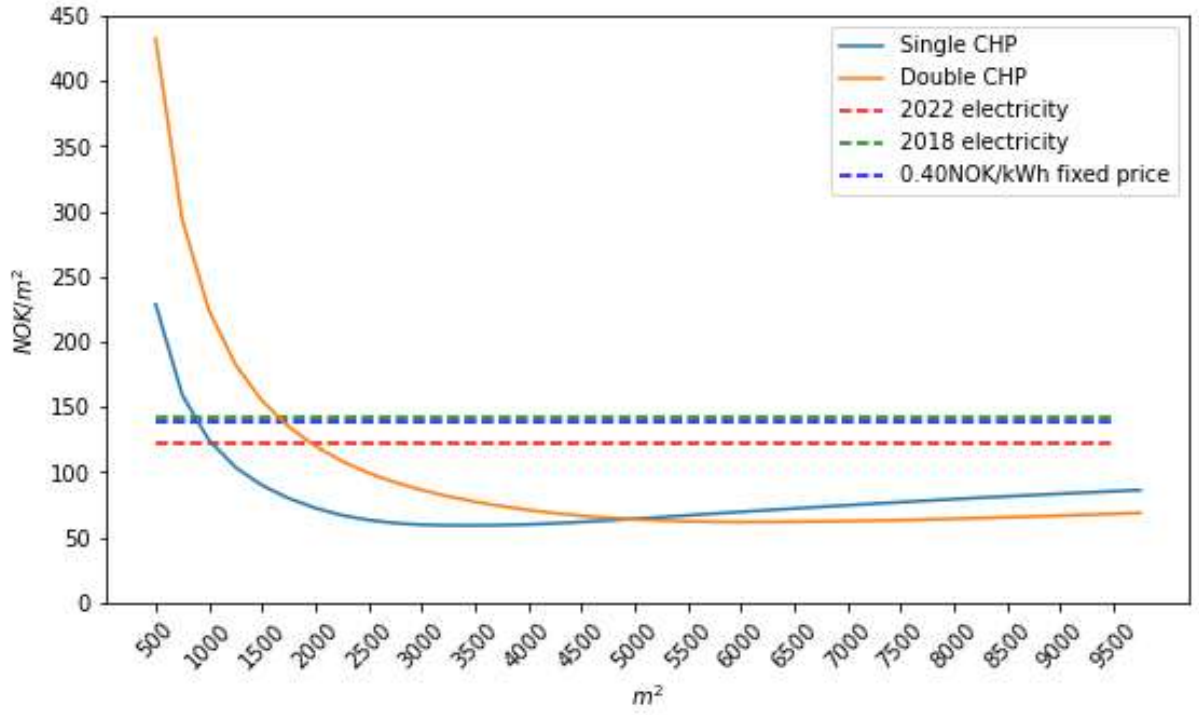

Figure 4.31 - Cost per square meter of 1 and 2 CHP module configuration, and 2018, 2022 and fixed electricity price scenarios for Karasjok

While similar to the ASHP results in Figure 4.29, costs of electricity price scenarios are shifted higher as heating demands are higher in Karasjok, as shown in Figure 4.31, than in Tromsø. This shows how temperature differences impacts CHP cost emission. The dynamic between single and double CHP resembles Figure 4.29, but the intersection between them is shifted to lower sizes.

The heating coverage for the lowest price scenario for the single CHP, with a price of 59.3 NOK/kWh, is 82.8%, while the maximal coverage is 87.9%. For the double CHP, the least costly option is 61.9 NOK/kWh with a heating coverage of 91.3% and a maximum of 99.0%. For the single CHP Karasjok has a lower heating coverage than Tromsø, while for the double CHP the coverage is slightly higher. This follows the same arguments as proposed in 4.4.2.

Single CHPs in Karasjok has a larger range where it has lower cost than electricity than Oslo. Double CHP perform better economically in Oslo than in Karasjok. How the location-specific conditions and different price zone dynamics between Karasjok and Oslo influences CHP

performance is clear between Figure 4.31 and Figure 4.28. The least costly options are similar between these two cases, but their initial parameters are substantially different.

4.4.4 Sensitivity analysis – Investment, electricity price and coverage

Increasing investment cost of module might provide additional insight into the arguments made for heating coverage in 4.4.2 and 4.4.3.

A 25% price increase results in a coverage percent of the least costly single CHP configuration of 85.6% and 90.2% for the double CHP configuration, which for the single CHP is identical to the initial investment cost, for the double CHP a reduction of 0.5 percentage points. Increasing the price 50% yields a reduction of heating coverage of 1.4 and 2.1 percentage points for single and double CHP configurations respectively. This implies that higher costs attributed to each square meter reduced the degree of optimal heating coverage, however as impacts are so low the local-specific conditions and price zones are relatively more impactful as shown between Tromsø and Oslo in 4.4.3.

The degree of heating coverage for the least costly option is with 2018 prices 84.8% and 91.2% for single and double CHP configurations respectively. Reductions of 3.2 and 7.9 percentage points respectively, showing a much clearer relation than investment cost increases.

Table 4.29 - Relative change in % from 2022 to 2018 electricity prices for single and double CHP configuration in Oslo

	$2000m^2$	$4000m^2$	$6000m^2$	$8000m^2$
Single CHP	-35.2	-46.9	-58.3	-64.3
Double CHP	-2.1	-4.5	-14.1	-27.3

Table 4.29 shows that as dependency on electricity increases with size the relationship between total cost of using CHP electricity prices is very clear.

4.4.5 CHP evaluation

The way CHPs are implemented are most impacted by electricity prices. Generally, economical performance is best when the CHP is utilized as much as possible. Resulting in a double CHP configuration being the most stable performer. In lower electricity price

scenarios, the yearly attributed cost of investment can shift the best economical approach to slightly dimension the CHPs under their max capacities.

There are uncertainties which must be attributed to the method for CHP estimations. Constant fuel prices over the whole lifetime of the CHP are unrealistic. Especially for CHPs, one would expect considerable yearly service and variable costs. High yearly costs will reduce the difference between the price per kWh delivered by CHP and electricity from the grid. Additionally, one must implement a heating infrastructure to deliver electricity and heating from a CHP in the ranges analysed, the cost of this is important when comparing with other heating and electricity providing systems. A feature which is not implemented, is the potential to sell electricity to the grid. This feature shows considerable effects for PV systems and might provide for additional saved costs for CHPs. These uncertainties result in a lower confidence to whether the estimations in this thesis corresponds to actual costs.

CHPs have the strength of delivering all building needs, which PV and ASHPs are not assumed to do. Another strength is that its output is unaffected by intermittency. However, there is some required downtime for each separate module, but with a double CHP configuration the hours in the year with no output is efficiently reduced. As price volatility and intermittency is related the continuity of CHPs can mitigate these effects in the power market if implemented in a substantial scale.

2.6.4 covers a discussion between biogenic and fossil carbon emissions, and sows doubt to the basis for which it is possible to conclude on the climatic impact of bioenergy CHPs. Muench & Guenther (2013) reports a range of both negative and positive emission factors for bioenergy use, which speaks to the uncertainty of how climatic impact of bioenergy should be handled. If bioenergy CHPs are a part of a processes which avoids methane emissions it might be labelled as climatically suited, but the scope of this thesis does not cover variability of potential avoided methane emissions. The results do not provide for any insights which allows for any confident general conclusion to the climatic impact of CHPs.

4.5 Implementation example

Based on the earlier results it is now possible to compare total costs for a concrete example house with energy technologies implemented against a grid electricity only example for 2022.

With a concrete house example PV and ASHP are suited to implement. CHPs are not compatible in the same way. If a relevant example for a concrete house was to be used for

CHP, first the intended supplied house size must be fixed. The most economical options for CHPs are in the scale of thousands of square meters. The cost for this size can then be scaled down to the intended house size.

Table 4.4 reports the costs per square meter for Tromsø in 2022. Using a $150m^2$ house it yields 2637 NOK, 10962 NOK and 1278 NOK to cover electrical needs, space heating and direct hot water respectively, amounting to a total cost of 14877NOK.

Implementing an east-west PV system in Tromsø, implicitly assuming that the house is oriented in such a way, the total cost of covering electrical needs with this configuration is 25.64 NOK/m^2, see Table 4.8. Amounting to 3846 NOK in total.

The cost of covering space heating needs in 2022 in Tromsø with an ASHPs is about 22.5 NOK/m^2, amounting to 3375 NOK in total.

In this example, DHW must be covered by electricity, and the total cost with implementing a PV system and ASHP is 8499 NOK, corresponding to a -42.9% relative change. A significant decrease, due to the ASHP.

The impact of the ASHP cannot be understated. There is no reason to be concerned for the economic performance of ASHPs in a low-temperature area such as Tromsø.

The total energy use to cover all needs in Tromsø is 32550 kWh, which based in grid electricity contributes to 618 kgCO2e, with a 0.019 kgCO2e/kWh GWP (Tuset, 2020). To ensure that climatic impacts is attributed correctly, see 2.3.2, the system specific emissions of the PV system must be attributed yearly to this example. A $150m^2$ with a 17kWp PV system configured east-west with $22°$ slope angle results in lifetime emissions of 25500 kgCO2e, resulting in 2125 kgCO2e/year over a 12-year lifetime, with emissions of 1500 kgCO2e/kWp.

In Tromsø the PV system produces 1023kWh. The yearly electrical needs for a $150m^2$ house amount to 6008 kWh. The hours where produced electricity covers housing needs and where electricity is sold is not identified. It is therefore unclear how much of the produced electricity is used to covers electrical needs. For this example is assumed that all produced electricity covers the house's building needs. This results in 4985 kWh that must be delivered by the grid, resulting in 95 kgCO2e.

Calculating the emission factor of a 15000 NOK ASHP, for a$150m^2$ house in Tromsø results in 0.0054 kgCO2e/kWh. With a space heating demand of 23582 kWh, the emission amount to 127 kgCO2e. Compared to electricity, with equivalently 448 kgCO2e, it is a relative change of -71.7%. Combining all emissions, where DHW heated with grid electricity emits 57 kgCO2e, results in 2404 kgCO2e/year. A relative change of 289%.

As for Oslo the total cost for a $150m^2$ house using only electricity from the grid in 2022 is 65222 NOK. With 15702 NOK for electrical needs, 41571 NOK for space heating and 7949 NOK for DHW.

With a PV system and ASHP implemented, electrical needs and space heating have respective costs of 3818 NOK and 9900 NOK, for a new total of 21667 NOK. While more expensive than exclusively using electricity in Tromsø it accounts for a -67.0% relative change. In isolation space heating has a relative change of -76.2%.

Covering the respective 6008 kWh, 16593 kWh and 2987 kWh for electrical needs, space heating and DHW in Oslo with electricity from the grid leads to emissions of 486 kgCO2e. The PV system produces 1380 kWh of electricity. The remaining electricity that needs to be covered from the grid thus emits 88 kgCO2e. The ASHP configuration in Oslo has an emission factor of 0.0057 kgCO2e/kWh, in accordance with Table 4.26, resulting in an emission of 94 kgCO2e. For space heating this results in a relative change of -70.2%. In total, emissions amount to 2363 kgCO2e in Oslo. A relative change of 386%.

Both economically and climatically results differ between Tromsø and Oslo. Comparing implementations in Tromsø and Oslo illustrate the importance of local-specific conditions and electricity prices. Isolated, ASHPs have similar effects for both locations. The PV system perform much better economically in Oslo than in Tromsø but will increase the total emissions relatively more in Oslo.

4.6 Comparing PV, ASHP and CHP

Comparing energy technologies includes how they are affected by intermittency, volatile power markets and local specific conditions, and the different technologies are subjected to their own assumptions.

Intermittency is most important for PV implementations, while ASHPs and CHPs are mostly unaffected by intermittency. If extending the concept of intermittency to the reduced

performance of ASHPs due to colder temperatures one would still argue that it is more impactful for PV systems. The use of ASHPs is more expensive in colder temperatures, due to the increased electricity use, but not comparable to the economic impact of a complete shutdown of PV output. CHPs might instead be a renewable intermittency mitigator. CHPs are, if done correctly, able to continuously produce renewable electricity and heat. While the majority of Norwegian grid electricity is not highly subjected to intermittency, interconnectivity with other power markets, higher shares of intermittent energy sources, and higher power demands might disrupt stable power delivery. Implementations of bioenergy CHP might be a part of stabilizing the grid.

Volatile, high priced power markets have the most impact on PV implementations. Whether or not a PV investment is cost saving or not changes between electricity price scenarios, as opposed to ASHPs which generally are cost saving regardless of electricity price scenario. Electricity price scenarios alters the range where CHPs are cost saving with higher reliance on back-up electricity.

Local-specific conditions such as solar irradiance and temperature have moderate impacts. Production potential for PV systems is important in volatile high prices power markets, but generally not as important as the electricity prices themselves. Lower temperatures can induce scenarios where heating-coverages from ASHPs or CHPs are lower than their maximums.

Better building efficiencies will definitely impact the results for ASHPs and CHPs. While a basis to discuss the economy of alternative efficiencies is not established the dynamics would be different. Scenarios with only electricity use would have lower costs, and the energy technologies would have less total energy to attribute saved costs to. A very efficient building could be more sensitive to over dimensioning, i.e. overinvesting in system size. Generally, this would not affect the results in this thesis as the heating technologies provide for lower cost solutions compared to electricity only scenarios.

5 Conclusion

PV systems performs climatically poor in relation to the GWP of Norwegian electricity. PV systems perform economically well in Oslo and Stavanger in an electricity price scenario such as 2022. PV systems are more sensitive to local-specific conditions and electricity prices than ASHPs and CHPs, with electricity prices being the most important factor. This thesis shows that an east-west configurations of a roof-top PV system gives lower cost compared to a south faced system. This despite having higher LCOE than south facing systems. Larger systems and better alignment with electricity prices are the main factors for this result. Clever adaptions of east-west configured systems in the electricity grid could also contribute positively to intermittency and volatility challenges.

ASHPs are very economically and climatically sensible implementations in all areas analysed. ASHPs are affected by volatility and intermittency, and they are implicitly affected by the changing electricity prices. Implementation of ASHPs will contribute to lower the use of electricity in Norway, as electricity is a common source of heating. The implementation of more ASHPs will contribute positively to volatility concerns in the power market. ASHPs are a technology which confidently show very efficient reductions of costs and climatic impact while being a purposeful implementation in the power market.

CHPs can produce both electricity and heat. They are not affected by intermittency; large penetration of CHPs could therefore mitigate volatility challenges in the power market. To cover larger areas of housing, CHPs show economic promise as wood chip prices are low compared to electricity. If yearly additional costs of implementing CHPs are low, they are economically well performing implementations, especially in high electricity price scenarios. As for the climatic impact of bioenergy CHPs, it is related to the production of its fuel, and based on this thesis nothing general can be concluded for how well bioenergy CHPs perform climatically.

From a prosumers perspective in Oslo and Stavanger a PV system implementation in an electricity scenario such as 2022 is more purposeful than it is in Tromsø, Trondheim and Bergen. In a less volatile electricity price scenario, such as 2018, the differences between locations diminishes. Temperature variances within Norway seems to have only moderate impacts on the total costs for ASHPs and CHPs, while the electricity price scenario is the main factor.

6 Future research

While the main focus of this thesis is exploring some important aspects concerning implementation of building integrated renewable energy technologies, the method of automatic data retrieval and processing could be generalized. The data which are preconditions of the performance of energy technologies given a location could be used as feature generation for machine learning purposes. The technologies in this thesis all are analysed independently, and future research should include synergetic optimal combination of the individual strengths. Machine learning and optimization approaches can be used to find local-specific synergetic optimal configurations. The brute force method applied in this method will surely be less efficient than alternative approaches.

Many other variables could have been the basis for analysis, for example different building types. The possible configurations of all variable parameters combined from PROFet, Frost and PVGIS combines to a very large number, and there are no methodological limitations of computing complete estimates for all combinations. Since a large part of the effort put into this thesis is automating and creating functions to compute estimations a potential of generating a large dataset of results is available with the same method. This thesis seeks out to investigate the estimations for pre-decided locations. An alternative approach, with such a large dataset available, could be to search for relevant patterns within the data.

The results in this thesis are only as reliable as its data basis and methodology. Future research could therefore be insuring higher quality data and implementing additional dynamics, such as discount rates and yearly variable costs. Some data from Frost is faulty, and a failsafe mechanism could be implemented, where values that are obviously wrong are replaced by modelled temperatures instead.

Smart-homes with automatic responses to power prices and production potential is an added dimension to the methodology which could provide very interesting results.

7 References

Aghaie, H. (2016). The impact of intermittent renewables on the resource adequacy in electricity markets. *2016 IEEE Electrical Power and Energy Conference (EPEC), Ottawa, ON, Canada* (pp. 1-5). https://doi.org/10.1109/EPEC.2016.7771743

Agrawal, K. K., Jain, S., Jain, A., & Dahiya, S. (2013). Assessment of greenhouse gas emissions from coal and natural gas thermal power plants using life cycle approach. *International Journal of Environmental Science and Technology*, *11*(4), 1157–1164. https://doi.org/10.1007/s13762-013-0420-z

Alam, E., & Xu, X. (2022). Life cycle assessment of photovoltaic electricity production by mono-crystalline solar systems: a case study in Canada. *Environmental Science and Pollution Research*, *30*(10), 27422–27440. https://doi.org/10.1007/s11356-022-24077-3

Alpaydin, E. (2020). *Introduction to machine learning* (4th ed.). The MIT Press

Ambec, S., & Crampes, C. (2021). Real-time electricity pricing to balance green energy intermittency. *Energy Economics*, *94*, 105074. https://doi.org/10.1016/j.eneco.2020.105074

Amillo, A. G., Huld, T., & Müller, R. (2014). A new database of global and direct solar radiation using the Eastern Meteosat satellite, models and validation. *Remote Sensing*, *6*(9), 8165–8189. https://doi.org/10.3390/rs6098165

Andersen, K.H, Lien, S.K, Walnum, H.T, Lindberg K.B, and Sartori, I. (2021). *Further development and validation of the "PROFet" energy demand load profiles estimator*. BuildSim 2021 Conference, 1-3 Sep., Bruges, BE.

Andersen, P. B. (2019, April 15). *halvledere* [semiconductors]. *Store Norske Leksikon.* Retrieved 18. March 2024 from https://snl.no/halvledere

Badr, O., Naik, S., O'Callaghan, P., & Probert, S. (1991). Expansion machine for a low power-output steam Rankine-cycle engine. *Applied Energy*, *39*(2), 93–116. https://doi.org/10.1016/0306-2619(91)90024-r

Blum, P., Campillo, G., Münch, W., & Kölbel, T. (2010). CO2 savings of ground source heat pump systems – A regional analysis. *Renewable Energy*, *35*(1), 122–127. https://doi.org/10.1016/j.renene.2009.03.034

Bojić, M., Cvetković, D., Marjanović, V., Blagojević, M., & Djordjević, N. (2013). Performances of low temperature radiant heating systems. *Energy and Buildings*, *61*, 233–238. https://doi.org/10.1016/j.enbuild.2013.02.033

Bunn, D. W., & Muñoz, J. I. (2016). Supporting the externality of intermittency in policies for renewable energy. *Energy Policy*, *88*, 594–602. https://doi.org/10.1016/j.enpol.2015.07.036

Delarue, E., & Morris, J. (2015). *Renewables Intermittency: Operational Limits and Implications for Long-Term Energy System Models*. https://dspace.mit.edu/handle/1721.1/95762

Donnison, C., Holland, R. A., Harris, Z., Eigenbrod, F., & Taylor, G. (2021). Land-use change from food to energy: meta-analysis unravels effects of bioenergy on biodiversity and cultural ecosystem services. *Environmental Research Letters*, *16*(11), 113005. https://doi.org/10.1088/1748-9326/ac22be

Energioversikt [Energy overview]. (2024, February 1). *Energirapporten* [The Energy Report]. https://www.energiaktuelt.no/energirapporten.573794.no.html

European Commission, (n.d.). *PVGIS data sources & calculation methods*. (n.d.). EU Science Hub. https://joint-research-centre.ec.europa.eu/photovoltaic-geographical-information-system-pvgis/getting-started-pvgis/pvgis-data-sources-calculation-methods_en

Finnegan, S., Jones, C. I., & Sharples, S. (2018). The embodied CO2e of sustainable energy technologies used in buildings: A review article. *Energy and Buildings*, *181*, 50–61. https://doi.org/10.1016/j.enbuild.2018.09.037

Forsberg, C. W., Stack, D. C., Curtis, D., Haratyk, G., & Sepulveda, N. A. (2017). Converting excess low-price electricity into high-temperature stored heat for industry and high-value electricity production. *The Electricity Journal*, *30*(6), 42–52. https://doi.org/10.1016/j.tej.2017.06.009

Garrett, P., & Rønde, K. (2012). Life cycle assessment of wind power: comprehensive results from a state-of-the-art approach. *The International Journal of Life Cycle Assessment*, *18*(1), 37–48. https://doi.org/10.1007/s11367-012-0445-4

Gibb, D., Rosenow, J., Lowes, R., & Hewitt, N. J. (2023). Coming in from the cold: Heat pump efficiency at low temperatures. *Joule*, *7*(9), 1939–1942. https://doi.org/10.1016/j.joule.2023.08.005

Gjerland, C.F., Gjerde, M. (2020). *Wind power production and electricity price volatility: an empirical study of the effect of increased wind power production on electricity price volatility in Norway* [Master thesis, Norges Handelshøgskole]. NHH Brage. https://openaccess.nhh.no/nhh-xmlui/handle/11250/2679448

Glenk, G., & Reichelstein, S. (2022). The economic dynamics of competing power generation sources. *Renewable & Sustainable Energy Reviews*, *168*, 112758. https://doi.org/10.1016/j.rser.2022.112758

Green, R., & Vasilakos, N. (2010). Market behaviour with large amounts of intermittent generation. *Energy Policy*, *38*(7), 3211–3220. https://doi.org/10.1016/j.enpol.2009.07.038

Hagos, D. A., Gebremedhin, A., & Bolkesjø, T. F. (2017). The prospects of bioenergy in the future energy system of Inland Norway. *Energy*, *121*, 78–91. https://doi.org/10.1016/j.energy.2017.01.013

Hansen, S. T., & Moe, E. (2022). Renewable energy expansion or the preservation of national energy sovereignty? Norwegian renewable energy policy meets resource nationalism. *Political Geography*, *99*, 102760. https://doi.org/10.1016/j.polgeo.2022.102760

Hartner, M., Ortner, A., Hiesl, A., & Haas, R. (2015). East to west – The optimal tilt angle and orientation of photovoltaic panels from an electricity system perspective. *Applied Energy*, *160*, 94–107. https://doi.org/10.1016/j.apenergy.2015.08.097

Havukainen, J., Nguyen, M. T., Väisänen, S., & Horttanainen, M. (2018). Life cycle assessment of small-scale combined heat and power plant: Environmental impacts of

different forest biofuels and replacing district heat produced from natural gas. *Journal of Cleaner Production*, *172*, 837–846. https://doi.org/10.1016/j.jclepro.2017.10.241

Hellström, J., Lundgren, J., & Yu, H. (2012). Why do electricity prices jump? Empirical evidence from the Nordic electricity market. *Energy Economics*, *34*(6), 1774–1781. https://doi.org/10.1016/j.eneco.2012.07.006

Hesaraki, A., Bourdakis, E., Ploskić, A., & Holmberg, S. (2015). Experimental study of energy performance in low-temperature hydronic heating systems. *Energy and Buildings*, *109*, 108–114. https://doi.org/10.1016/j.enbuild.2015.09.064

Hofstad, K. (2021, October 12). *varmefaktor* [Heat factor]. *Store norske leksikon*. Retrieved 19. March 2024 from https://snl.no/varmefaktor

Hofstad, K. (2023, January 2). *fotovoltaisk effekt* [photovolatic effect]. *Store norske leksikon*. Retrieved 19. March 2024 from https://snl.no/fotovoltaisk_effekt

Holmberg, H. (2007). *Biofuel drying as a concept to improve the energy efficiency of an industrial CHP plant*. [Doctoral dissertation, Aalto University]. Aalto Thesis Database. https://aaltodoc.aalto.fi/items/12e4f38f-83f8-471f-b52a-a49ff3722622

Inderberg, T. H. J., Sæle, H., Westskog, H., & Winther, T. (2020). The dynamics of solar prosuming: Exploring interconnections between actor groups in Norway. *Energy Research & Social Science*, *70*, 101816. https://doi.org/10.1016/j.erss.2020.101816

Iqbal, M. (1983). Chapter 1 - SUN–EARTH ASTRONOMICAL RELATIONSHIPS,Editor(s): Muhammad Iqbal. *An Introduction to Solar Radiation*. Academic Press. Pages 1-28. https://doi.org/10.1016/B978-0-12-373750-2.50006-9

Ivanko, D., Walnum, H. T., & Nord, N. (2020). Development and analysis of hourly DHW heat use profiles in nursing homes in Norway. *Energy and Buildings*, *222*, 110070. https://doi.org/10.1016/j.enbuild.2020.110070

Jacobsen, H. K., & Zvingilaite, E. (2010). Reducing the market impact of large shares of intermittent energy in Denmark. *Energy Policy*, *38*(7), 3403–3413. https://doi.org/10.1016/j.enpol.2010.02.014

Jaraitė, J., Kažukauskas, A., Brännlund, R., Chandra, K., & Kriström, B. (2019). Intermittency and pricing flexibility in electricity markets. Social Science Research Network. https://doi.org/10.2139/ssrn.3389768

Jasolar 365. (n.d.). Solcellespesialisten.no. Retrieved 4 May, 2024 from https://www.nettbutikk.solcellespesialisten.no/jasolar/jam60s21-365-mr-30mm/jasolar-365wp-all-black-30mm-all-black-30mm

Jåstad, E. O., Bolkesjø, T. F., Trømborg, E., & Rørstad, P. K. (2021). Integration of forest and energy sector models – New insights in the bioenergy markets. *Energy Conversion and Management*, *227*, 113626. https://doi.org/10.1016/j.enconman.2020.113626

Kamel, R. S., & Fung, A. S. (2014). Modeling, simulation and feasibility analysis of residential BIPV/T+ASHP system in cold climate—Canada. *Energy and Buildings*, *82*, 758–770. https://doi.org/10.1016/j.enbuild.2014.07.081

Keeble, J., Abraham, N. L., Archibald, A. T., Chipperfield, M. P., Dhomse, S., Griffiths, P. T., & Pyle, J. A. (2020). Modelling the potential impacts of the recent, unexpected increase in CFC-11 emissions on total column ozone recovery. *Atmospheric Chemistry and Physics*, *20*(12), 7153–7166. https://doi.org/10.5194/acp-20-7153-2020

Khatib, T., & Deria, R. (2022). East-west oriented photovoltaic power systems: model, benefits and technical evaluation. *Energy Conversion and Management*, *266*, 115810. https://doi.org/10.1016/j.enconman.2022.115810

Kirkerud, J. G., Nagel, N. O., & Bolkesjø, T. F. (2021). The role of demand response in the future renewable northern European energy system. *Energy*, *235*, 121336. https://doi.org/10.1016/j.energy.2021.121336

Knopf, B., Nahmmacher, P., & Schmid, E. (2015). The European renewable energy target for 2030 – An impact assessment of the electricity sector. *Energy Policy*, *85*, 50–60. https://doi.org/10.1016/j.enpol.2015.05.010

Laleman, R., Albrecht, J., & Dewulf, J. (2011). Life Cycle Analysis to estimate the environmental impact of residential photovoltaic systems in regions with a low solar irradiation. Renewable & Sustainable Energy Reviews, 15(1), 267–281. https://doi.org/10.1016/j.rser.2010.09.025

Li, Z., Wei, W., Wei, W., Sun, Y., Wang, Y., Lin, Y., Huang, C., & Deng, S. (2024). Experimental study on the effects of melted frost icing on the operating performances of air source heat pump. *Applied Thermal Engineering*, *238*, 122136. https://doi.org/10.1016/j.applthermaleng.2023.122136

Libra, M., Mrazek, D. A., Tyukhov, I., Severová, L., Poulek, V., Mach, J., Šubrt, T., Beránek, V., Svoboda, R., & Sedláček, J. (2023). Reduced real lifetime of PV panels – Economic consequences. *Solar Energy*, *259*, 229–234. https://doi.org/10.1016/j.solener.2023.04.063

Lindberg, M. B., & Inderberg, T. H. J. (2023). Just sharing? Energy injustices in the Norwegian solar policy mix for collective prosuming. *Energy Research & Social Science*, *103*, 103219. https://doi.org/10.1016/j.erss.2023.103219

Lindberg, K. B., Bakker, S. J., & Sartori, I. (2019). Modelling electric and heat load profiles of non-residential buildings for use in long-term aggregate load forecasts. *Utilities Policy*, *58*, 63–88. https://doi.org/10.1016/j.jup.2019.03.004

Liu, W., Zhang, Z., Xie, X., Yu, Z., Von Gadow, K., Xu, J., Zhao, S., & Yang, Y. (2017). Analysis of the global warming potential of biogenic CO2 emission in life cycle assessments. *Scientific Reports*, *7*(1). https://doi.org/10.1038/srep39857

Longi 410, (n.d.). Solcellegrossisten.no. Retrieved 4 May, 2024 from https://www.solcellegrossisten.no/products/solcellepaneler-pakkepris

Lorentzen, G. (2018, July 9). *kuldeanlegg* [Cooling systems]. *Store norske leksikon*. Retrieved 19. mars 2024 from https://snl.no/kuldeanlegg

Lynch, J., Cain, M., Pierrehumbert, R. T., & Allen, M. (2020). Demonstrating GWP*: a means of reporting warming-equivalent emissions that captures the contrasting impacts of short- and long-lived climate pollutants. *Environmental Research Letters*, *15*(4), 044023. https://doi.org/10.1088/1748-9326/ab6d7e

Mandley, S., Daioglou, V., Junginger, H., Van Vuuren, D. P., & Wicke, B. (2020). EU bioenergy development to 2050. *Renewable & Sustainable Energy Reviews*, *127*, 109858. https://doi.org/10.1016/j.rser.2020.109858

Masruroh, N. A., Li, B., & Klemeš, J. J. (2006). Life cycle analysis of a solar thermal system with thermochemical storage process. *Renewable Energy*, *31*(4), 537–548. https://doi.org/10.1016/j.renene.2005.03.008

Masternak, C., Meunier, S., Reinbold, V., Sælens, D., Marchand, C., & Leroy, Y. (2024). Potential of air-source heat pumps to reduce environmental impacts in 18 European countries. *Energy*, 130487. https://doi.org/10.1016/j.energy.2024.130487

Meireles, I., Sousa, V., Bleys, B., & Poncelet, B. (2022). Domestic hot water consumption pattern: Relation with total water consumption and air temperature. *Renewable & Sustainable Energy Reviews*, *157*, 112035. https://doi.org/10.1016/j.rser.2021.112035

Meng, F., & Dillingham, G. (2018). Life Cycle Analysis of Natural Gas-Fired Distributed Combined Heat and Power versus Centralized Power Plant. *Energy & Fuels*, *32*(11), 11731–11741. https://doi.org/10.1021/acs.energyfuels.8b02949

Mitsubishi Kaiteki 6300. (n.d.) Varmpeumpermesteren.no. Retrieved April 26, 2024 from https://www.varmepumpemesteren.no/product/mitsubitshi-varmepumpe-kaiteki-6600/

Mitsubishi Kaiteki 6600. (n.d.) Varmpeumpermesteren.no. Retrieved April 26, 2024 from https://www.varmepumpemesteren.no/product/mitsubitshi-varmepumpe-kaiteki-6600/

Mitsubishi Kaiteki 8700. (n.d.) Varmpeumpermesteren.no. Retrieved April 26, 2024 from https://www.varmepumpemesteren.no/product/mitsubitshi-varmepumpe-kaiteki-6600/

Muench, S., & Guenther, E. (2013). A systematic review of bioenergy life cycle assessments. *Applied Energy*, *112*, 257–273. https://doi.org/10.1016/j.apenergy.2013.06.001

Naumann, G., Schropp, E., & Gaderer, M. (2022). Life cycle assessment of an Air-Source heat pump and a condensing gas boiler using an attributional and a consequential approach. Procedia CIRP, 105, 351–356. https://doi.org/10.1016/j.procir.2022.02.058

Nord, N., Ding, Y., Skrautvol, O., & Eliassen, S. F. (2021). Energy pathways for future Norwegian residential building areas. *Energies*, *14*(4), 934. https://doi.org/10.3390/en14040934

Núñez-Regueiro, M. M., & Siddiqui, S. (2020). Effects of bioenergy on biodiversity arising from land-use change and crop type. *Conservation Biology*, *35*(1), 77–87. https://doi.org/10.1111/cobi.13452

Otovo. (n.d.). Otovo.no. Retrieved 10 December, 2023 from https://solar.otovo.com/nb-no/products/1bde2e84-62b2-4293- 9fa4- c9e6fe12c88b?

Pandey, M., Winkler, D., Sharma, R., & Lie, B. (2021). Using MPC to Balance Intermittent Wind and Solar Power with Hydro Power in Microgrids. *Energies*, *14*(4), 874. https://doi.org/10.3390/en14040874

Qiu, G., Shao, Y., Li, J., Liu, H., & Riffat, S. (2012). Experimental investigation of a biomass-fired ORC-based micro-CHP for domestic applications. *Fuel*, *96*, 374–382. https://doi.org/10.1016/j.fuel.2012.01.028

Raadal, H. L., Gagnon, L., Modahl, I. S., & Hanssen, O. J. (2011). Life cycle greenhouse gas (GHG) emissions from the generation of wind and hydro power. *Renewable & Sustainable Energy Reviews*, *15*(7), 3417–3422. https://doi.org/10.1016/j.rser.2011.05.001

Raadal, H. L., Vold, B. I., Myhr, A., & Nygaard, T. A. (2014). GHG emissions and energy performance of offshore wind power. *Renewable Energy*, *66*, 314–324. https://doi.org/10.1016/j.renene.2013.11.075

Ranta, T., Laihanen, M., & Karhunen, A. (2020). Development of the bioenergy as a part of renewable energy in the Nordic countries: A comparative analysis. *Journal of Sustainable Bioenergy Systems*, *10*(03), 92–112. https://doi.org/10.4236/jsbs.2020.103008

Rasmussen, C.S. (2021). Analysis of Correlations between Energy Consumption, Structural Specifications and Climate-Induced Variables to increase Energy Efficiency in Households and Buildings through a Prediction Model. [Master's thesis, Institute of physics and technology]. UiT Munin. https://munin.uit.no/handle/10037/22105

Reichelstein, S., & Sahoo, A. (2015). Time of day pricing and the levelized cost of intermittent power generation. *Energy Economics*, *48*, 97–108. https://doi.org/10.1016/j.eneco.2014.12.005

Ruhnau, O., Hirth, L., & Praktiknjo, A. (2019). Time series of heat demand and heat pump efficiency for energy system modeling. *Scientific Data*, *6*(1). https://doi.org/10.1038/s41597-019-0199-y

Sadeghi, H., Ijaz, A., & Singh, R. M. (2022). Current status of heat pumps in Norway and analysis of their performance and payback time. *Sustainable Energy Technologies and Assessments*, *54*, 102829. https://doi.org/10.1016/j.seta.2022.102829

Sadiku, M.N.O. (2015). *Elements of electromagnetism.* Oxford University Press.

Santoyo-Castelazo, E., Solano–Olivares, K., Martínez, E., Garcia, E., & Santoyo, E. (2021). Life cycle assessment for a grid-connected multi-crystalline silicon photovoltaic system of 3 kWp: A case study for Mexico. *Journal of Cleaner Production*, *316*, 128314. https://doi.org/10.1016/j.jclepro.2021.128314

Savola, T., & Fogelholm, C. (2007). MINLP optimisation model for increased power production in small-scale CHP plants. *Applied Thermal Engineering*, *27*(1), 89–99. https://doi.org/10.1016/j.applthermaleng.2006.05.002

Solanki, S. K., Krivova, N. A., & Haigh, J. D. (2013). Solar irradiance variability and climate. *Annual Review of Astronomy and Astrophysics*, *51*(1), 311–351. https://doi.org/10.1146/annurev-astro-082812-141007

Solanki, C.S. 2015. *Solar Photovolatics – Fundamentals, Technologies and Applications* (3rd ed.). PHI Learning Private Limited.

Solenergi Norge. (n.d.). solenerginorge.no. Retrieved 10 December, 2023 from https://www.solenerginorge.no/tips-og-nyheter/solcellepakker-til-landbruk-industri-og-naering/

Spotpriser. (n.d.). Forbrukerrådet ["Norwegian Consumer Council"]. Retrieved April 26, 2024 from https://www.forbrukerradet.no/strompris/spotpriser

Statnett. (2022, October 3). *Derfor har vi prisområder* [Why we have price zones]. Retrieved May 27. 2024 from https://www.statnett.no/om-statnett/bli-bedre-kjent-med-statnett/om-strompriser/fakta-om-prisomrader/

Sterman, J. D., Siegel, L., & Rooney-Varga, J. N. (2018). Does replacing coal with wood lower CO 2 emissions? Dynamic lifecycle analysis of wood bioenergy. *Environmental Research Letters*, *13*(1), 015007. https://doi.org/10.1088/1748-9326/aaa512

Stokkan, G. (2019, December 6). *doping – teknikk* [doping – technique]. *Store Norske Leksikon.* Retrieved 18. March 2024 from https://snl.no/doping_-_teknikk

Sutherland, B. R. (2020). Solar materials find their band gap. *Joule*, *4*(5), 984–985. https://doi.org/10.1016/j.joule.2020.05.001

Svenska Kraftnät. (2023, September 29). *Map of the national grid*. Retrieved May 27. 2024 from https://www.svk.se/en/national-grid/map-of-the-national-grid/

Tongwei 415. (n.d.). Solcellespesialisten.no. Retrieved 4 May, 2024 from https://www.nettbutikk.solcellespesialisten.no/solcellepanel/th415pmb7-44scf/tongwei-415wp-all-black-shingled

Torvanger, A. (2021, December 6). *Forest-based bioenergy in Norway's green transition: Balancing production and other societal interests*. https://pub.cicero.oslo.no/cicero-xmlui/handle/11250/2834949

Toshiba Daisekai 25. (n.d.). Ventdel.no. Retrieved April 26, 2024 from https://ventdel.no/produkt/varmepumper-tilbehor/toshiba-varmepumper/toshiba-daiseikai-9-25-6700-w

Toshiba Daisekai 35. (n.d.). Ventdel.no. Retrieved April 26, 2024 from https://ventdel.no/produkt/varmepumper-tilbehor/toshiba-varmepumper/toshiba-daiseikai-9-35-7700-w

Toshiba Polar 25. (n.d.). Toshibavarmepumper.no. Retrieved April 26, 2024 from https://www.toshibavarmepumper.no/varmepumper-luft-luft/toshiba-polar-25/

Toshiba Polar 35. (n.d.). Toshibavarmepumper.no. Retrieved April 26, 2024 from https://www.toshibavarmepumper.no/varmepumper-luft-luft/toshiba-polar-35/

Toshiba Seiya Nordic 25. (n.d.). Toshibavarmepumper.no. Retrieved April 26, 2024 from https://www.toshibavarmepumper.no/varmepumper-luft-luft/toshiba-seiya-nordic-25/

Toshiba Seiya Nordic 35. (n.d.). Toshibavarmepumper.no. Retrieved April 26, 2024 from https://www.toshibavarmepumper.no/varmepumper-luft-luft/toshiba-seiya-nordic-35/

Toshiba Sinatur 25 (n.d.). Toshibavarmepumper.no. Retrieved April 26, 2024 from https://www.toshibavarmepumper.no/varmepumper-luft-luft/signatur-25/

Toshiba Sinatur 35 (n.d.). Toshibavarmepumper.no. Retrieved April 26, 2024 from https://www.toshibavarmepumper.no/varmepumper-luft-luft/signatur-25/

Trømborg, E. (2011, December). IEA Bioenergy task 40–Country report 2011 for Norway. In *IEA Bioenergy Task*.

Tuset, J.K. (2024, March 20). *Hvor kommer strømmen fra?* [Where does the power come from?]. NVE - Noregs vassdrag- og energidirektorat [The Norwegian Water Resources and Energy Directorate]. Retrieved April 24, 2024 from https://www.nve.no/energi/energisystem/kraftproduksjon/hvor-kommer-stroemmen-fra/.

Ulica 455. (n.d.). Solcellespesialisten.no. Retrieved 4 May, 2024 from https://www.nettbutikk.solcellespesialisten.no/solcellepanel/ul-455m-144hv/ulica-solar-ul-455m-144hv-455w

Van Fan, Y., Klemeš, J. J., & Ko, C. (2020). Bioenergy carbon emissions footprint considering the biogenic carbon and secondary effects. *International Journal of Energy Research*, *45*(1), 283–296. https://doi.org/10.1002/er.5409

Volter. (2023, February 27). *Walter powerplant*. Retrieved 31. October 2023 https://volter.fi/en/products/walter-powerplant/

Walker, R., & Pavía, S. (2015). Thermal performance of a selection of insulation materials suitable for historic buildings. Building and Environment, 94, 155–165. https://doi.org/10.1016/j.buildenv.2015.07.033

Walpole, R.E., Myers, R.H., Myers, S.L. & Ye, Keying (2012). *Probability & Statistics for Engineers & Scientists* (9th ed.). Pearson Prentice Hall.

Wang, L., Wang, Y., Du, H., Zuo, J., Li, R. Y. M., Zhou, Z., Bi, F., & Garvlehn, M. P. (2019). A comparative life-cycle assessment of hydro-, nuclear and wind power: A

China study. *Applied Energy*, *249*, 37–45. https://doi.org/10.1016/j.apenergy.2019.04.099

Aldersey-Williams, J., & Rubert, T. (2019). Levelised cost of energy –A theoretical justification and critical assessment. *Energy Policy*, *124*, 169–179. https://doi.org/10.1016/j.enpol.2018.10.004

Winther, T., Westskog, H., & Sæle, H. (2018). *Like having an electric car on the roof: Domesticating PV solar panels in Norway*. https://sintef.brage.unit.no/sintef-xmlui/handle/11250/2576205

Wu, C., Liu, F., Li, X., Wang, Z., Xu, Z., Zhao, W., Yao, Y., Wu, P. C., Xu, C., & Wang, Y. (2022). Low-temperature air source heat pump system for heating in severely cold area: Long-term applicability evaluation. *Building and Environment*, *208*, 108594. https://doi.org/10.1016/j.buildenv.2021.108594

Xu, L., Pang, M., Zhang, L., Poganietz, W., & Marathe, S. D. (2018). Life cycle assessment of onshore wind power systems in China. *Resources, Conservation and Recycling*, *132*, 361–368. https://doi.org/10.1016/j.resconrec.2017.06.014

Yang, Z., Feng, B., Ma, H., Zhang, L., Duan, C., Liu, B., Zhang, Y., Chen, S., & Yang, Z. (2021). Analysis of lower GWP and flammable alternative refrigerants. *International Journal of Refrigeration*, *126*, 12–22. https://doi.org/10.1016/j.ijrefrig.2021.01.022

Zainali, S., Lindahl, J., Lindén, J., & Stridh, B. (2023). LCOE distribution of PV for single-family dwellings in Sweden. *Energy Reports*, *10*, 1951–1967. https://doi.org/10.1016/j.egyr.2023.08.042

Appendix A

Appendix A contains tables which provide additional information for 4.1.2.

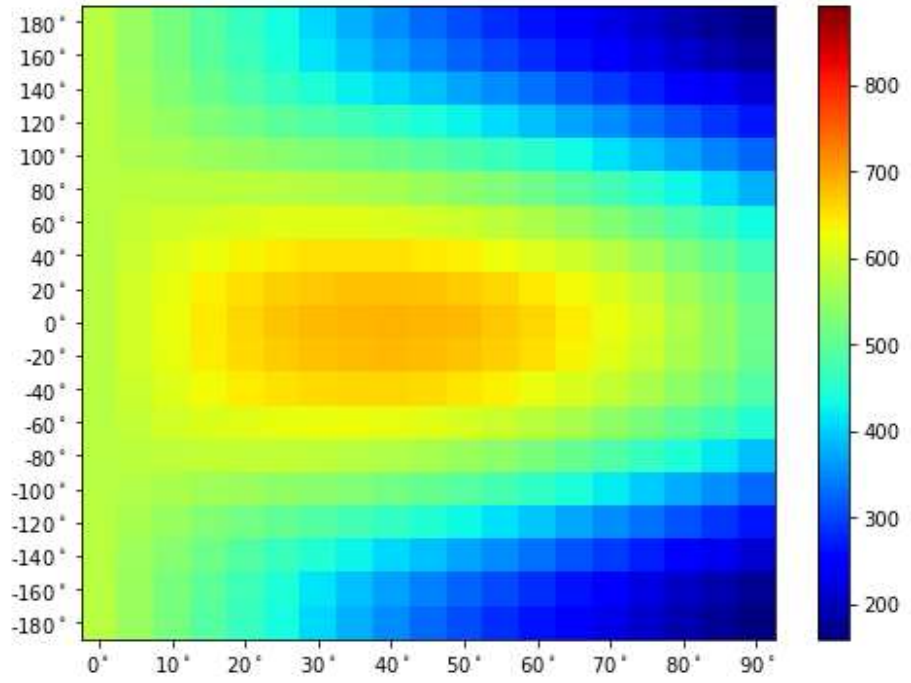

Figure A1 - Total yearly production of different azimuth and slope relations in Bergen for 1kWp [kWh/kWp]

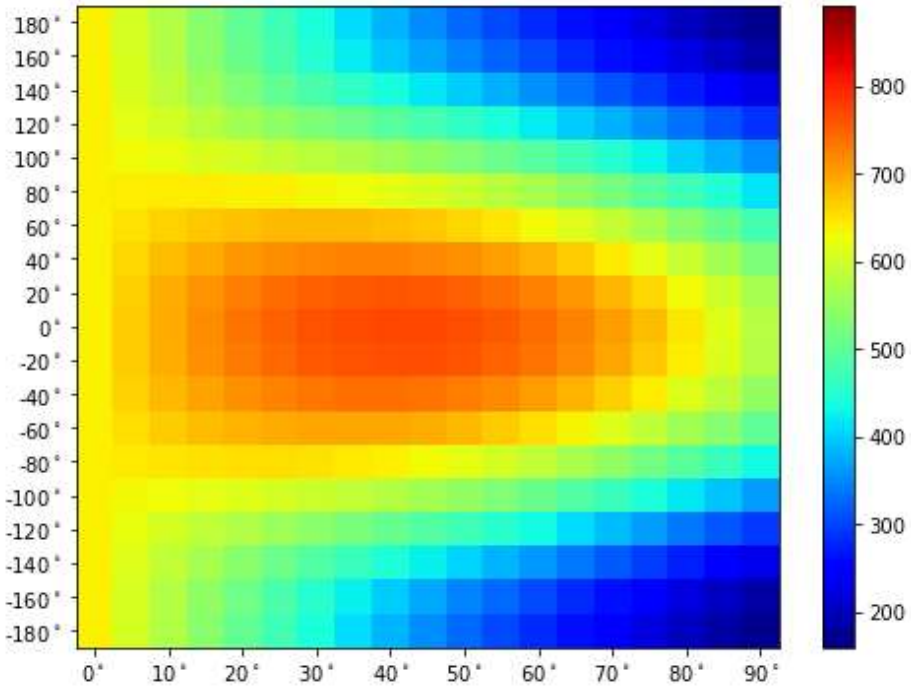

Figure A2 - Total yearly production of different azimuth and slope relations in Stavanger for 1kWp [kWh/kWp]

Appendix B

Appendix B contains tables and a figure which provide additional information for 4.2.4 and 4.2.5.

Table B1- Cost of covering electrical needs with economically optimized PV system implementation in NOK/m2 based in 0.40NOK/kWh fixed price

	$50m^2$	$100m^2$	$150m^2$	$200m^2$	$250m^2$
Oslo	42.41	32.21	28.94	27.33	26.36
Tromsø	44.1	33.18	29.62	27.84	26.77
Bergen	43.68	32.91	29.42	27.69	26.65
Stavanger	43.02	32.56	29.18	27.51	26.51
Trondheim	43.25	32.72	29.3	27.6	26.58

Table B2 - Cost of covering electrical needs with south facing PV system implementation in NOK/m2 based in 0.40NOK/kWh fixed price

	$50m^2$	$100m^2$	$150m^2$	$200m^2$	$250m^2$
Oslo	41.14	54.39	55.88	55.36	52.45
Tromsø	43.28	58.37	60.47	60.25	57.16
Bergen	42.95	57.79	59.81	59.55	56.49
Stavanger	42.03	56.06	57.82	57.44	54.45
Trondheim	41.95	55.92	57.65	57.26	54.28

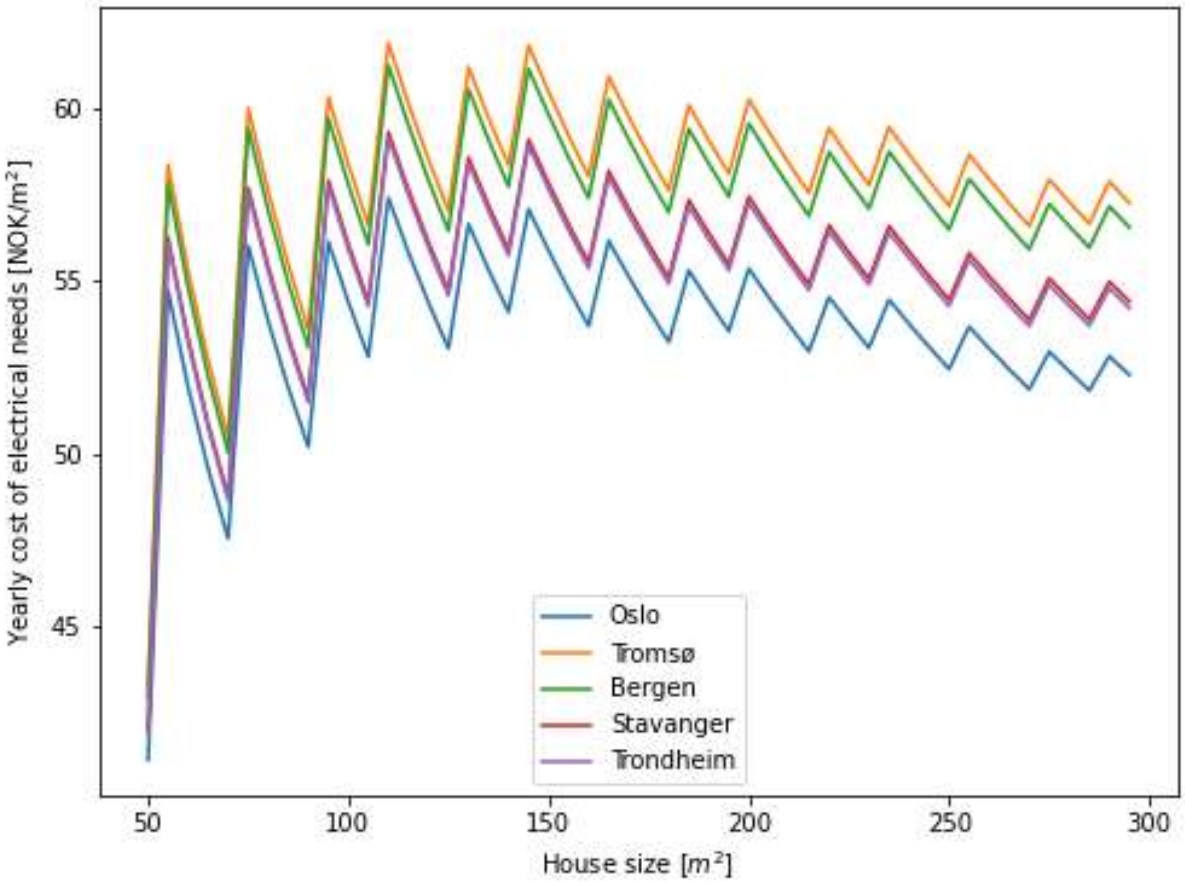

Figure B3 - Cost of covering electrical needs with south facing PV system implementation in NOK/m2 based in 0.40NOK/kWh fixed price

Appendix C

Appendix C contains tables which provide additional information for 4.2.8.

Table C1 - Emission factor in kgCO2e/kWh for PV panels with configurations 12-, 20- and 30-year lifetime facing south or east-west based in Bergen

	South		**East-west**	
	1500 kgCO2e/kWp	2500 kgCO2e/kWp	1500 kgCO2e/kWp	2500 kgCO2e/kWp
12 years	0.1940	0.3234	0.2252	0.3753
20 years	0.1164	0.194	0.1351	0.2252
30 years	0.0776	0.1293	0.0901	0.1501

Table C2 - Emission factor in kgCO2e/kWh for PV panels with configurations 12-, 20- and 30-year lifetime facing south or east-west based in Stavanger

	South		**East-west**	
	1500 kgCO2e/kWp	2500 kgCO2e/kWp	1500 kgCO2e/kWp	2500 kgCO2e/kWp
12 years	0.1688	0.2813	0.2008	0.3347
20 years	0.1013	0.1688	0.1205	0.2008
30 years	0.0675	0.1125	0.0803	0.1339

Table C3 - Emission factor in kgCO2e/kWh for PV panels with configurations 12-, 20- and 30-year lifetime facing south or east-west based in Trondheim

	South		**East-west**	
	1500 kgCO2e/kWp	2500 kgCO2e/kWp	1500 kgCO2e/kWp	2500 kgCO2e/kWp
12 years	0.1665	0.2776	0.2098	0.3496
20 years	0.0999	0.1665	0.1259	0.2098
30 years	0.0666	0.111	0.0839	0.1398

Appendix D

Appendix D contains figures which provide additional information for 4.4.2.

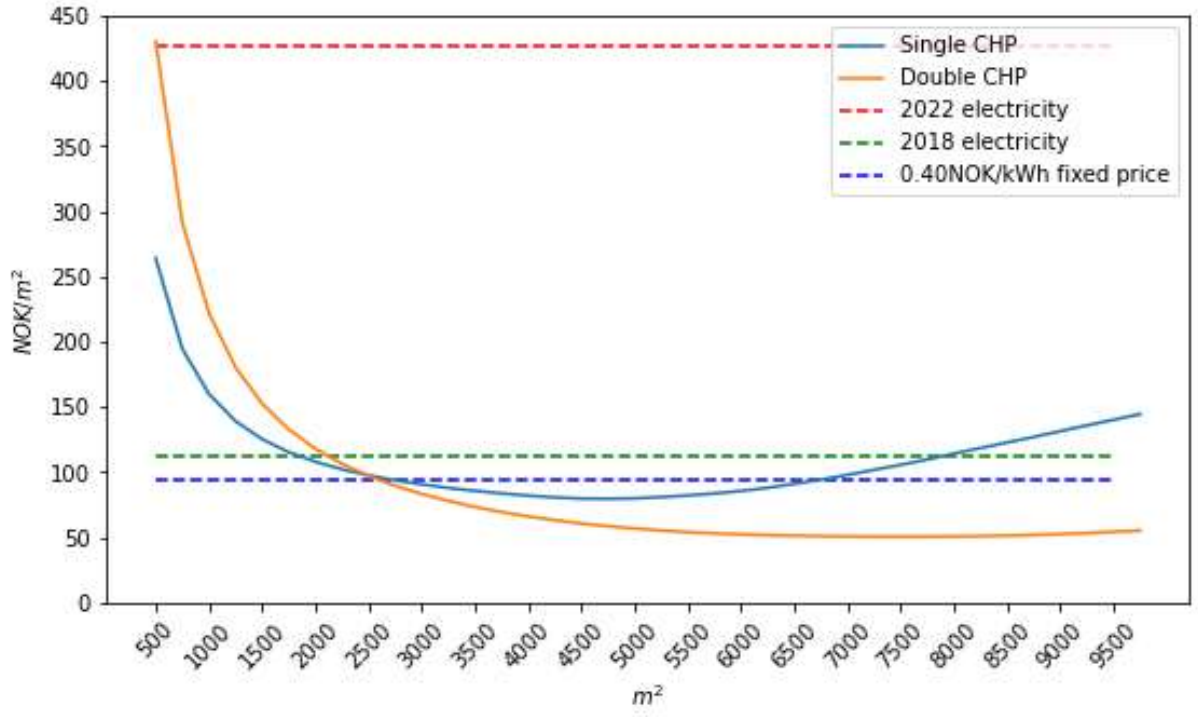

Figure D1 - Cost per square meter of 1 and 2 CHP module configuration, and 2018, 2022 and fixed electricity price scenarios for Bergen

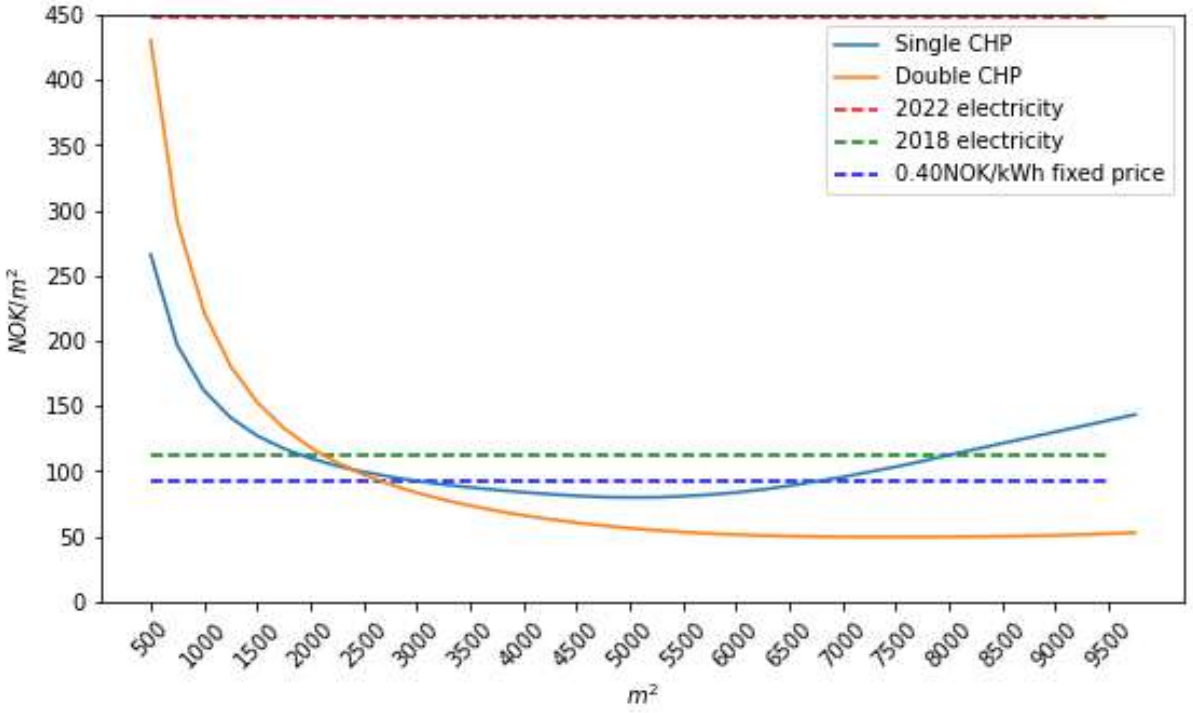

Figure D2 - Cost per square meter of 1 and 2 CHP module configuration, and 2018, 2022 and fixed electricity price scenarios for Stavanger

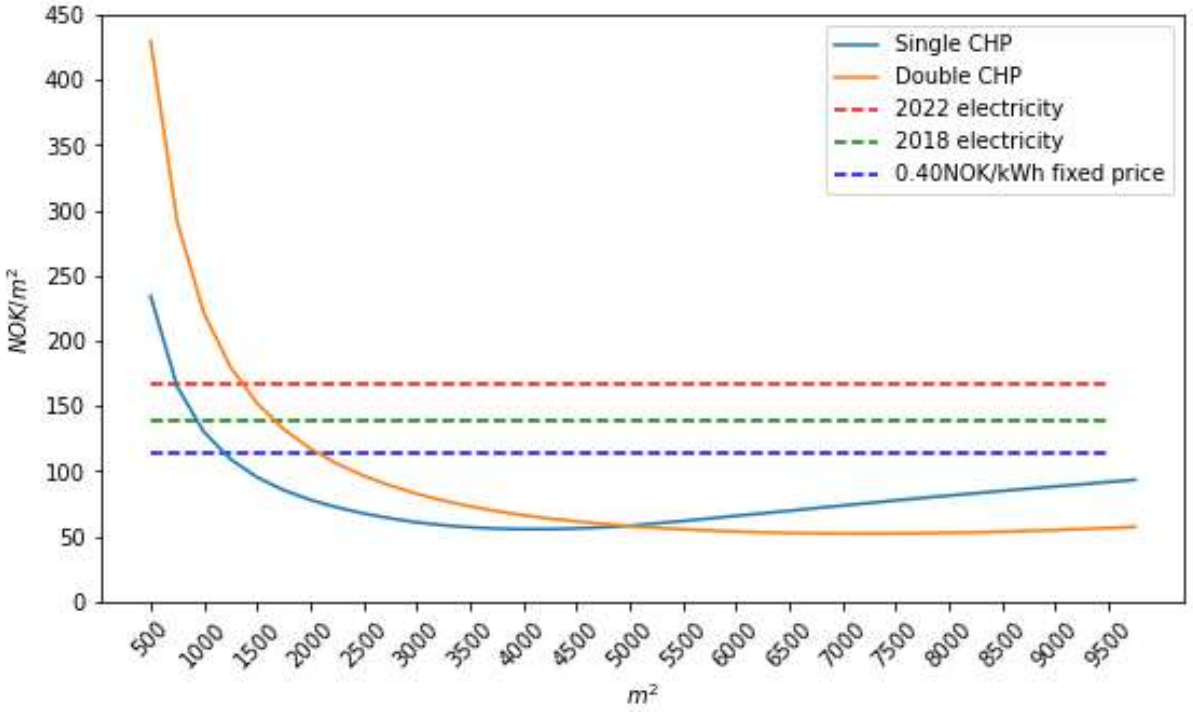

Figure D3 - Cost per square meter of 1 and 2 CHP module configuration, and 2018, 2022 and fixed electricity price scenarios for Trondheim